CLEARINGHOUSE FOR FEDERAL SCIENTIFIC AND TECHNICAL INFORMATION CFSTI
DOCUMENT MANAGEMENT BRANCH 410.11

LIMITATIONS IN REPRODUCTION QUALITY

ACCESSION # AD609068

- [x] 1. WE REGRET THAT LEGIBILITY OF THIS DOCUMENT IS IN PART UNSATISFACTORY. REPRODUCTION HAS BEEN MADE FROM BEST AVAILABLE COPY.
- [ ] 2. A PORTION OF THE ORIGINAL DOCUMENT CONTAINS FINE DETAIL WHICH MAY MAKE READING OF PHOTOCOPY DIFFICULT.
- [ ] 3. THE ORIGINAL DOCUMENT CONTAINS COLOR, BUT DISTRIBUTION COPIES ARE AVAILABLE IN BLACK-AND-WHITE REPRODUCTION ONLY.
- [ ] 4. THE INITIAL DISTRIBUTION COPIES CONTAIN COLOR WHICH WILL BE SHOWN IN BLACK-AND-WHITE WHEN IT IS NECESSARY TO REPRINT.
- [ ] 5. LIMITED SUPPLY ON HAND: WHEN EXHAUSTED, DOCUMENT WILL BE AVAILABLE IN MICROFICHE ONLY.
- [ ] 6. LIMITED SUPPLY ON HAND: WHEN EXHAUSTED DOCUMENT WILL NOT BE AVAILABLE.
- [ ] 7. DOCUMENT IS AVAILABLE IN MICROFICHE ONLY.
- [ ] 8. DOCUMENT AVAILABLE ON LOAN FROM CFSTI (TT DOCUMENTS ONLY).
- [ ] 9.

PROCESSOR: G. Lee

TSL-107-10/64

AD 609068

June, 1960

Index No. NS712-100 S.T. 2

CONESCO

consultants in

engineering science

SHIP HULL VIBRATIONS – 2

THE DISTRIBUTION OF EXCITING FORCES GENERATED BY PROPELLERS

F. E. Reed

R. T. Bradshaw

COPY 1 OF 1	
HARD COPY	$. 6.00
MICROFICHE	$. 1.25

Contract No. NObs 77150

CONESCO Report No. F-101-2

40 massachusetts avenue • arlington 74, massachusetts

CONESCO consultants in engineering science

40 Massachusetts Avenue

Arlington 74, Massachusetts

SHIP HULL VIBRATIONS - 2

THE DISTRIBUTION OF EXCITING FORCES GENERATED BY PROPELLERS

by

F. E. Reed

R. T. Bradshaw

Contract No. NObs 77150

Bureau of Ships, Department of the Navy

Code 345

June 1960

CONESCO Report No. F-101-2

Index No. NS712-100 S. T. 2

ABSTRACT

A study of the forces acting on a hull as a consequence of the propeller action. Develops calculation forms for computing the dynamic forces and moments generated by a propeller operating in a variable wake. Describes a program for computing the shaft-bearing reactions resulting from these propeller forces. Presents a method of computing hull pressure forces resulting from the propeller pressure field.

The various procedures are illustrated by numerical examples.

PREFACE

This report describes the principal effort of CONESCO under Contract NObs 77150 "Propeller Excited Hull Vibrations"; a previous report (F-101-1) presented a bibliography of significant published work in this field.

In writing the present report, the authors have departed from the traditional form and have adopted an organization which, it is believed, will make the contents accessible to a greater variety of readers.

Thus, the report is divided into two sections, the first of which contains a purely verbal description of the main problems, the methods used for their solution, and the significant results obtained. The second section contains the analytical development of these topics, but with greater continuity and clearer motivation than would be realized were the work presented as a series of appendices.

The authors would like to acknowledge their indebtedness to Mr. F. F. Vane and Mr. A. R. Paladino of the Bureau of Ships; to Mr. R. T. McGoldrick of the David W. Taylor Model Basin; and to Dr. J. P. Breslin of the Davidson Laboratory, Stevens Institute of Technology. The information and assistance received from these gentlemen contributed substantially to the preparation of this report.

The authors are particularly grateful for the efforts of:

Dr. O. K. Mawardi and Mr. M. Yildiz of CONESCO who contributed Appendix E on the interaction of a rigid wedge and a radiating dipole.

Dr. E. H. Cuthill and Mrs. Y. Smith of the Applied Mathematics Laboratory, David W. Taylor Model Basin, who contributed Appendix F on the programming of the methods developed for the computation of propulsion train characteristics.

TABLE OF CONTENTS

LIST OF FIGURES

LIST OF TABLES

NOMENCLATURE

a - axial inflow factor in propeller hydrodynamics

- cross sectional area of shaft

a' - rotational inflow factor in propeller hydrodynamics

A - a function of the Theodorsen parameter, k

A_n - coefficient in a Fourier expansion

b - one-half the chord length of a blade section

B - a function of the Theodorsen parameter, k

B_n - coefficient in a Fourier expansion

c - chord length of a blade section

- speed of sound

C - complex Theodorsen function $C(k) = F(k) + i\,G(k)$

d - axial distance of a reference point on the propeller blade face from a coordinate axis

D - overall diameter of a propeller

E - Young's Modulus of Elasticity - an elliptic integral

F - a Theodorsen flutter function

- axial force per unit length on propeller blade

- a general force

G - a Theodorsen flutter function

- tangential force per unit length on a propeller blade h - height of an airplane above a plane surface

- motion of an airfoil normal to the stream

I, I_s - Diametrical moment of inertia

J - Polar moment of inertia

k - Theodorsen reduced frequency - $\frac{\omega b}{U}$

- wave number = $\frac{\omega}{c}$

l - length of a section of shafting between supports

L - lift force

L_o - steady lift force in steady motion

M - a Theodorsen flutter function

- mass of a concentrated element

- moment in a propeller on a shaft (see page 61 for definition of components)

n - propeller speed in R.P.S. - order number of a vibration

N - a Theodorsen flutter function

- propeller speed in R.P.M.

p - pressure

P - varying lift force on an airfoil subjected to flow variations

Q - torque in a propeller

- shear force in shafting

r - radius of propeller blade element

- radius vector

R - tip radius of a propeller

s - distance from the point of action of a harmonic force to a point where pressure is measured

t - time

u - displacement of shaft element

U - stream velocity

U_o - average stream velocity

V - velocity of ship

W - weight

w_g - gust velocity, normal to stream

W_l - longitudinal wake fraction

W_t - tangential wake fraction

x, y, z - coordinate axes -

In propeller calculations

x is along the axis	+ forward
y is vertical	+ upward
z is transverse	+ starboard

In shafting calculations

x - vertical	+ upward
y - transverse	+ starboard
z - along the shaft	+ forward

α - angle of attack of section, measured from zero lift orientation

- shaft parameter $\sqrt[4]{\frac{\mu \omega^2}{E I_s}}$

α_o - angle of attack due to blade camber

α_{nt} - angle of attack due to lift of nose and tail

β - solid angle of a wedge

- bending rigidity, EI_s

ϕ - angular location of blade element of a propeller

- linear deflection of shaft

ζ - non-dimensional quantity used in propeller force determination

η - propeller blade section efficiency

θ - angle of a propeller blade from the vertical

- pitch angle of a propeller blade

- angular deflection of shaft

μ - mass of shaft per unit length

- pressure intensification factor

ν - non-dimensional quantity used in propeller force determination

ξ - non-dimensional quantity used in propeller force determination

ρ - mass density

σ - ratio of harmonic to average stream velocity

- solidity ratio of a propeller at a given radius

ϕ - hydrodynamic pitch angle of propeller

- pitch angle of propeller lift line

Φ - potential function

ψ - advance angle of a propeller

ω - circular frequency - radians per sec.

Ω - rotational velocity - radians per sec.

INTRODUCTION

A problem of major interest in Naval Architecture is the prediction of vibrations in a ship's hull. The problem has two main aspects, viz. the estimation of forces exciting vibrations, and the response of the hull to this excitation. The present report is concerned with the former and, in particular, with the estimation of those forces which arise from the action of the propeller. While the report develops and presents several original contributions to the prediction of hull forces, its primary purpose is to render existing techniques into forms suitable for the practical calculation of these forces.

Hull forces arising from the action of a ship's propeller can be divided into two main categories:

(1) Those forces and moments generated by the propeller as it moves through the varying wake and which are transmitted to the hull via the shafting and bearings.

(2) Oscillating fluid pressures arising from the moving pressure fields associated with the blades of the loaded propeller.

Consider first the forces generated at the propeller. A method was developed (by Burrill)[1] for the calculation of blade forces when the propeller operates in a wake which varies radially but which is uniform circumferentially. This method has been used to compute forces in a circumferentially varying wake by assuming that the forces developed at any angular position are those that would be developed if the local conditions of the wake existed at all angular locations. Ritger and Breslin[2] showed that this "quasi-steady-state" analysis is inaccurate since it neglects the influence of fluid inertia which delays and modulates the circulations appropriate to local wake conditions. Methods of treating these unsteady-flow effects have been developed by aerodynamicists in the study of wing flutter and their results are incorporated in the work reported here.

Turning now to the transmission of propeller forces through the propulsion train, the literature shows that the dynamics of the shaft system has received a fair amount of theoretical and experimental attention. Many of the theoretical treatments have idealized the system into discrete masses and stiffnesses (i.e. lumped parameter analysis); however, some have treated the whirling of the propeller-shaft-gear ensemble with considerable generality (Jasper).[3,4] The specific problem of the bearing reactions caused by oscillatory propeller forces has apparently not been considered in any detail. In the present report this subject has been dealt with in detail and a description is given of a program for machine computation of the dynamical characteristics of the propulsion train.

With regard to the fluctuating pressures produced on the surface of the ship by propeller action, these are believed to be two or three times as large as the direct propeller forces in the case of a twin-screw ship, and of approximately the same magnitude as direct propeller forces in the case of single-screw ships. Experimental determinations of these pressures have been carried out by Lewis,[5,6] Lewis and Tachmindji,[7] and Tachmindji and Dickerson.[8] Within recent years Breslin[9,10,11,12] has made advances in the theoretical study of such pressures.

The problem is closely related to that of determining the noise radiated from aircraft propellers – a topic that was first considered by Gutin[13] in 1936 and has since been studied by NASA personnel [14,15,16] at Langley Field. The complexity of the problem when there is a rigid boundary present makes it necessary to find pressures by first calculating the free-field values and then multiplying by an intensification factor which accounts for reflections from the boundary.

In the present report, the methods developed by aeronautical engineers are used in modified form. These modifications are primarily a neglect of elastic-wave effects which is justified on the grounds that the physical dimensions of propellers, tip-clearances, etc. are small in comparison with the wavelength of sound at the frequencies of interest. In addition, there is presented an original theoretical study of the pressure distribution on a wedge inserted in the acoustic field produced by a harmonically varying dipole. The wedge is intended as an approximation of the submerged surface at the stern of a ship.

In Section I which follows, there is given a purely verbal description of these studies while Section II describes in greater detail the various derivations and calculations.

SECTION I.

1. The origin of the forces sustained by the propeller.

The simplest forces associated with the propeller are those due to geometric imperfections or lack of symmetry. Thus, static and dynamic mass unbalance will give rise to transverse forces and moments which rotate at shaft speed. Variations in pitch from one blade to another will result in there being different forces and moments associated with each blade, so that the complete array of blades experiences a resultant force and moment which will again rotate at shaft speed. However, due to the precision with which propellers are currently made, these forces are undoubtedly small.

A more important source of excitation arises from the fact that the propeller operates in a variable wake; thus, as a blade passes cyclically from regions of high velocity to regions of low velocity there will be a cyclic variation in the axial load on the blade. Also, since forces which lie in the plane of the disc will vary, there will be oscillating transverse forces. The axial and transverse forces will produce moments on the hub so that there will arise a general system of oscillating forces and moments on the hub viz. axial, vertical and horizontal forces, and axial (torsional), vertical and horizontal moments.

A further source of propeller excitation - one that is not generally recognized - arises from the turbulent nature of the ship's boundary layer. The wake in the region of the propeller is not constant with time as is assumed in blade force calculations, but varies in a more or less random manner as large scale turbulent eddies interact with the propeller. Since the propeller will modify these random fluctuations with its own periodicity, a harmonic excitation may be generated. While this source of excitation is mentioned here, the resulting forces and moments are not treated in the body of the work.

2. <u>The magnitude and distribution of forces sustained by the propeller</u>.

The calculation of propeller forces is normally carried out on the basis of an assumed distribution of the wake over the disc, this distribution being inferred from model tests on either the ship and propeller in question or another ship and propeller of approximately similar design. The calculations are of a quasi-steady-state nature, i. e. for any given angular position of a blade, the axial and circumferential wake components at a given radius are used to find the resulting 'forward' velocity and angle of attack of a blade element at that radius; these quantities are then used to compute the elementary lift and drag forces which would be experienced by an element operating at these steady-state conditions. Since the wake is surveyed at as many as 24 angular positions with 4 radial points on each, and since the calculations are carried out for each of these 96 positions, the computation of propeller loads is a tedious job.

Aside from tedium, the principal defect of this method is that dynamic effects are not taken into account. The force on an aerofoil can be considered to arise from the interaction of a uniform stream velocity and a circulating flow around the aerofoil. If the magnitude or direction of the incident stream changes, a new circulation will result and the force experienced by the aerofoil will change. Obviously, this new circulation will not be established instantaneously, but will require an interval (albeit quite short) to become fully developed, hence, an aerofoil operating in a rapidly varying stream will experience forces which may differ substantially (in both magnitude and phase) from those predicted by the quasi-steady-state analysis.

Changes in the relative velocity between stream and propeller can also arise from axial and rotational movements of the propeller caused by axial and torsional oscillations in the shafting.

Dynamic effects of the preceding phenomena can be accounted for by considering the three following topics:

(i) A harmonic variation in the velocity of approach of the fluid to the surface.

(ii) Impingement of harmonic gusts acting in a direction normal to the orientation of the surface for zero lift.

(iii) Harmonic translation of the surface in a direction perpendicular to its orientation for zero lift.

The case of an aerofoil subjected to a harmonic velocity superimposed on the main stream velocity was first considered by Isaacs,[17] later, Greenberg[18] presented a simpler solution that agreed closely with Isaac's work, and it is Greenberg's solution that has been used here. Fig. (1) illustrates the oscillatory forces predicted by Greenberg's formulae.

Solutions (due to Theodorsen and others) exist for (ii) and (iii) and are most conveniently summarized in the volume "Aeroelasticity" by Bisplinghoff, Ashley, and Halfman.[19] Formulae quoted in that work refer to the flutter of aircraft wings which have ailerons, tabs, etc. These formulae have been modified to correspond to the simpler, rigid, lifting surface represented by the propeller blade and have been used to evaluate the dynamic effects in question. The results are summarized in Fig. (2).

Turning now to the question of incorporating these results into the formal computation of propeller forces, this is accomplished in the following way:

At any given radius, the wake variation can be expressed as a mean velocity with a number of superimposed harmonic (Fourier) components. The forces (due to the mean velocity) experienced by a blade element at this radius can be calculated and the contribution from each harmonic component of the wake can be found from these by relatively simple ratios based on the Fourier coefficient of each component. In this way the cyclic variation of thrust and torque (for an element of radius) can be computed for a given radius. If this procedure is repeated for a number of selected radii (at least 4) a quite detailed picture of the cyclic thrust and torque variation can be obtained with considerably less effort than the method previously

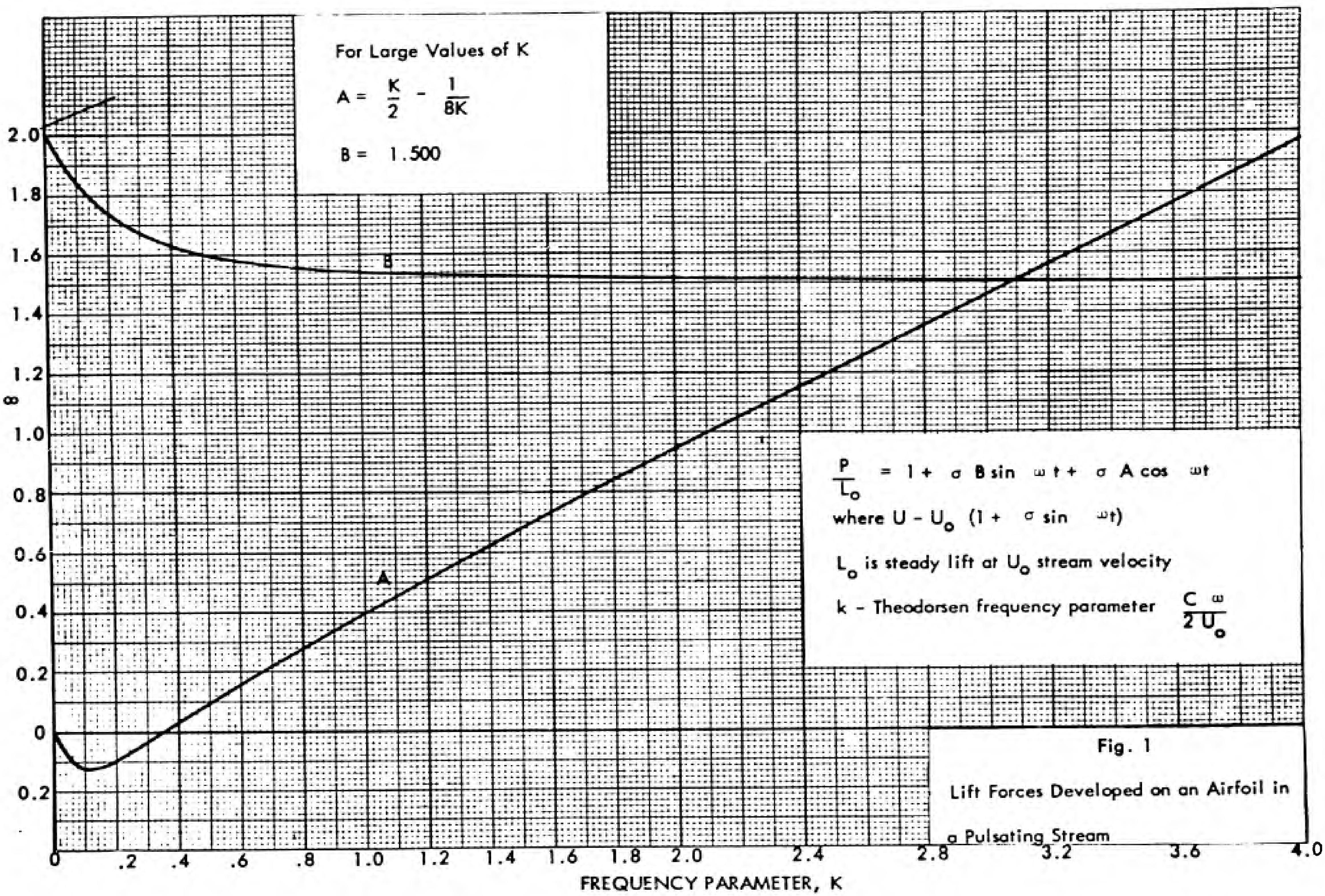

Fig. 1

Lift Forces Developed on an Airfoil in a Pulsating Stream

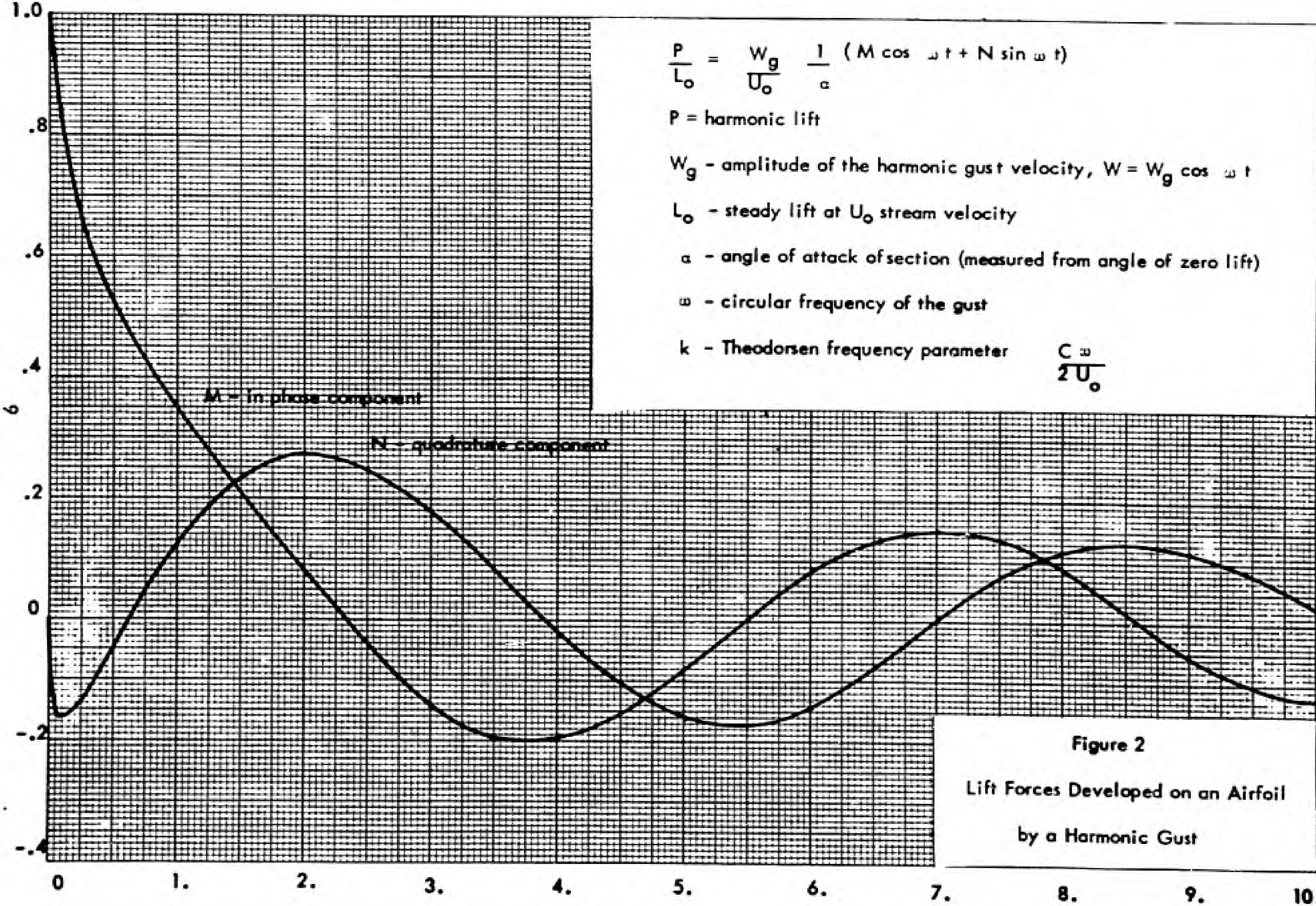

Figure 2

Lift Forces Developed on an Airfoil by a Harmonic Gust outlined.

Forms have been devised to facilitate this method of computation and their use is illustrated in appendices which follow Section II.

3. Transmission of propeller forces through the sea to the hull.

Since the forces experienced by the blades of the propeller react against the surrounding sea, there will be a time-varying pressure field at the stern of the ship. This pressure field has been investigated on the basis of potential flow in an incompressible fluid and as a problem of radiation through a compressible fluid. The former approach is best exemplified by the work of Breslin[9,10,11,12] in which a blade of the propeller is treated as a rotating line vortex which sheds a trailing helical vortex from its tip. The pressure at any point in the field due to an elemental length of this line vortex is computed, and the result is integrated over the whole line to get the total of all contributions.

The radiation approach was first used by Gutin[13] who represented the force on a blade element as an oscillating potential dipole and proceeded to solve the wave equation and find the pressure at some distance from the radiating source.

In both cases the field was considered to be without boundaries.

The method of finding free-field pressures developed in this work is based on the potential solution of Lamb[20] as used by Gutin,[13] but with the wave character of the expression suppressed. The solution as then written gives the pressure in terms of a differential expression containing the X, Y, Z components of the applied force and the coordinates of the point of application and the point at which the pressure is computed. The components of force are derived quite simply from the axial (thrust) and tangential (torque) components of the blade-element force, and the coordinates are of course the radial and angular location of the blade element. The pressure appears (after some approximations) as a Fourier series whose terms have multiples of the blade angle as arguments and have power series as coefficients. These power series are functions of the coordinates of the point at which the pressure is being computed and, for locations at a reasonable distance from the propeller disc, are rapidly convergent.

Since the blade-element forces can themselves be expressed as Fourier series of the blade angle, the pressure at a point becomes the product of two Fourier series. The terms of these various series are given in detail in Section II.

An alternative method would be to calculate the pressure for a number of different blade positions and in this way obtain a description of the pressure variation as the blade rotates.

In both of these methods, the total pressure at a point must be found by summing the contributions from all the blade elements.

The fact that the blade-element forces have a chord-wise distribution is discussed in Appendix D and can be shown to be a minor influence except in the vicinity of the propeller hub.

The presence of a boundary (such as the ship's hull) can materially alter the pressure field, generally by increasing the pressure over the value in the free-field. It is believed that the most feasible method of determining the pressure on the boundary is to compute the pressure that would exist if the boundary did not exist and to multiply this free-field pressure by a factor (referred to as the pressure intensification factor and designated by μ) which gives the ratio of the pressure on the boundary to the free-field pressure for the particular surface under consideration.

The value of the pressure intensification factor, μ , is an easily determined quantity only in the case of a rigid, plane surface of infinite extent and in this case is 2. The value of μ has been determined theoretically for sources located between two intersecting infinite surfaces having certain subtended angles of less than 180° and for a source outside an infinite circular cylinder

Since many of the parts of a ship cannot be approximated by the shapes for which the pressure on the boundary has been studied, some attention has been given to surfaces that will represent the hull more adequately, particularly the narrow surfaces such as the section forward of the propeller in single screw ships, the rudders and the portion of the hull directly over the propeller in a single screw ship.

The idealized representation considered in this study consists of an infinite, rigid, wedge inserted in the field produced by a sinusoidal force (represented mathematically by an oscillating dipole). The solution developed by M. Yildiz and O. K. Mawardi which is given in Appendix E represents an extremely powerful new technique for the treatment of wave propogation in partially bounded fields.

To choose an intensification factor that includes the effects of dimensions on the wedge and integrates all the locations and orientations of the propeller force, will require more detailed study than time permits. In all cases, the intensification factor at the apex of the wedge is found to be equal to $(1 + \frac{2\pi}{2\pi - \beta})$ where β is the solid angle of the wedge. At points on the surface remote from the apex, it is probably adequate to take the intensification factor equal to 2 on the surface over which the force is acting and 0 on the shaded surface and this situation represents quite accurately the case of a skeg.

Since the pressures generated by a propeller fall off rapidly with the distance from the propeller, much of the hull where the pressures are significatnt can be represented by either infinite plane surfaces or as an infinite wedge; hence, reasonably good estimates of the hull forces can be obtained by the integration of the pressures on these idealized sections.

4. Transmission of propeller forces through the propulsion system to the hull

In Part 2. of this section there was described a method of calculating the cyclic variation of thrust and torque on the propeller. These forces, along with those arising from dynamic unbalance or from pitch variations in the blades, can be represented by a general set of forces and moments acting on the outboard end of the tailshaft. Due to the action of these forces, the propulsion train will be excited into a state of transverse (flexural) and axial (torsional and extensional) vibrations, which, in turn, will produce oscillating reactions at the various bearings and will thereby excite the hull into some compatible state of vibration.

Ideally, an analysis of the vibration characteristics of the propulsion system would take into account the fact that it is coupled to another elastic system (in the hull), but, for the present, it is considered sufficient to treat the shafting, etc. as supported in elastic bearings which are supported by rigid foundations.

The methods developed to treat the dynamics of the propulsion system can be described as follows:

(a) Transverse Vibration

If the standard solution of the equation of flexural vibration of a beam is successively differentiated and multiplied by appropriate constants, a series of four equations can be obtained which represent the deflection, slope, bending moment, and shear force at any section of the beam. These equations contain the inertial and elastic properties of the beam, the frequency of vibration, the location of the section, and four undetermined constants which are eventually determined by boundary conditions on the beam. If the equations are written in matrix form, there appears a relation between two vectors or column matrices, one of which has for its terms the deflection, slope, moment and shear, while the other vector is composed of the four undetermined constants. This matrix equation can now be manipulated to identify the four undetermined constants with known conditions of deflection, slope, moment and shear at some other point in the beam. There now appears a fourth order matrix which relates deflection, slope, etc. at one point to corresponding conditions at another. This matrix, which conveniently summarizes the dynamical properties of the length of the beam lying between the points in question, has been dubbed a 'transfer' matrix, and the two vectors which it relates are referred to as 'condition' vectors. Since the solution of a boundary value problem depends on finding a relation between two condition vectors, of which, part of each is known, it can be seen that such a solution requires that an overall transfer matrix be built up. To take a simple example of this process, consider the case of a cantilever made up of a number of lengths of different cross-sections, modulii of elasticity, and densities, the assembly being excited at some frequency with known moment and shear at one end. The individual transfer matrices for each span can be written down directly, and the overall transfer matrix is the cumulative product of these. This cumulative product provides the four equations whose solution gives the unknown deflection and slope at the excited end and the unknown moment and shear at the fixed end. If conditions of deflections, slope, moment or shear are required at an intermediate point, it is simply required to write down a transfer matrix which will transfer the (now known) conditions at one end up to that point and make the transfer, i. e. the multiplication.

While discontinuities in the physical or material properties of the system are important, probably more importance can be attached to discontinuous changes in the condition vector at various points in the system. Such changes can be brought about by elastic constraints, concentrated masses, pin joints, etc. which produce discontinuous changes in one or more of the components of the condition vector (deflection, slope, etc.). In each case the discontinuity can be assigned a characteristic matrix which contains terms representing the effects of inertia, elasticity, etc. depending on the nature of the discontinuity. This 'discontinuity' matrix can now be incorporated in the process of accumulation which yields the final overall transfer matrix. As before, the relatively simple solution of this overall transfer equation yields the unknown parts of the boundary condition vectors, and knowledge of the condition vector at an interior point (specifically, at a discontinuity) can again be found by transferring a boundary condition up to that point.

Up to now, this discussion has been limited to those transverse vibrations which occur in one plane only. However, the more general case of cross-coupling between vibrations in mutually perpendicular planes can be treated by an extension of the ideas already introduced. In the discussion which follows, cross-coupling is always assumed to exist at localized places. Thus, there is specifically excluded that type of distributed coupling which arises from the gyroscopic action of a spinning shaft whose cross-sections rotate due to flexure. While distributed gyroscopic coupling is excluded, the localized coupling caused by discs attached to the shaft are not.

To treat the case of cross-coupled vibrations, the concepts of transfer matrices, condition vectors, discontinuity matrices, etc. are still valid, but the order of these must now be doubled. Thus, a condition vector will now have eight components, viz. four for one plane and four for the other, while transfer and discontinuity matrices will be of eighth order (8 x 8). In the case of a circular shaft a transfer matrix for a uniform length or run will consist of two identical fourth order matrices arranged along the principal diagonal. The biggest difference between the one-plane and two-plane vibration occurs in the discontinuity matrix. In addition to the previous elastic and inertial terms, there will be new terms which relate the forces arising in one plane with displacements and accelerations arising in the other. Force-acceleration terms appear when there is a rotating disc to provide gyroscopic reactions, while force-displacement terms appear when an elastic constraint does not have its principal axes lying in the planes used to describe the vibration, i. e. when a force in one plane produces a component of displacement in the other plane.

Using these more general forms of the various matrices the methods of accumulating an overall transfer matrix can be carried out as before.

At this point it is probably well to confirm the reader's suspicions about the amount of numerical calculation involved. In only the simpler cases (involving, say, two or three bearings and vibration in one plane) is it feasible to carry out the computations with a desk machine. For a larger number of bearings and for vibration in two planes it is necessary to use automatic computing equipment; this is particularly true for vibration in two planes since phase differences between effects in these planes result in complex terms arising in various matrices.

(b) Axial Vibration

Turning now to the question of axial vibration, it can be shown that the general matrix techniques already outlined can be adapted to the treatment of torsional and extensional vibrations. Taking the steady-state (sine and cosine) solution of the extensional wave equation, differentiating it once and multiplying by the cross-sectional area yields an expression for axial force. If this is taken together with the original solution for the displacement, the two equations can be written in a matrix form in which a column vector of two components (displacement and force) is related to a column vector composed of the two undetermined constants of the solution. Once again, by appropriate manipulation, this matrix equation can be rendered into a form which relates displacement and force at one point to corresponding conditions at another. The agent of this relation is a second order transfer matrix which expresses the dynamical properties (in extension) of the intervening length of the shaft.

If the torsional equation is treated in the same way, there results a method of transferring angular deflection and torsional moment from one point to another.

Discontinuities in extensional forces can arise at localized masses (e.g. the propeller) or stiffnesses (thrust bearing stiffness); discontinuities in torsional forces can arise at localized masses (again the propeller), while discontinuities in angular deflection occur at gears.

In a ship's propulsion system, the propeller represents a very important type of discontinuity. It is responsible for the principal gyroscopic coupling between vertical and horizontal flexural vibrations and it produces coupling between extensional and torsional vibrations. The mechanism by which this latter coupling is produced has already been mentioned in the discussion of propeller forces. Thus, torsional oscillations will result in harmonic variations of approach velocity of the propeller blade with attendant oscillations of the axial (thrust) component of the blade force, while axial oscillations correspond to harmonic gusts across the blade and result in variations of propeller torque. These coupling effects are generally quite weak and for this reason they have not been treated in any detail. (There are mechanical systems other than a propeller shaft in which coupling between torsional and extensional vibrations is significant. One such example is the crankshaft of a multi-cylinder engine in which, for certain configurations of the crank webs, there can be a substantial coupling action.)

The coupled torsional-extensional vibrations of the shaft system can be treated by combining the torsional and extensional matrix relations into a single fourth order matrix equation in much the same way that the two-plane transverse vibration expressions were combined. As before, the accumulation of an overall transfer matrix and the solution of the resulting simultaneous equations completes the solution of the boundary value problem.

A significant advantage of the techniques outlined lies in the fact that a fairly simple computer program can be written and applies equally well to the coupled transverse vibration problem and to the coupled torsion-extension problem. The only difference between the two lies in the individual terms of the component matrices.

The derivations of the above techniques are treated in more detail in Section II of this report and form the basis of a computer program written by the Staff of the David W. Taylor Model Basin.

SECTION II

1. FORCES DEVELOPED ON A PROPELLER WORKING IN AN IRREGULAR WAKE

(a) Dynamic Effects due to Wake Variation

Calculations of the thrust and torque experienced by a propeller operating in a variable wake are usually of a quasi-steady-state nature. Forces are computed for each angular position of the blade as if each blade element were operating in a steady stream whose velocity and angle of attack correspond to the local conditions in the wake. Since the fluid has appreciable inertia it may be expected that the circulation will not follow rapid variations in wake, consequently, there is good reason to question the accuracy of quasi-steady-state predictions of lift forces.

The methods developed here to treat dynamic effects can be described briefly as follows. If the wake is described in terms of a Fourier series, the first (constant) term of this series can be considered to represent the true steady-state velocity experienced by the blade. The other Fourier components represent harmonic oscillations in blade approach velocity and harmonic gusts in a direction normal to the blade. Thus, the dynamic effects of the wake can be treated by finding the oscillatory forces developed on a blade which experiences harmonic gusts parallel to, and normal to, the main stream. There are two other dynamic effects associated with blade forces, namely, those in which the blade velocity (rather than the stream velocity) contains harmonic components parallel to, and normal to, the main velocity. These are of importance in providing coupling between rotational and axial vibrations of the blades, and in providing damping of blade vibration.

(1) Effect of oscillations in stream velocity

Some attention was given to this problem by Von Karman and Burger[21] and a solution is given for the lift of a two dimensional lifting element starting from rest. The case of an airfoil subjected to a harmonic velocity superposed on the mean stream velocity was first considered by Isaacs.[17] Later, Greenberg[18] presented a simpler solution that agreed closely with Isaac's work. In this note, Greenberg gives the lift force as

$$\frac{P}{L_o} = (1 + \frac{\sigma^2}{2}F) + \sigma\left(\frac{k}{2} + G\right)\cos\omega t + \sigma(1+F)\sin\omega t - \frac{\sigma^2}{2}F\cos 2\omega t + \frac{\sigma^2 G}{2}\sin 2\omega t$$

when the approach velocity is

$$U = U_o\,(1 + \sigma\sin\omega t)$$

In these expressions

L_o = steady lift at a uniform stream velocity, U_o

P = lift force, positive upward

k = the 'reduced frequency' = $\dfrac{b\,\omega}{U_o}$

where $b = \dfrac{1}{2}$ chord width

ω = circular frequency

$$F = \frac{J_1 \, (J_1 + Y_o) + Y_1 \, (Y_1 - J_o)}{(J_1 + Y_o)^2 + (Y_1 - J_o)^2}$$

$$G = \frac{Y_1 \, Y_o + J_1 \, J_o}{(J_1 + Y_o)^2 + (Y_1 - J_o)^2}$$

The argument of the Bessel functions being the reduced frequency k, F (k) and G (k) are the "Theodorsen" functions.[22]

A plot of the coefficient of the first order sine and cosine terms of $\frac{P}{L_o}$ is given in Fig. (1). Since the second order harmonics have coefficients containing σ^2, they can be neglected on the grounds that σ is a small quantity. On the same basis the first term becomes unity, leaving the harmonic part of the response to be two terms in quadrature. This can be put in the alternative form of a single harmonic term which is out of phase with the oscillations in the main stream.

Since the constant terms from the Fourier analyses of the axial and tangential wakes can be combined to give L_o, and the harmonic components (axial and tangential) can be similarly combined to give various values of σ, all that is required is to calculate the steady force corresponding to L_o whereupon all the other (harmonic) contributions from variations in stream velocity can be calculated by the above expression.

(2) Effects of harmonic gusts normal to the stream

The treatment of this problem is to be found in standard texts on flutter, e.g. "Aeroelasticity"[19] or, "Introduction to the Study of Aircraft Vibration and Flutter".[23] The following equation is given for the lift force per unit length of an infinitely long airfoil:

$$P = 2 \pi \rho U_o b \; w_g \left\{ C(k) \; [J_o (k) - i J_1 (k)] + i J_1 (k) \right\} e^{i \omega t}$$

where, in addition to the quantities already defined, w_g is the amplitude of the gust velocity, $C(k) = F(k) + i\,G(k)$, and it is understood that the real part of the expression is taken.

This equation may be written in the form

$$P = 2 \pi \rho \bar{U}_o b w_g \; (M \cos \omega t + N \sin \omega t)$$

where M and N are functions of the reduced frequency, k.

Since $2 \pi \rho U_o 2 b \alpha$ is the lift L_o corresponding to a steady angle of attack, α, (measured from the "no-lift" attitude of the airfoil), we may write:

$$\frac{P}{L_o} = \frac{w_g}{U_o} \frac{1}{\alpha} (M \cos \omega t + N \sin \omega t)$$

Values of M and N are plotted in Fig. 2

Since the values of w_g/U_o can be found from the amplitudes of the Fourier components of the axial and tangential wake, the above formula yields the resulting oscillatory lift forces.

(3) Effects of blade oscillations normal to stream

It has been pointed out that blade oscillations parallel to, and normal to, the main stream will give rise to oscillatory blade forces. The former of these has apparently not been treated, but the latter is discussed by Bisplinghoff et al, [19] Page 272 and by Scanlan and Rosenbaum,[23] Page 395.

When certain conditions on the rigidity of the blade are met, the lift force is given by the expression

$$P = -\pi \rho b^2 (U_o \dot{\alpha} + \ddot{h} - ba \ddot{\alpha}) - 2\pi\rho U_o b C(k) [U_o \alpha + \dot{h} + b(\frac{1}{2} - a) \dot{\alpha}]$$

where P = lift force, positive upward

ρ = density of the fluid

$b = \frac{1}{2}$ chord width of the airfoil

h = vertical displacement, positive upward

$C(k)$ = Theodorsen's function $= F(k) + i\, G(k)$

$k = \frac{b\omega}{U_o}$ = the 'reduced frequency'

ω = circular frequency of oscillation

U_o = forward speed of the airfoil

α = inclination of blade to "no-lift" attitude

For a propeller blade which does not twist, α is constant and the above equation reduces to

$$P = -\pi \rho b^2 (\ddot{h}) - 2\pi\rho U_o^2 b C(k) [\alpha + \frac{\dot{h}}{U_o}]$$

In this equation the quantity $\pi \rho b^2 \ddot{h}$ represents the inertia of entrained fluid and is normally included in vibration calculations.

The quantity $2\pi\rho U^2 b C(k)$ in the second term might be expected to represent the steady lift on the section. It is not clear why this should contain

$C(k)$ where α is steady.

The quantity $2\pi\rho U_0 b \dot{h} C(k) = 2\pi\rho U_0 b \dot{h} [F(k) + i G(k)]$ represents forces proportioned to, and for $F(k)$, opposite in direction to, the velocity - hence it represents a damping term. The imaginary part of the expression represents a component of force which is proportional to the velocity $\dot{h}$ but is out of phase.

The Theodorsen functions $F(k)$ and $G(k)$ have been defined previously.

(b) Calculation of Forces and Moments including Dynamic Effects

Calculations of forces and moments generated by a propeller in an irregular wake have been carried out by several investigators. In 1935, Lewis[5] gave a method of calculating bearing forces arising from the propeller action. The David W. Taylor Model Basin has developed a quasi-steady-state procedure based on Burrill's "Method of Calculation of Marine Propeller Performance Characteristics"[1]. This method was used in 1955 by Noonan, Knopfle, and Feldman in their calculation of propeller shaft bending stresses in the USNS LT. JAMES E. ROBINSON.[24] Breslin pointed out that all of these methods neglected the effects of fluid inertia and, in 1958, Ritger and Breslin[2] considered these effects. Their report considers fluid inertia only with regard to the cross flow and computes the variable thrust and torque but not the bearing forces and moments.

The present work gives a detailed procedure for calculating the three components of variable force and the three components of variable moment (for each order of vibration) from an experimentally determined wake variation. The Theodorsen effects in both cross flow and variable stream flow are included, and the assumption is made that such effects will alter the variable lift forces in the propeller (modified as these are by induced flow, tip effects and centrifugal effects) in the same proportion that they modify the forces in an infinitely long airfoil.

The first step in the calculation is to make a Fourier analysis of the wake. In general, some interpolation of experimentally determined values will be required and this is most easily done by radial cross-plots at different angular positions. A typical wake survey using a fine interval of 15° is given in Fig. 3, and the curves of longitudinal and tangential wake given in Figs. 4 through 7 are based on this survey. The sign convention adopted is such that a tangential wake opposing the propeller rotation is considered positive.

When the wake has been determined by interpolation at the required positions the appropriate values are entered in the Harmonic Analyses Schedules and, by following the procedures detailed there, the harmonic content of the wake is determined. For single screw ships,wake determinations are usually made at angular intervals of 15° and for this scheme a 24-ordinate schedule is used. For multiple screw ships it is common to use a 22 1/2° angular interval and for this scheme a 16 ordinate schedule is used. Copies of these are displayed (along with instruction sheets) in Appendix A, while the numerical example presented in Appendix I

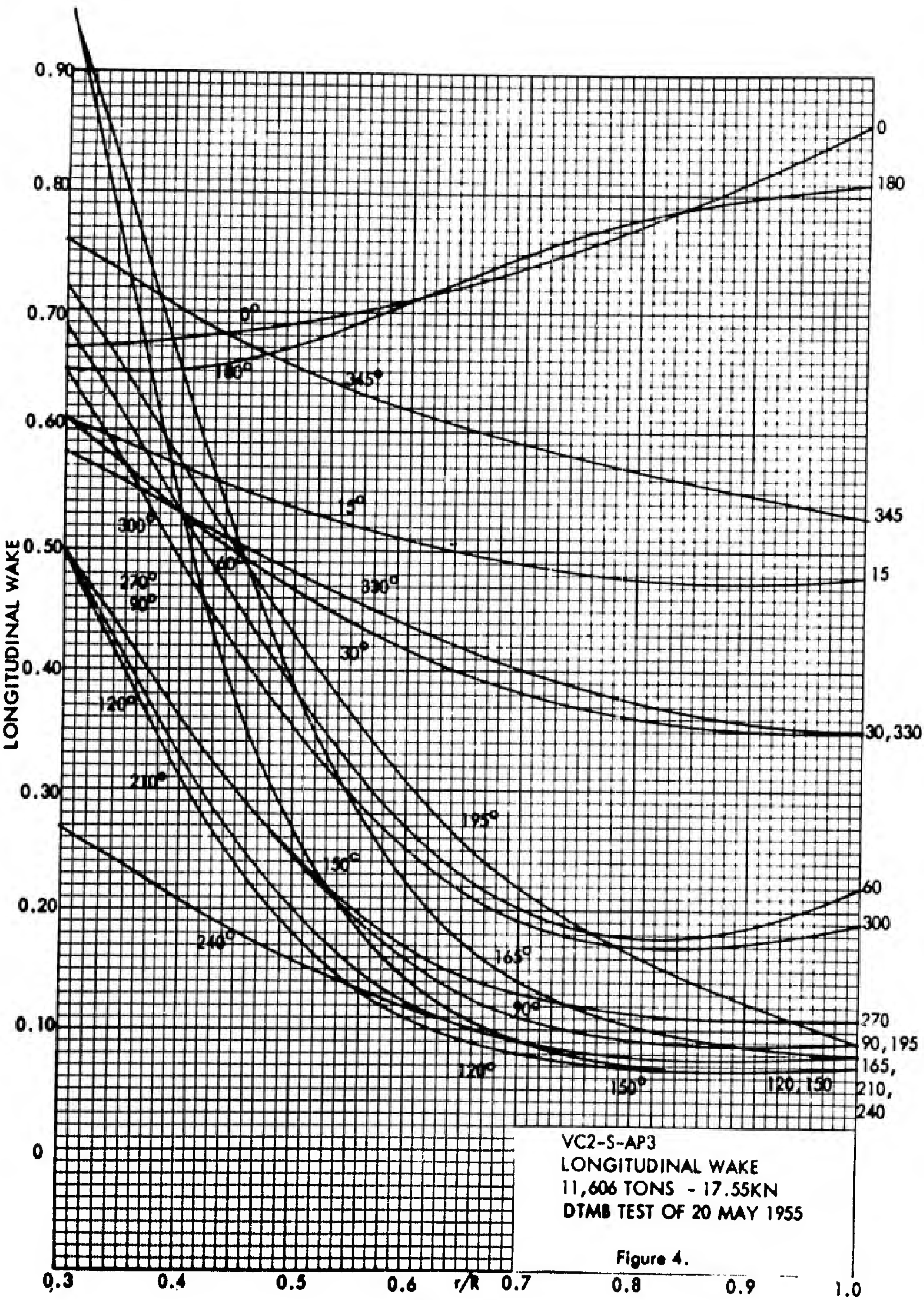

VC2-S-AP3
LONGITUDINAL WAKE
11,606 TONS - 17.55KN
DTMB TEST OF 20 MAY 1955

Figure 4.

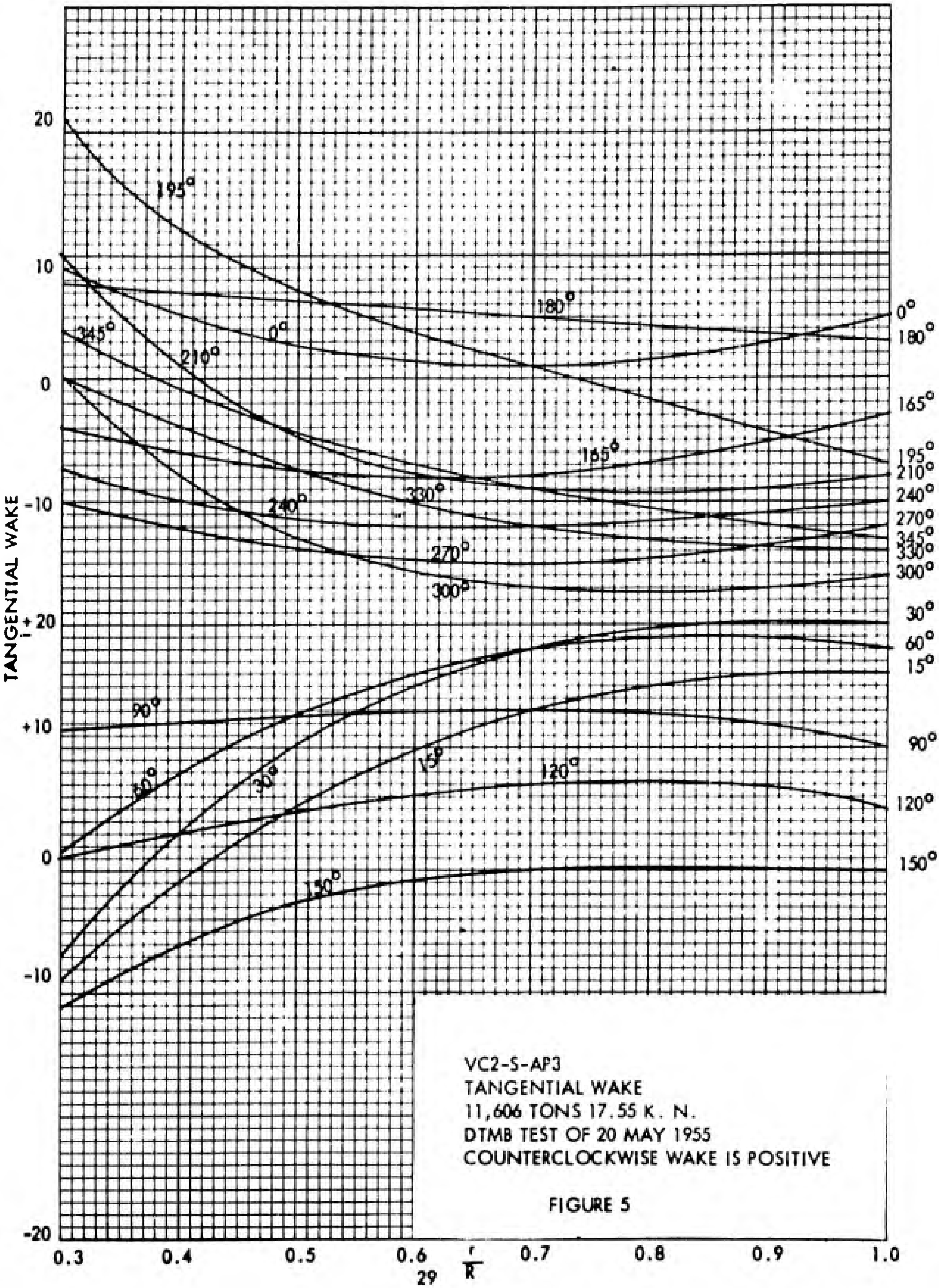

VC2-S-AP3
TANGENTIAL WAKE
11,606 TONS 17.55 K. N.
DTMB TEST OF 20 MAY 1955
COUNTERCLOCKWISE WAKE IS POSITIVE

FIGURE 5

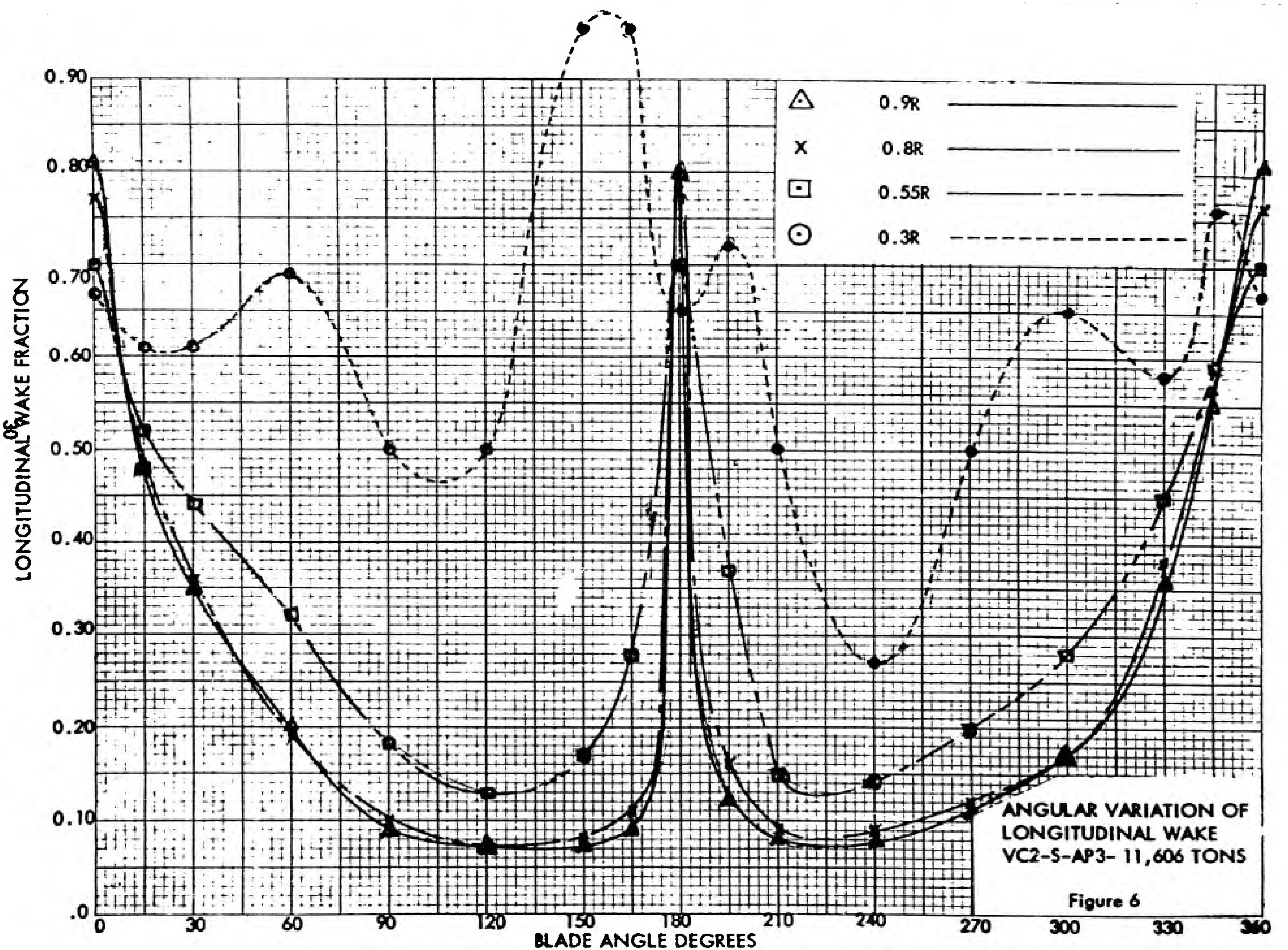

ANGULAR VARIATION OF LONGITUDINAL WAKE VC2-S-AP3- 11,606 TONS

Figure 6

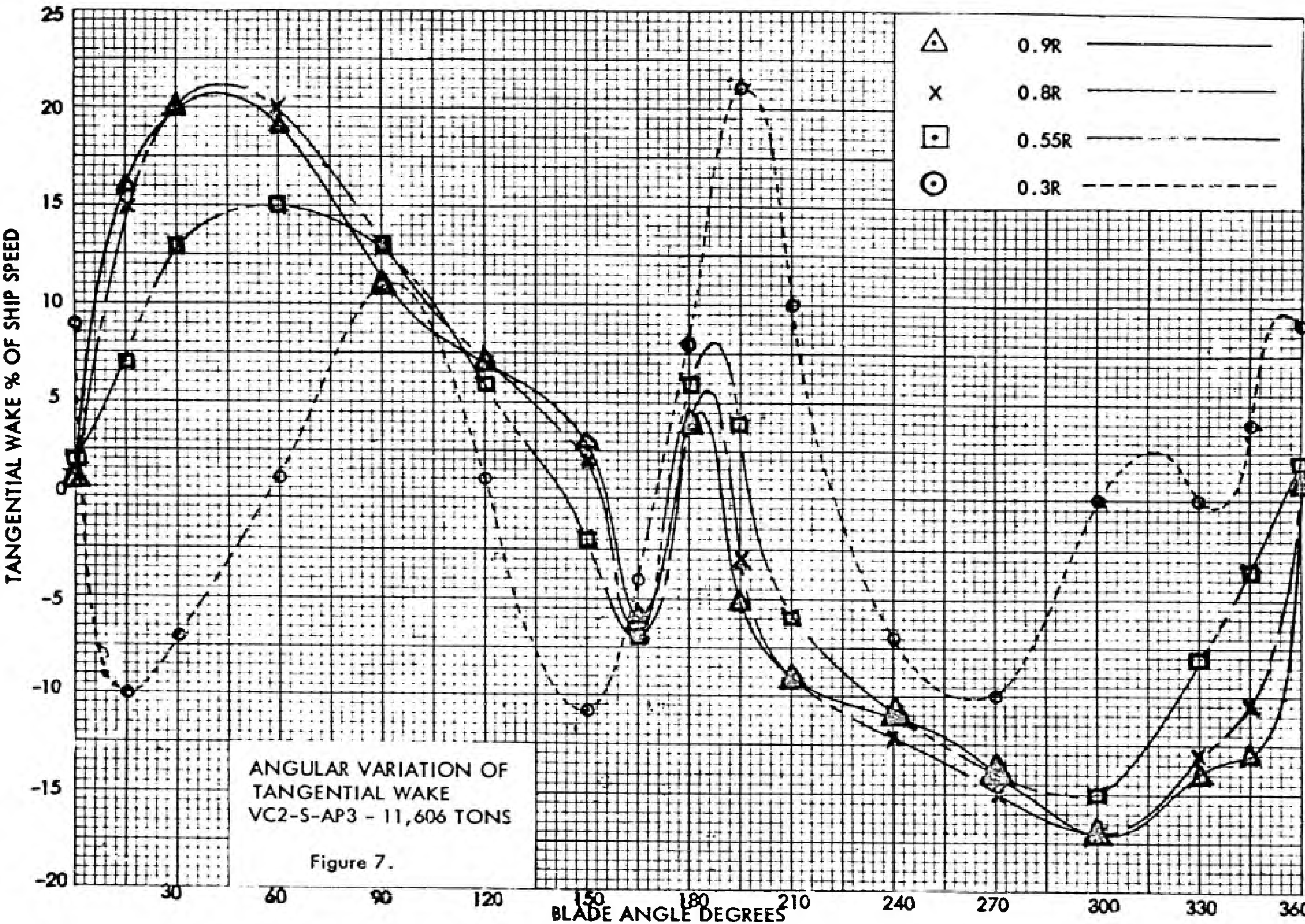

ANGULAR VARIATION OF TANGENTIAL WAKE VC2-S-AP3 - 11,606 TONS

Figure 7.

illustrates their use.

The second step involves the computation of the steady thrust and tangential forces resulting from the mean wake as given by the constant term of the harmonic analysis. This calculation is based on Burrill's[1] method and uses the schedules and instructions displayed in Appendix B. For the basis of the procedure and the many curves required in the calculation it is necessary to refer to Burrill's original paper.[1] For convenience, the calculation of forces per unit length of blade is carried out at 0.3R, 0.55R, 0.8R, and 0.9R, so that the harmonic analysis must be based on interpolated wake values corresponding to these radii. By integrating the thrust force and the moment of the tangential force along the blade it is possible to obtain a check with known propeller characteristics.

Turning to the third step, we now have available the harmonic analysis of the wake and the steady values of the forces resulting from the average wake. It is now necessary to convert the amplitudes of the harmonic components of the wake to equivalent gust and stream fluctuations so that these can be used with Figure 1 and Figure 2 to obtain the amplitudes of the oscillatory blade forces.

This conversion (and the calculation of the forces) is accomplished in a routine manner by use of the schedule and instructions displayed in Appendix C. However, a word of explanation of the form is desirable.

Using Burrill's nomenclature and referring to the sketch in Fig. 8, we

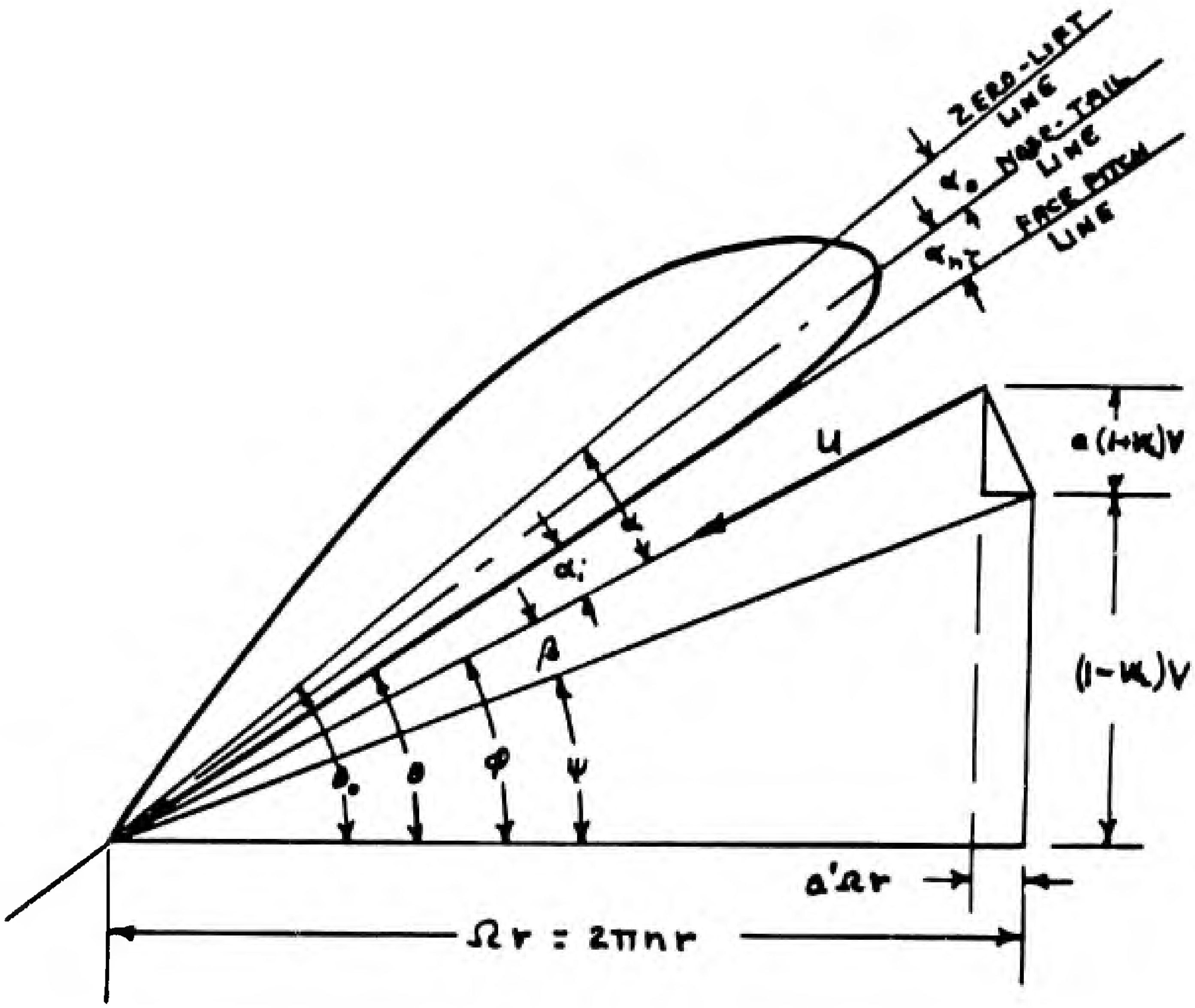

DIAGRAM OF ANGLES

Figure 8

may write

$$U^2 = [V(1-w_l)(1+a)]^2 + [(\Omega r + Vw_t)(1-a')]^2$$

$$\tan \phi = \frac{V(1-w_l)(1+a)}{(\Omega r + Vw_t)(1-a')}$$

Differentiating the former gives

$$2U \Delta U = 2[V(1-w_l)(1+a)]V(1+a)(-\Delta w_l) + 2[(\Omega r + Vw_t)(1-a')](1-a')V\Delta w_t$$

hence $$\frac{\Delta U}{U} = (\sin^2 \phi)\frac{(-\Delta w_l)}{(1-w_l)} + (\cos^2 \phi)\frac{(V\Delta w_t)}{(\Omega r + Vw_t)}$$

Differentiating the latter gives

$$\mathrm{Sec}^2 \phi \Delta \phi = \frac{(\Omega r + Vw_t)(1-a')V(1+a)(-w_l) - V(1-w_l)(1+a)(1-a')V \quad \Delta w_t}{[(\Omega r + Vw_t)(1-a')]^2}$$

$$\Delta \phi = \cos^2 \phi \left[(\tan \phi)\frac{(-w_l)}{(1-w_l)} - (\tan \phi)\frac{(V\Delta w_t)}{(\Omega r + Vw_t)}\right.$$

$$= \sin \phi \cos \phi \left[\frac{-w_l}{1-w_l} - \frac{V\Delta w_t}{\Omega r + Vw_t}\right]$$

Now, since $\Delta a = -\Delta \phi$ and Vw_t is small

$$\Delta a = \sin \phi \cos \phi \left[\frac{w_l}{1-w_l} + \frac{V\Delta w_t}{\Omega r}\right]$$

For the nth harmonic, $\Delta w_l = w_{ln}$, $\Delta w_t = w_{tn}$, $\Delta U = U_n$ and $\Delta a = a_n$

where w_{ln} and w_{tn} are complex numbers. Hence

$$\frac{U_n}{U} = -\sin^2\phi \quad \frac{w_{ln}}{1 - w_{lo}} \quad + \cos^2\phi \quad \frac{Vw_{tn}}{\Omega r}$$

and $$\alpha_n = \sin\phi\cos\phi\left[\frac{w_{ln}}{1 - w_{lo}} + \frac{V}{\Omega r} \quad w_{tn}\right]$$

These two effects together give a resultant lift force

$$P = L_o \quad \left[(M+iN) \quad \frac{\alpha_n}{\alpha} \quad + (B+iA) \quad \frac{U_n}{U}\right]$$

Hence $$G_n = G_o \left[(M+iN) \quad \frac{\alpha_n}{\alpha} \quad + (B+iA) \quad \frac{U_n}{U}\right]$$

and $$F_n = F_o \left[(M+iN) \quad \frac{\alpha_n}{\alpha} \quad + (B+iA) \quad \frac{U_n}{U}\right]$$

Where G_n is the n^{th} harmonic component of the tangential force and F_n is the n^{th} harmonic component of the thrust force.

At the conclusion of the calculation form, the values of G_n and F_n and their moments are multiplied by integrating factors and summed to obtain the total thrust and tangential moments on the blade. The integrating factors contain a "Simpson's Rule" multiplier and the radial location of the section.

Thus, the integrating factor for 0.3R is:

$$\frac{(0.25 \times R = \text{the interval})}{3} \quad \times (1 = \text{Simpson's multiplier}) = \frac{1}{12} \; R = \frac{1}{24} \quad D$$

Likewise the integrating factor for 0.8R is:

$$\frac{0.25R}{3} \times 1 + \frac{0.1R}{3} \times 1 = \left(\frac{1}{12} + \frac{1}{30}\right) \; R = \frac{7}{60} \; R = \frac{7}{120} \quad D$$

It should be noted that it would be possible to simplify this form slightly by not finding the values of the force per unit radius. However, these values give an indication of the accuracy of the calculations and are used in computations of the hull pressure forces.

The fourth step, namely, the summation of the force and moment contributions from all the blades, is carried out using the form and instructions in the remainder of this Appendix C. Again, a word of explanation is desirable.

The net harmonic thrust and torque are simply the vector sums of the harmonic components for each blade. If all the blades are identical and therefore produce identical components displaced from one another in space, then, for all orders except multiples of the number of blades, this vector sum is zero. For orders that are multiples of the number of blades the sum is non-zero.

The vertical and horizontal forces and moments require further consideration. For example, the vertical force from one blade is G sin θ where θ is the angle of the blade to the vertical. G is expressed as the real part of the series.

$$G = A_o + (A_1+B_1 i)\, e^{i\theta} + (A_2 + B_2 i)\, e^{2i\theta} + \cdots + (A_n + B_n i)\, e^{in\theta} + \ldots\ldots$$

hence, expressing sin θ as $\dfrac{e^{i\theta} - e^{-i\theta}}{2i}$, the n^{th} term of G sin θ

is $\quad \mathrm{Re}\, \dfrac{(A_n + B_n i)}{2i}\, e^{i(n+1)\theta} - \mathrm{Re}\, \dfrac{(A_n + B_n i)}{2i}\, e^{i(n-1)\theta}$

When these quantities are summed over all the blades of the propeller there is a vector cancellation for all orders except when (n+1) and(n-1) are multiples of the number of blades. Hence if there are s blades the value of the s^{th} order is

$$\mathrm{Re}\left[\frac{A_{s-1}+B_{s-1}i}{2i} - \frac{A_{s+1}+B_{s+1}i}{2i}\right]e^{is\theta}$$

Similar reasoning applies to the other transverse forces and moments.

(c) Numerical Example

To illustrate the use of the computational scheme that has been described, the following example has been chosen.

In May 1943, the David W. Taylor Model Basin made a series of tests on a model of a ship designated VC2-S-AP3. The ship has a single four-bladed screw of 20.5 ft. diameter and a very complete wake survey was made. The result of this survey at 11,600 tons is illustrated in Fig. 3, and all the computations made here are based on this wake description.

The first step in the calculation is to make cross-plots for interpolating the wake survey as described earlier. Figures 4 and 5 illustrate these while Figures 6 and 7 show the interpolated values plotted against angular position.

The second step - the harmonic analysis of the wake - makes use of the tabular procedure described in Appendix A and results in Tables I-1-4 describing the longitudinal wake, and Tables I-5-8describing the tangential wake. The radial locations chosen are 0.3R, 0.55R, 0.8R, and 0.9R.

The third step is the determination of the average thrust and torque intensity at each calculation radius and makes use of the calculation forms described in Appendix B. Tables I-9-16 demonstrate the procedure applied to the wake and propeller in question. It is advisable at this point to integrate these force intensities over the propeller blade in order to check with the (generally known) steady forces developed by the propeller. This is done in Table I-17.

The fourth step is the computation of dynamic forces and moments from the now known average values and the harmonic components of the wake. Use of the methods detailed in Appendix C results in Tables I-18-20 for the 4th order forces and moments. The summary of all the results finally appears in Table I-21.

The 4th order harmonic thrust, 35,048 pounds, is about 29% of the average thrust. The 4th order harmonic torque, 93,051 pounds feet, is about 20% of the average torque. The 4th order vertical harmonic force of 1,327 pounds and the 4th order horizontal harmonic force of 1,149 pounds are about 1% of the average thrust. The 4th order moments of 23,840 pounds feet about the horizontal axis and 28,286 pounds feet about the vertical axis are about 5% and 6% of the average torque.

The value of the harmonic thrust is about twice the value computed by Ritger and Breslin[2] but is about as much lower than the quasi-steady state values given by Ritger and Breslin as might be expected from the Theodorsen parameters. The values of harmonic thrust and harmonic torque are about twice those that are generally assumed in vibration calculations. It is believed that the large values of harmonic thrust and torque occur because the averaging effect of propeller blade width on the wake is neglected. One way to treat this would be to consider the average wake over the width of the propeller blade at each angular position. It might be, however, that the variations in lift would be more accurately represented by wake variations at the leading edge of the propeller rather than at the center of the chord. In either case, the harmonic thrust and torques would be reduced.

2. PRESSURES ON THE HULL DUE TO PROPELLER ACTION

(a) Pressure Field due to a Rotating Propeller

(1) Comparison of Breslin's approach with that of Gutin

Breslin treats the propeller as a rotating line vortex which moves axially, shedding helical line vortices from its ends. Taking the pressure induced at a point by an elementary length of these vortices, he then integrates over the complete length of the vortex line to find the total field at the point. Gutin, on the other hand, considers that a point on a propeller disc receives a pulse of force as the blade passes. This pulse can be considered as the cumulative effect of a number of harmonic force components, so that the pressure at some distant point is the cumulative effect of the radiated pressure from all of these harmonically varying forces.

It is interesting to compare the results of these two approaches, based as they are on different approximations to the solution of the flow equation. Breslin solves the steady-state flow problem neglecting all wave effects and obtains pressures from changes in flow velocities. This is justifiable since the frequencies of the excitation are low and because only those pressures in the vicinity of the propeller are of interest. In contrast, Gutin (who was concerned with far-field acoustic radiation from aircraft propellers) neglects the steady-state flow and deals only with wave effects.

To compare more clearly these two approaches it is desirable to consider the complete equations for irrotational flow and to explore the nature of the assumptions in both cases. The difference in the results yielded by both methods is then most easily demonstrated by considering the case of the pressure generated on the ground by a flying aircraft.

The equations are:

Continuity: $\frac{1}{c^2}\frac{\partial p}{\partial t} + \Delta \phi \; \frac{+ w \cdot \text{grad } p}{c^2} = 0$

Generalized Bernoulli equation $\frac{\partial \phi}{\partial t} + \frac{w^2}{2} + p - U = f(t)$

(See Prandtl-Tietgens",[25] p. 129)

In this, c is the speed of sour i in the fluid

w is the fluid velocity vector

ϕ is the potential function of the velocity field

p is the pressure

U is the force function of the body forces. (This will be omitted since the only pressures of interest are those that are changes from the average.)

If the coordinate axes are taken to rotate with the propeller and the fluid is incompressible then, since $c \rightarrow \infty$, the equations reduce to:

$$\Delta \phi = 0 \text{ and } \frac{w^2}{2} + p = f(t)$$

These are the equations on which Breslin's solution is based.

If the fluid is considered to be compressible but w so small that $\frac{w \cdot \text{grad } p}{c^2}$ and $\frac{w^2}{c^2}$ are negligible, then the equations become:

$$\frac{1}{c^2} \cdot \frac{\partial p}{\partial t} + \Delta \Phi = 0 \quad \text{and} \quad \frac{\partial \Phi}{\partial t} + p = f(t)$$

and these are the equations on which Gutin's work is based.

Turning now to the application of these two methods to the prediction of the pressure produced by a force located above a plane, the 'incompressible' solution (using the same basis as Breslin's work) is given in Prandtl-Tietgens[26] under the heading "Transfer of Airplane Weight to the Surface of the Earth". p. 186 This gives a pressure $p = \frac{Lh}{2\pi s^3}$ where L is the total force, h is the vertical distance from the earth to the aircraft and s is the distance from the aircraft to the point at which the pressure is measured.

Using (as Gutin did) the potential function developed in Lamb's "Hydrodynamics"[20] for a harmonically varying force in free space, we may write

$$p = -\frac{L}{4\pi} \frac{\partial}{\partial x} \frac{e^{i\omega(t-s/c)}}{S}$$

In this, $Le^{i\omega t}$ is the force acting at a point and the calculated pressure exists at a point whose coordinates are x, y with respect to the 'force' point. Obviously,

$$S = \sqrt{x^2 + y^2}$$

Carrying out the differentiation and noting that x = h the expression for pressure becomes

$$\left(\frac{Lh}{4\pi s^3} \sqrt{1 + \frac{\omega^2 s^2}{c^2}} \right) e^{i\omega \left(t - s/c + \tan^{-1} \omega s/c\right)}$$

Taking the modulus of this expression and doubling to account for the presence of the rigid boundary, we have $p = \frac{Lh}{2\pi s^3} \sqrt{1 + \frac{\omega^2 s^2}{c^2}}$. From this it can be seen that for low frequencies, the value of the pressure approaches that given by the incompressible solution.

Some important features of the pressure generated by a harmonic force can be recognized in the above example. For example, it can be seen that the pressure falls off with at least the square of the distance from the source, consequently it is important that the forces on the propeller-tip adjacent to the hull surface be accurately represented. Unfortunately this is the most difficult part of the propeller to represent well and the most poorly defined of the wake regions.

(2) Calculation on basis of moving force

Since a previous part of this report has shown how the forces on an element of the propeller blade can be calculated, it is now possible to calculate the free-field pressure resulting from such elementary forces as they move with the blade. Also, since our discussion involves distances which are quite small compared with the wavelengths of sound (at the frequencies corresponding to ship propeller speeds), it is possible to ignore the wave character of the pressure field and write the pressure in the form $P = -\frac{1}{4\pi}\left(F_x \frac{\partial}{\partial x} + F_y \frac{\partial}{\partial y} + F_z \frac{\partial}{\partial z}\right)\frac{1}{S}$

where F_x, F_y, F_z are the components of the force and S is the distance from the force to the point at which the pressure is calculated.

If the coordinate axes are chosen such that x lies along the propeller axis and is positive in the direction of forward motion, y is vertical and positive upwards, then z will be positive to starboard for a right handed system.

Let a propeller blade element rotate in the plane x = d and let the angular position of a blade be θ with respect to the vertical, then the coordinates of the blade element at radius r of the propeller are

$$x_1 = d$$

$$y_1 = r \cos\theta$$

$$z_1 = r \sin\theta$$

The forces acting on an element are an axial force F and a tangential force G, hence the cartesian force components are

$$F_x = F$$

$$F_y = -G \sin\theta$$

$$F_z = G \cos\theta$$

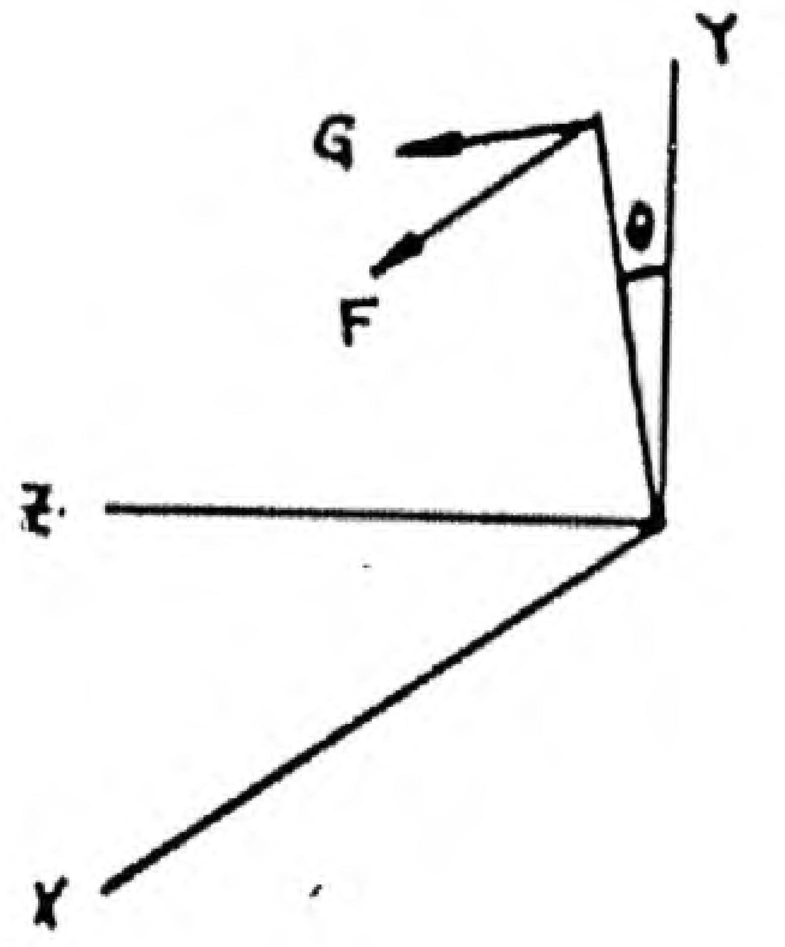

The free-field pressure which results from the x-component is

$$P_x = \frac{F}{4\pi} \frac{x-d}{\left[(x-d)^2 + (y - r\cos\theta)^2 + (z - r\sin\theta)^2 \right]^{3/2}}$$

$$= \frac{F}{4\pi R^2} \frac{(x-d)}{R} \left[\left(\frac{x-d}{R}\right)^2 + \left(\frac{y - r\cos\theta}{R}\right)^2 + \left(\frac{z - r\sin\theta}{R}\right)^2 \right]^{-3/2}$$

where R is the propeller radius.

Let $\left(\frac{x-d}{R}\right)^2 + \left(\frac{y}{R}\right)^2 + \left(\frac{z}{R}\right)^2 + \left(\frac{r}{R}\right)^2 = \nu^2$

$$\frac{yr}{\nu^2 R^2} = \xi \qquad \frac{zr}{\nu^2 R^2} = \zeta$$

Then $P_x = \frac{F}{4\pi R^2} \frac{(x-d)}{R} \nu^{-3} (1 - 2\xi\cos\theta - 2\zeta\sin\theta)^{-3/2}$

For sufficiently large values of y and z, ξ and ζ will be small enough to make the sum of the harmonic terms less than unity and the above expression can be expanded binomially, giving

$$P_x = \frac{F}{4\pi R^2} \frac{(x-d)}{R} \nu^{-3} \sum_n \left[A_n(\xi,\zeta)\cos n\theta + B_n(\xi,\zeta)\sin n\theta \right]$$

The coefficients of the Fourier series are:

$$A_o = \frac{1}{2}\left[1 + \frac{3.5}{2.4}(2\xi^2 + 2\zeta^2) + \frac{3.5.7.9}{2.4.6.8}(6\xi^4 - 12\xi^2\zeta^2 + 6\zeta^4) + \cdots\cdots \right]$$

$$A_1 = \frac{1}{2}\left[\frac{3}{2}\xi + \frac{3.5.7}{2.4.6}(3\xi^3 + 3\xi\zeta^2) + \cdots\cdots \right]$$

$$A_2 = \frac{1}{2}\left[\frac{3.5}{2.4}(\xi^2 - \zeta^2) + \frac{3.5.7.9}{2.4.6.8}(4\xi^4 - 4\zeta^4) + \cdots\cdots \right]$$

$$A_3 = \frac{1}{2}\left[\frac{3.5.7}{2.4.6}\left(\xi^3 - 3\xi\zeta^2\right) + \text{-----}\right]$$

$$A_4 = \frac{1}{2}\left[\frac{3.5.7.9}{2.4.6.8}\left(\xi^4 - 6\xi^2\zeta^2 + \zeta^4\right) + \text{-----}\right]$$

$$A_5 = \frac{1}{2}\left[\frac{3.5.7.9.11}{2.4.6.8.10}\left(\xi^5 - 10\xi^3\zeta^2 + 5\xi\zeta^4\right) + \text{-----}\right]$$

etc.

and

$$B_1 = \frac{1}{2}\left[-\frac{3}{2}\zeta - \frac{3.5.7.}{2.4.6}\left(3\xi^2\zeta + 3\zeta^3\right) + \text{-----}\right]$$

$$B_2 = \frac{1}{2}\left[\frac{3.5}{2.4}(-2\xi\zeta) + \frac{3.5.7.9}{2.4.6.8}\left(-8\xi^3\zeta - 8\xi\zeta^3\right) + \text{-----}\right]$$

$$B_3 = \frac{1}{2}\left[\frac{3.5.7}{2.4.6.}\left(-3\xi^2\zeta + \zeta^3\right) + \text{------}\right]$$

$$B_4 = \frac{1}{2}\left[\frac{3.5.7.9}{2.4.6.8}\left(-4\xi^3\zeta + 4\xi\zeta^3\right) + \text{----}\right]$$

$$B_5 = \frac{1}{2}\left[\frac{3.5.7.9.11}{2.4.5.8.10}\left(-5\xi^4\zeta + 10\xi^2\zeta^3 - \zeta^5\right) + \text{------}\right]$$

etc.

The pressure resulting from the y component of force is

$$P_y = -\frac{G\sin\theta}{4\pi}\ \frac{(y - r\cos\theta)}{\left[(x-d)^2 + (y - r\cos\theta)^2 + (z - r\sin\theta)^2\right]^{3/2}}$$

and that from the z component is

$$P_z = \frac{G\cos\theta}{4\pi}\ \frac{(z - r\sin\theta)}{\left[(x-d)^2 + (y - r\cos\theta)^2 + (z - r\sin\theta)^2\right]^{3/2}}$$

adding these two scalar quantities gives

$$\frac{G}{4\pi R^2 \nu^3} \quad \frac{(-y\sin\theta + z\cos\theta)}{R} \,(1 - 2\xi\cos\theta - 2\zeta\sin\theta)^{-3/2}$$

$$= \frac{G}{4\pi R^2} \quad \frac{R}{\nu r} \,(-\xi\sin\theta + \zeta\cos\theta)\,(1 - 2\xi\cos\theta - 2\zeta\sin\theta)^{-3/2}$$

Once again expanding binomially this can be written

$$\frac{G}{4\pi R^2} \quad \frac{R}{\nu r} \sum_n \left[A_n'(\xi,\zeta)\cos n\theta + B_n'(\xi,\zeta)\sin n\theta\right]$$

where $A_o' = 0$

$$A_1' = \left[\zeta + \frac{3.5}{2.4}(\xi^2\zeta + \zeta^3) + \frac{3.5.7.9}{2.4.6.8}(-20\xi^2\zeta^3 + 2\xi^4\zeta + 2\zeta^5) + ---\right]$$

$$A_2' = \left[3\xi\zeta + \frac{3.5.7}{2.4.6}(4\xi^3\zeta + 4\xi\zeta^3) + ----\right]$$

$$A_3' = \left[\frac{3.5}{2.4}(3\xi^2\zeta - \zeta^3) + \frac{3.5.7.9}{2.4.6.8}(9\xi^4\zeta + 6\xi^2\zeta^3 - 3\zeta^5) + ----\right]$$

$$A_4' = \left[\frac{3.5.7}{2.4.6}(4\xi^3\zeta - 4\xi\zeta^3) + -----\right]$$

$$A_5' = \left[\frac{3.5.7.9}{2.4.6.8}(5\xi^4\zeta - 10\xi^2\zeta^3 + \zeta^5) + -----\right]$$

etc.

and $$B_1' = \left[\xi + \frac{3.5}{2.4}(\xi^3 + \xi\zeta^2) + \frac{3.5.7.9}{2.4.6.8}(2\xi^5 - 20\xi^3\zeta^2 + 2\xi\zeta^4) + ---\right]$$

$$B_2' = \left[\frac{3}{2}(\xi^2 - \zeta^2) + \frac{3.5.7}{2.4.6}(2\xi^4 - 2\zeta^4) + ----\right]$$

$$B_3' = \left[\frac{3.5}{2.4}(\xi^3 - 3\xi\zeta^2) + \frac{3.5.7.9}{2.4.6.8}(3\xi^5 - 6\xi^3\zeta^2 + 9\xi\zeta^4) + ----\right]$$

$$B_4' = \left[\frac{3.5.7}{2.4.6}(\xi^4 - 6\xi^2\zeta^2 + \zeta^4) + -----\right]$$

$$B_5' = \left[\frac{3.5.7.9}{2.4.6.8}(\xi^5 - 10\xi^3\zeta^2 + 5\xi\zeta^4) + -----\right]$$

etc.

The above expressions give the free-field pressure at some point in terms of the angular position θ of the blade - which, for a propeller rotating at constant speed, represents the pressure as a function of time. Since the blade forces F and G are also known as functions of angle (or time), finding the net pressure at a point requires the formation of the product of the above Fourier series with the Fourier series representing the blade loads.

There is an alternative method of computing free-field pressures which might be somewhat easier to apply. In this approach, the blade forces would be computed for each radial section at a number of different angular positions in the vicinity of the point at which the pressure is to be found.

Summing the pressure contributions from all blade elements for each angular position of the blade in turn will then give a description of the variation in pressure as the blade passes. If the process is carried out for a number of angular positions around the propeller disc, the total effect of a number of blades can be found by superposition.

The decision as to which of the above methods is the more practical will have to be based on trials of each on an actual case.

In the preceding discussions it is assumed that the forces on a blade element can be considered to act at a point in the element. An improvement on this assumption would be to consider the blade element forces to have a uniform chordwise distribution and to act on a line which, due to the pitch of the blade, is skewed with respect to the shaft axis. The effects of pitch and of lift distribution are considered in Appendix D.

(b) Pressures in a Field Containing a Boundary

Since the basic problem in hull vibration is the estimation of pressure on the hull surface it is necessary to find how the presence of such a surface affects the free-field pressure.

The method of images can be used to show that the existence of a rigid plane boundary effectively doubles the free-field pressure at the location of the boundary. This will only be true so long as the presence of the boundary does not materially alter the operation of the propeller.

If two identical propellers operate with opposite senses of rotation, and, if they are sufficiently far apart that the flow from one does not materially affect the operation of the other, then there is no flow across an infinite plane located midway between the two propellers. Consequently, this plane can be made a rigid boundary. Since the pressure at this plane is the sum of the pressures from the propellers it is twice the pressure generated in a free-field by one propeller.

The image method does not require that the 'mirror' plane be parallel to the axis of the propeller but it does require the plane to be of infinite extent. In the case of a multi-screw ship it is probably acceptable to represent the hull by a plane surface, however, many of the more serious ship vibration problems occur where the reacting surfaces are not continuous flat surfaces. It is important to know whether or not it is possible to obtain reliable estimates of pressures on such surfaces as bossings, skegs, and rudders in terms of free-field pressures. Regier and Hubbard[27] made free-field measurements and measurements on plane and cylindrical surfaces near the tips of a rotating propeller. In general, these data seem to show that pressures on the cylindrical surface are 1-1/2 times the free-field values. The tests were carried out using a cylinder whose diameter was equal to that of the propeller and a tip clearance of approximately $\frac{1}{12}$ of the propeller diameter. Measurements on a flat plane gave the expected value of twice the free-field pressure.

(1) A new generalized modal technique

When a non-planar surface is introduced into the pressure field, matters become quite complicated; the method of images becomes of limited value and can only be used with success in a restricted class of problems. If the bounding surface completely encloses the fluid and has a geometry that lends itself to treatment by one of the standard co-ordinate systems, problems of elastic wave action within the fluid can be treated in terms of the 'normal modes' which can exist in the space. These modes are discrete and each mode has an associated characteristic or 'natural' frequency. However, when the surface does not completely enclose the fluid, i. e. the field is only partially bounded, modes and frequencies are no longer discrete but have a continuous spectrum.

Dr. O. K. Mawardi and Mr. M. Yildiz of CONESCO have extended the modal technique to the case of a partially bounded three-dimensional space and have solved the specific problem of the diffraction of elastic waves by a wedge shaped surface. The wave source considered was an oscillating potential dipole which represents a fluctuating force (see Lamb's "Hydrodynamics.")[20]

The development of this technique is quite lengthy and is given in detail in Appendix E.

(2) Pressures on a wedge shaped boundary

The analysis described in Appendix E leads to an expression for the pressure amplitude in the space exterior to a wedge shaped boundary and is best expressed in the form of a dimensionless ratio μ. This function is the ratio of the pressure around the wedge to the free-field pressure that would exist if the wedge were absent; it takes the form:

$$\mu = \frac{2\pi}{2\pi - \beta} \; \frac{(ikR_w - 1)}{(ikR_f - 1)} \left(\frac{R_f}{R_w}\right)^3 e^{ik(R_w - R_f)} \left\{ \left[r' \cos\theta' - r\cos\theta \right] \cos\theta^* \right.$$

$$+ \left[r' \sin\theta' - r\sin\theta \cos\frac{\pi\phi}{2\pi-\beta} \cos\frac{\pi\phi'}{2\pi-\beta} \right] \cos(\phi^* - \phi') \sin\theta^*$$

$$\left. + \frac{\pi}{2\pi-\beta} \; r\sin\theta\sin\theta' \cos\frac{\pi\phi}{2\pi-\beta} \sin\frac{\pi\phi'}{2\pi-\beta} \; \sin\theta^* \sin(\phi^* - \phi') \right\}$$

$$\left\{ \left[r'\cos\theta' - r\cos\theta \right] \cos\theta^* + \left[r'\sin\theta' - r\sin\theta\cos(\phi - \phi') \right] \cos(\phi^* - \phi') \right.$$

$$\left. \sin\theta^* - r\sin\theta\sin\theta' \sin(\phi - \phi') \sin(\phi^* - \phi') \sin\theta^* \right\}^{-1}$$

$$\text{where } R_w = \left[r^2 + r'^2 - 2rr' \left(\cos\theta\cos\theta' + \sin\theta\sin\theta' \cos\frac{\pi\phi}{2\pi-\beta} \cos\frac{\pi\phi'}{2\pi-\beta}\right) \right]^{1/2}$$

$$R_f = \left[r^2 + r'^2 - 2rr' \left(\cos\theta\cos\theta' + \sin\theta\sin\theta'\cos(\phi - \phi')\right) \right]^{1/2}$$

where: β ; r, θ, ϕ ; r', θ', ϕ' ; θ^*, ϕ^* are defined in Figure 9

$k = \frac{\omega}{c}$

ω = radian frequency of the excitation

c = speed of sound in the fluid

A graph showing the value of μ for a special orientation and location of a dipole excitation is given in Figure 10.

(c) Calculation of Pressures on a Rigid Plane Surface

The calculation methods based on a moving force can be used to find the pressures developed on a plane surface in the neighborhood of the propeller. While this may not satisfactorily represent a ship's hull in the region around the propeller, the results give some useful insights into the nature of pressure distributions that can be expected, and allow some inferences to be drawn as to the effects of clearances.

The method of calculation is demonstrated in the example below which

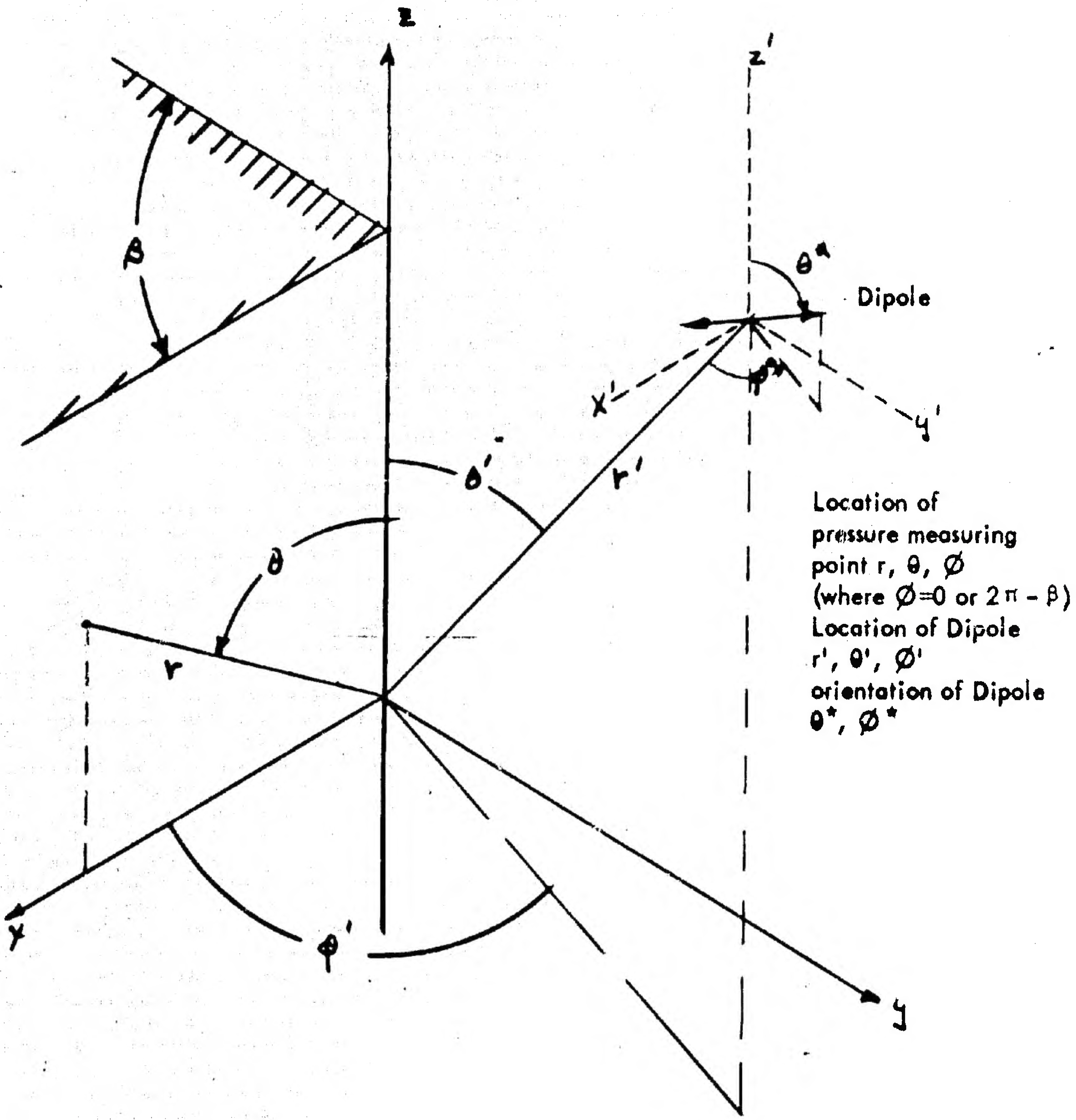

Coordinates in Study of Pressures
on a Wedge

Fig. 9

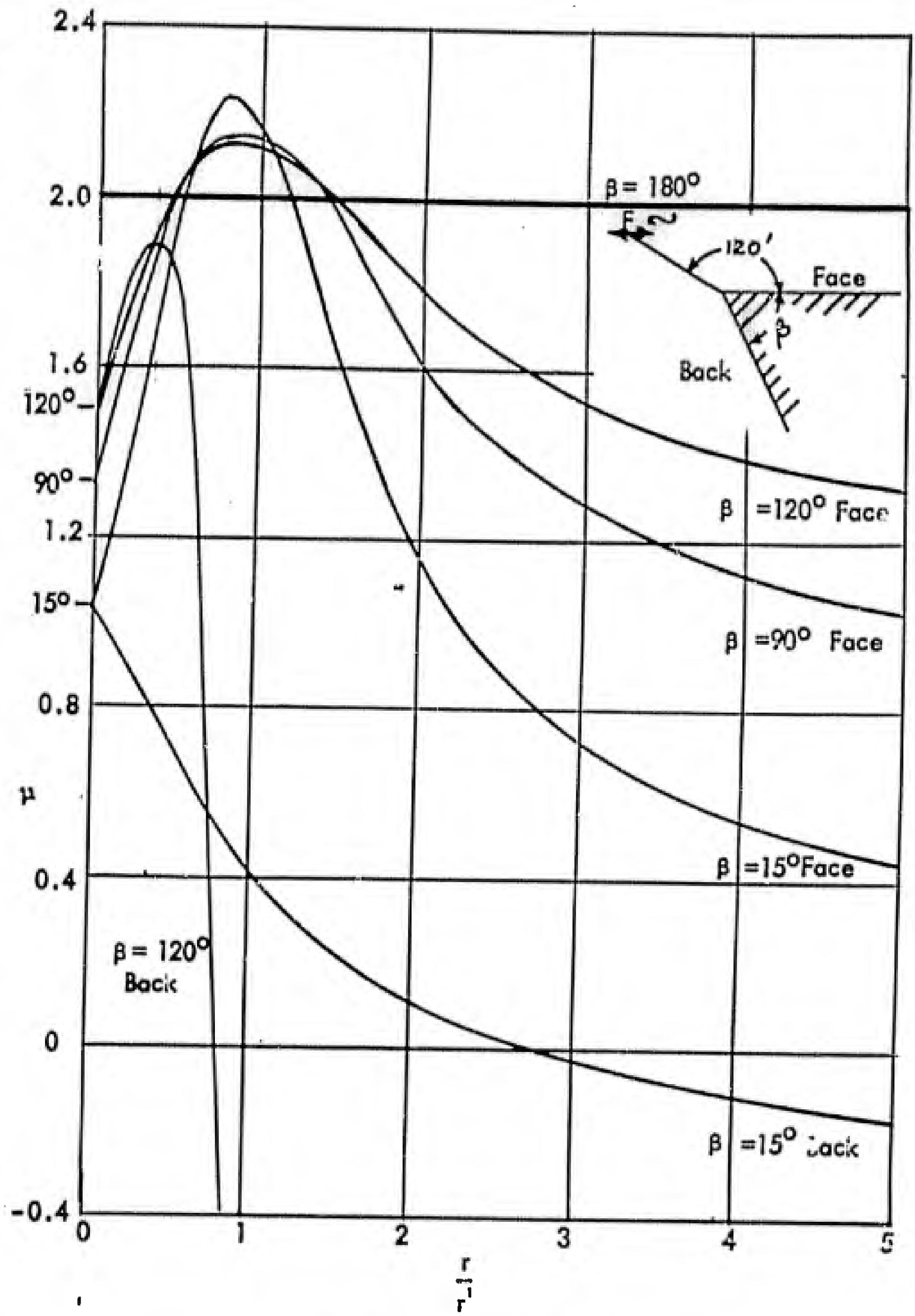

Fig. 10 Pressures on Wedges Caused by a Harmonic Force

considers a propeller working with a tip clearance of 0.2D. The values used for G and F are those obtained from the VC2 steady-state calculations made in Appendix I of this report.

Consider first the pressures along a line formed by the intersection of a plane containing the propeller disc and the plane surface lying parallel with the propeller axis.

Recapitulating;

The pressure due to thrust forces $P_F = \frac{F}{4\pi R^2} \cdot \frac{a-d}{R} \cdot \frac{1}{\nu^3}\left[1-2\xi\cos\theta - 2\zeta\sin\theta\right]^{-3/2}$

The pressure due to tangential forces $P_G = \frac{G}{4\pi R^2}(-\xi\sin\theta + \zeta\cos\theta)\left[1-2\xi\cos\theta - 2\zeta\sin\theta\right]^{-3/2}$

$$\text{where } \nu^2 = \left(\frac{a-d}{R}\right)^2 + \left(\frac{b}{R}\right)^2 + \left(\frac{c}{R}\right)^2 + \left(\frac{r}{R}\right)^2$$

$$\xi = \frac{br}{\nu^2 R^2} \qquad \zeta = \frac{cr}{\nu^2 R^2}$$

Choosing coordinates such that a = 0 . c = 0, gives b = 1.4R

The above expressions have been previously expanded in Fourier series and were seen to have the following fourth order terms.

$$P_F = \frac{F}{4\pi R^2} \cdot \frac{a-d}{R} \cdot \frac{1}{\nu^3}\left\{\left[\frac{3.5.7.9}{2.4.6.8}(\xi^4 - 6\xi^2\zeta^2 + \zeta^4) + \text{-----}\right](e^{4i\theta} - e^{-4i\theta}) + \left[\frac{3.5.7.9}{2.4.6.8}(-4\xi^3\zeta - 4\xi\zeta^3) + \text{-----}\right] i\,(e^{4i\theta} - e^{-4i\theta})\right\}$$

$$P_G = \frac{G}{4\pi R^2} \cdot \frac{R}{\nu r}\left\{\frac{3.5.7}{2.4.6}(4\xi^3\zeta - 4\xi\zeta^3)\cos 4\theta - \frac{3.5.7}{2.4.6}(\xi^4 - 6\xi^2\zeta^2 + \zeta^4)\sin 4\theta\right\}$$

Since there are 4 blades, these quantities must be multiplied by 4 to give the free-field pressure, also, since the presence of a rigid plane surface will double the pressure at the location of the surface, these expressions must be further multiplied by 2.

Hence,

$$P = \frac{16F}{4\pi R^2}\,\frac{a-d}{R}\cdot\frac{1}{\nu^3}\,\frac{3.5.7.9}{2.4.6.8}\left\{(\xi^4-6\xi^2\zeta^2+\zeta^4)\cos 4\theta + (4\xi^3\zeta-4\xi\zeta^3)\sin 4\theta\right\}$$

$$+\ \frac{8G}{4\pi R^2}\cdot\frac{R}{\nu r}\cdot\frac{3.5.7}{2.4.6}\left\{(4\xi^3\zeta-4\xi\zeta^3)\cos 4\theta - (\xi^4-6\xi^2\zeta^2+\zeta^4)\sin 4\theta\right\}$$

At the point 0.9R

$a = 0$

$$d = \begin{cases} -0.9\times 19'' \text{ due to rake} \\ -8.03\times\dfrac{22.90}{\pi\times 20.5\times 0.9} \text{ due to skewback}\end{cases}$$

$= -17.1 - 3.18 = -20.28''$ or -1.90 ft.

$b = 1.4R$

$c = 0$

θ must be corrected for skewback. The correction is

$$\frac{8.03/12}{\pi\times 20.5\times 0.9}\times 360 = 4.18^\circ$$

The fourth order of this is 16.7°

$\frac{a-d}{R} = \frac{1.90}{10.25} = 0.185$; $\frac{b}{R} = 1.4$; $\frac{c}{R} = 0$; $\frac{r}{R} = 0.9$

$$\nu^2 = (.0344 + 1.96 + .81) = 2.804 \therefore \nu = 1.676$$

$$\xi = \frac{1.4 \times 0.9}{2.804} = 0.449 \quad ; \quad \xi^4 = 0.0405 \quad ; \quad \zeta = 0$$

$$F_o = -4660^{\#} \qquad G_o = 2080^{\#}$$

Substituting these values gives

$$P._{9R} = \frac{1}{\pi R^2} (52.6 \cos 4\theta - 239.3 \sin 4\theta)$$

Repeating this calculation for several other radial points on the blades and summing the results yields the total of all contributions to the surface pressure. The in-phase component is plotted as point A in Figures 11 and 12 while the quadrature component is plotted as point B.

The above calculations were carried out for a number of different locations on the rigid surface and Figures 11 & 12 show the distribution of pressure on this surface (at the location of the propeller).

Reference to Figure 11 shows the very different characters of the distributions of in-phase and quadrature pressures and emphasizes the importance of measuring phase in experimental determinations of hull pressures: (In this connection an in-phase component is one which has a maximum when a blade is normal to the surface.)

Curves of pressure appear to have roughly equal areas above and below the axis, consequently, if the fore and aft pressure distribution is the same at all points

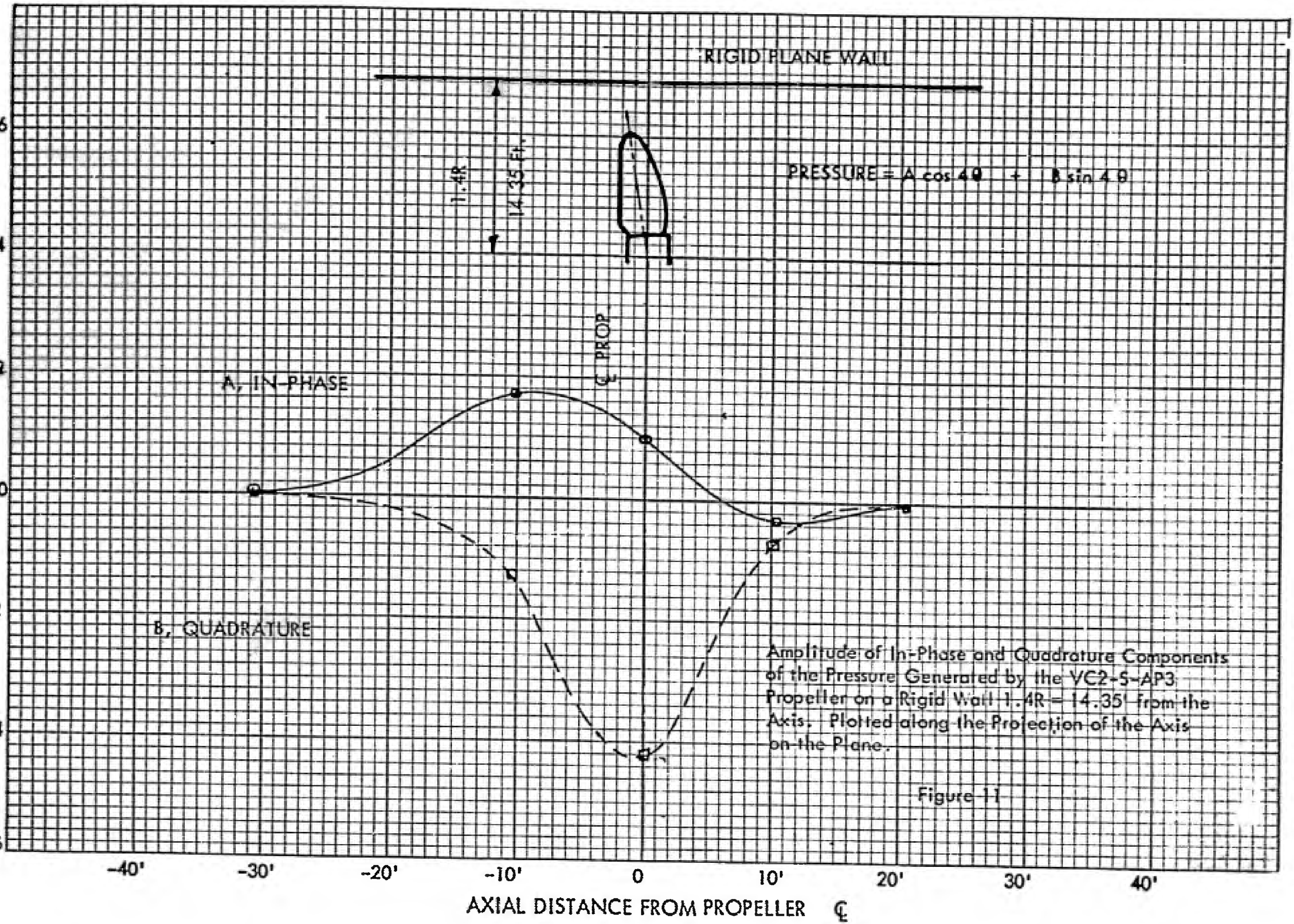

Amplitude of In-Phase and Quadrature Components of the Pressure Generated by the VC2-S-AP3 Propeller on a Rigid Wall 1.4R = 14.35' from the Axis. Plotted along the Projection of the Axis on the Plane.

Figure 11

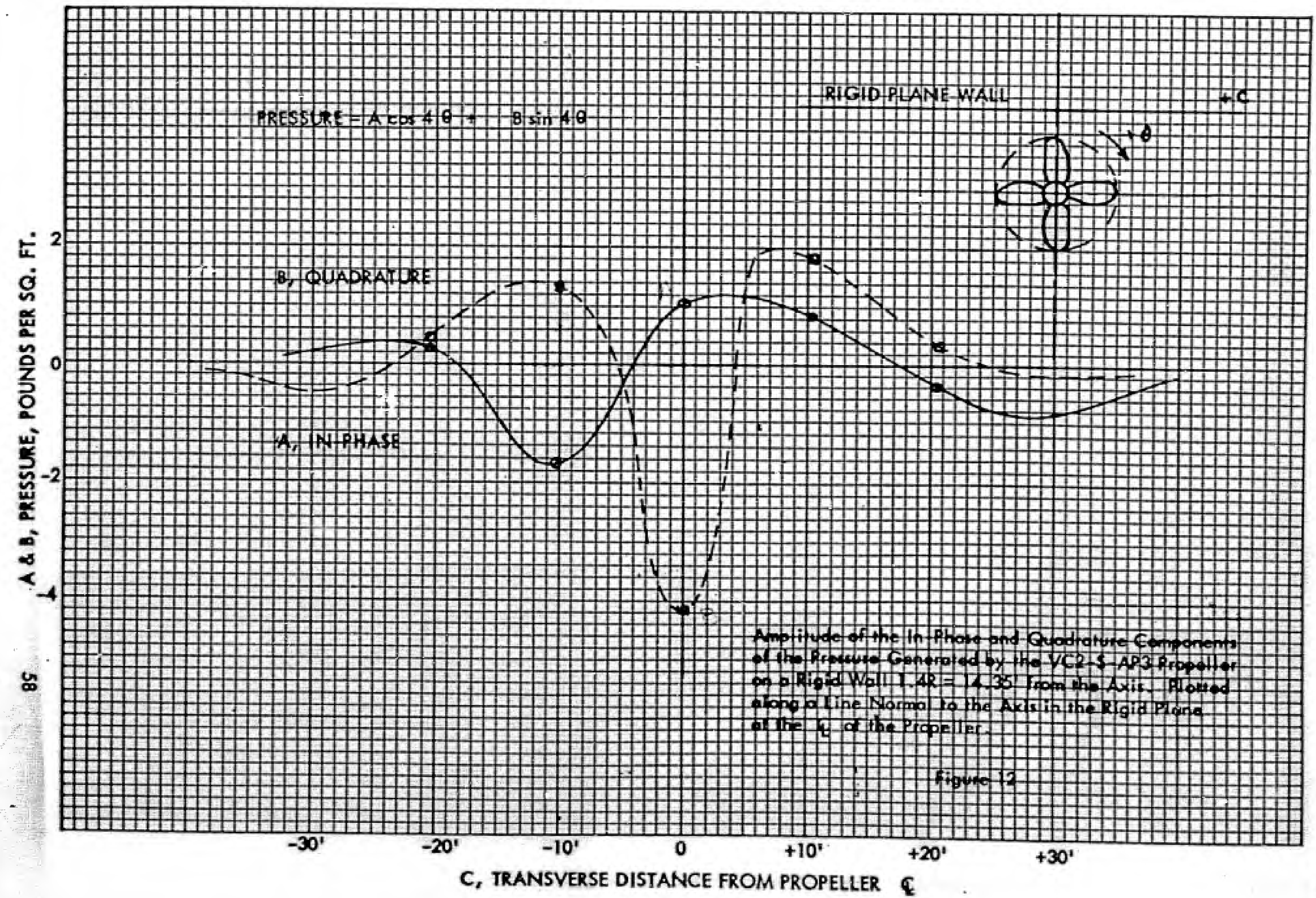

Amplitude of the In-Phase and Quadrature Components of the Pressure Generated by the VC2-S-AP3 Propeller on a Rigid Wall 1.4R = 14.35' from the Axis. Plotted along a Line Normal to the Axis in the Rigid Plane at the ℄ of the Propeller.

Figure 12

across the plane surface the net force on the surface could be zero.

Surface pressures decrease quite rapidly with distance from the propeller. Fig.11 shows that pressures become negligible at a distance greater than one diameter fore and aft of the propeller, while Fig. 12 shows a slower decay in the transverse direction. In this case, pressures do not become negligible until at least two diameters away.

The effects of hull clearance, surfaces other than flat and of planes inclined to the propeller axis are all worth investigation and methods developed in this report allow many of these questions to be studied. However, time does not permit that these questions be taken up under the present contract.

3. DYNAMICAL PROPERTIES OF THE PROPULSION SHAFTING AND THE CALCULATION OF BEARING REACTIONS

The flexible shafting of a ship's propulsion system will be excited into a state of transverse and axial vibration by the variable forces developed by the rotating propeller. This vibratory motion will give rise to reactions at the various bearings which in turn will excite the hull into transverse vibration.

The general treatment of the dynamics of a flexible rotating shaft includes the gyroscopic coupling action which is distributed along the length of the shaft, the effects of rotatory inertia about axes perpendicular to the planes of bending, and deflections due to shear.

The analyses presented here ignore these effects and utilize the simple equation of a vibrating beam, however, the form of each analysis is such that these effects can be incorporated by allowing certain terms to become complex. In order to justify the adoption of the simple beam equation, Appendix G presents a novel treatment of the effects of including the inertial terms mentioned above and shows them to be of minor importance.

Appendix H makes a simplified evaluation of the effect of propeller blade flexibility. It is shown that, for frequencies in the excitation range of the propeller, the propeller behaves essentially as a rigid mass.

In the present study, coupling between horizontal and vertical bending modes is considered to arise at various discrete points. Thus, gyroscopic actions of attached masses (i.g. propeller, thrust bearings, etc.) will produce such coupling, as will anisotropic stiffnesses in the various support bearings.

The nomenclature and sign conventions adopted in the flexural analysis are illustrated by the following:

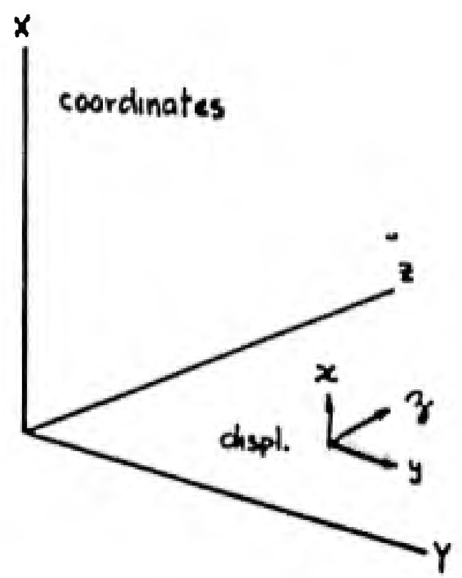

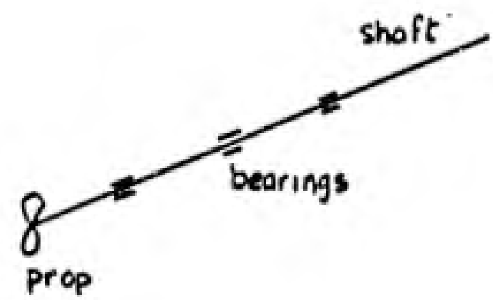

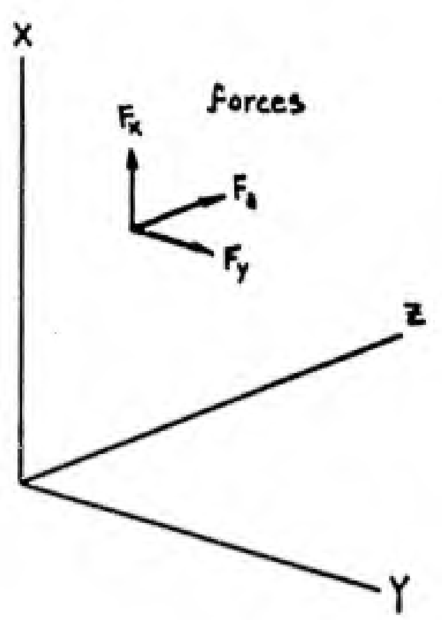

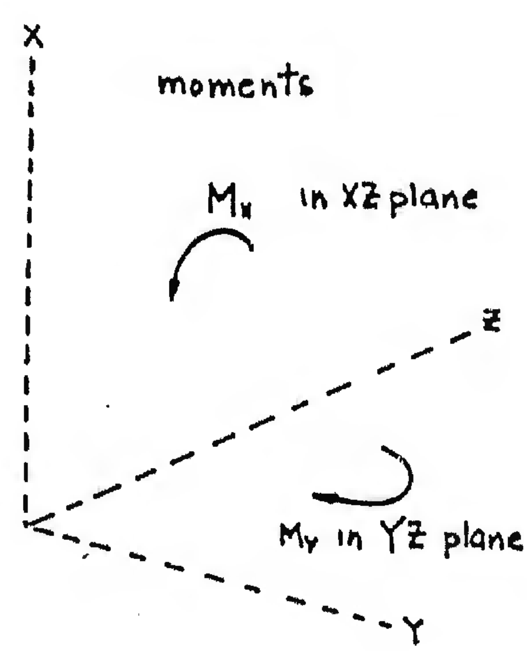

(a) Matrix Treatment of Flexural Vibration

The following paragraphs describe the use of matrix method in shaft vibrations.

(1) Transverse Vibration in one plane

Definitions: μ = mass/unit length of shaft

ω = $2\pi f$ where f = frequency of vibration

E = Young's modulus

I_s = moment of inertia of section about diameter

y = transverse deflection

The differential equation has the form

$$\frac{\partial^4 y}{\partial x^4} + \frac{\mu}{EI_s}\frac{\partial^2 y}{\partial t^2} = 0$$

and admits the steady-state solution $Ye^{i\omega t}$ where Y has the form

$$Y = A_1 e^{\alpha_1 x} + A_2 e^{\alpha_2 x} + A_3 e^{\alpha_3 x} + A_4 e^{\alpha_4 x}$$

In this, $\alpha_1, \alpha_2, \alpha_3, \alpha_4$ are roots of the reduced equation corresponding

to $\dfrac{d^4 y}{dx^4} - \dfrac{\mu\omega^2}{EI_s} Y = 0$

Thus deflection $= Y = \sum_i \left(A_i e^{\alpha_i x}\right) \qquad i = 1,2,3,4$

$$\text{slope} = \frac{dy}{dx} = \sum_i \left(\alpha_i A_i e^{\alpha_i x}\right)$$

$$\text{moment} = EI_s \frac{d^2y}{dx^2} = EI_s \sum_i \left(\alpha_i^2 A_i e^{\alpha_i x}\right)$$

$$\text{shear} = -EI_s \frac{d^3y}{dx^3} = -EI_s \sum_i \left(\alpha_i^3 A_i e^{\alpha_i x}\right)$$

which equations can be written in matrix form as follows:

$$\begin{bmatrix} \text{defl.} \\ \text{slope} \\ \text{moment} \\ \text{shear} \end{bmatrix} = \begin{bmatrix} \delta_y \\ \theta_y \\ M_y \\ F_y \end{bmatrix} = \begin{bmatrix} 1 & 1 & 1 & 1 \\ \alpha_1 & \alpha_2 & \alpha_3 & \alpha_4 \\ EI_s\alpha_1^2 & EI_s\alpha_2^2 & EI_s\alpha_3^2 & EI_s\alpha_4^2 \\ -EI_s\alpha_1^3 & -EI_s\alpha_2^3 & -EI_s\alpha_3^3 & -EI_s\alpha_4^3 \end{bmatrix} \begin{bmatrix} e^{\alpha_1 z} & & & \\ . & e^{\alpha_2 z} & & \\ . & . & e^{\alpha_3 z} & \\ . & . & . & e^{\alpha_4 z} \end{bmatrix} \begin{bmatrix} A_1 \\ A_2 \\ A_3 \\ A_4 \end{bmatrix}$$

This can be written in abbreviated form

$$B_y = \mathfrak{Z}\,\mathcal{E}_z \begin{bmatrix} A_1 \\ A_2 \\ A_3 \\ A_4 \end{bmatrix}$$

When $z = 0$, the vector B_y becomes $(B_y)_{z=0}$ i.e. a vector of boundary conditions at the origin – while $\mathcal{E}$ becomes the identity matrix 1.

Thus

$$(B_y)_{z=0} = \mathfrak{Z} \begin{bmatrix} A_1 \\ A_2 \\ A_3 \\ A_4 \end{bmatrix}$$

hence
$$\begin{bmatrix} A_1 \\ A_2 \\ A_3 \\ A_4 \end{bmatrix} = \mathfrak{Z}^{-1} (B_y)_{x=0}$$

and the expression for $(B_y)_x$ may be written

$$(B_y)_x = \mathfrak{Z} \mathcal{E}_x \mathfrak{Z}^{-1} (B_y)_{x=0}$$

$$\text{or} \quad (B_y)_x = T_x \; (B_y)_{x=0}$$

Hence, conditions of deflection, slope, moment, and shear at any point may be 'transferred' to another point by this transformation.

The 'transfer matrix' T_x has elements which are functions of the elastic properties of the shaft and the distance between the two points. The vector B will, in general, be discontinuous in x . For example, if the complete beam is divided into two sections which are connected by a spring-like member, there can be discontinuities in slope and deflection; if the two sections are pin-jointed there will be continuity of deflection but a discontinuity in slope.

If the beam is physically continuous, discontinuities in moment and shear will arise at the location of a concentrated mass, or at a point where the beam is elastically supported or otherwise constrained. In such a case, the vector B can be transferred up to the location of the discontinuity, the discontinuity added, and the resulting vector transferred to the next point.

Physical discontinuities in the form of abrupt changes in cross-section of the beam will result in changes in the ζ and $\mathcal{E}$ matrices. In such cases, the appropriate ζ and $\mathcal{E}$ matrices must obviously be used when transferring the B vector from one change of section to another.

The utility of the transfer matrix is that it can provide a relationship between two points at which some of the conditions are known viz. the boundary conditions. This relationship will be in the form of four simultaneous equations whose solution yields the unknown conditions at the boundaries. In any given problem then, it is required to build up an overall transfer matrix which will include the effects of all discontinuities intervening between the two points at which some conditions are known. The method of doing this will now be described:

Form of the elementary transfer matrix:

The four roots of the reduced differntial equation are $\pm\ \alpha$, $\pm\ i\ \alpha$ (where $\alpha^4 = \frac{\mu\omega^2}{EI_s}$) and, if the product EI_s is designated β, the form of the T matrix is found to be:

$$\begin{bmatrix} \frac{1}{2}(\cos\alpha x + \cosh\alpha x) & \frac{1}{2\alpha}(\sin\alpha x + \sinh\alpha x) & \frac{1}{2\beta\alpha^2}(-\cos\alpha x + \cosh\alpha x) & \frac{1}{2\beta\alpha^3}(\sin\alpha x - \sinh\alpha x) \\ \frac{\alpha}{2}(-\sin\alpha x + \sinh\alpha x) & \frac{1}{2}(\cos\alpha x + \cosh\alpha x) & \frac{1}{2\beta\alpha}(\sin\alpha x + \sinh\alpha x) & \frac{1}{2\beta\alpha^2}(\cos\alpha x - \cosh\alpha x) \\ \frac{\beta\alpha^2}{2}(-\cos\alpha x + \cosh\alpha x) & \frac{\beta\alpha}{2}(-\sin\alpha x + \sinh\alpha x) & \frac{1}{2}(\cos\alpha x + \cosh\alpha x) & \frac{1}{2\alpha}(-\sin\alpha x - \sinh\alpha x) \\ \frac{\beta\alpha^3}{2}(-\sin\alpha x - \sinh\alpha x) & \frac{\beta\alpha^2}{2}(\cos\alpha x - \cosh\alpha x) & \frac{\alpha}{2}(\sin\alpha x - \sinh\alpha x) & \frac{1}{2}(\cos\alpha x + \cosh\alpha x) \end{bmatrix}$$

The treatment of discontinuities

As has been pointed out, a shaft which is physically continuous will experience discontinuous changes of bending moment and shear force at the locations of concentrated masses or elastic constraints. Let the condition vectors before and after a discontinuity be:

$$\begin{bmatrix} \delta \\ \theta \\ M \\ F \end{bmatrix} \quad \text{and} \quad \begin{bmatrix} \delta \\ \theta \\ M + \Delta M \\ F + \Delta F \end{bmatrix}$$

If both elastic and inertial effects are involved in the discontinuity – say, a heavy disc located at an elastic bearing – the change in bending moment will have a component $(-I_d\,\omega^2\,\theta)$ due to inertial effects of the disc, and a component $(k_{32}\cdot\theta)$ due to the angular stiffness of the bearing. The change in shear force will have a component ($-m_d \omega^2 \delta$) due to inertial effects and a component ($k_{41} \delta$) due to the linear stiffness of the bearing. Hence, the effects of the discontinuity can be characterized by the following matrix equation:

$$\begin{bmatrix} \cdot & \cdot & \cdot & \cdot \\ \cdot & \cdot & \cdot & \cdot \\ \cdot & (k_{32} - I_d \omega^2) & \cdot & \cdot \\ (k_{41} - m_d \omega^2) & \cdot & \cdot & \cdot \end{bmatrix} \begin{bmatrix} \delta \\ \theta \\ M \\ F \end{bmatrix} = \begin{bmatrix} \cdot \\ \cdot \\ \Delta M \\ \Delta F \end{bmatrix}$$

Or, if the square matrix is designated by K and the condition vector before the discontinuity B, the change in B is KB. Hence, the condition vector after the discontinuity is (I + K) B where I is the identity matrix. It can thus be seen that if a shaft is divided into n sections by (n-1) discontinuities, the overall transfer matrix is:

$$\mathcal{T} = T_n \; (I + K_{n-1}) \; T_{n-1} \; (I + K_{n-2}) \; . \; . \; . \; . \; . \; T_2 \; (I + K_1) \; T_1$$

where T_j is the transfer matrix corresponding to the j^{th} section of the shaft. Since the various transfer matrices can be written down from knowledge of the length, diameter, and elastic modulus of each section of the shaft, and the K matrices can be formed from knowledge of the elastic properties of the bearings, etc., the formation of the overall transfer matrix can be carried out directly. This overall transfer matrix relates the boundary vectors B_o and B_n and part of each of these is known from the 'end conditions' of the shaft.

Take for example the case

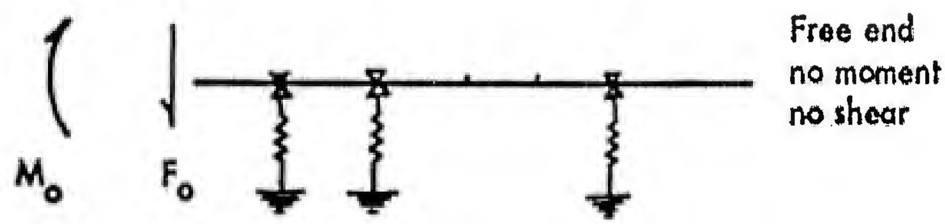

$$B_o = \begin{bmatrix} \delta_o \\ \theta_o \\ M_o \\ F_o \end{bmatrix}$$

M_o and F_o being known

$$B_n = \begin{bmatrix} \delta_n \\ \theta_n \\ 0 \\ 0 \end{bmatrix}$$

The transfer relation $B_n = \mathcal{T} B_o$ can be expanded and partitioned as follows:

$$\left[\begin{array}{cc|cc} t_{11} & t_{12} & t_{13} & t_{14} \\ t_{21} & t_{22} & t_{23} & t_{24} \\ \hline t_{31} & t_{32} & t_{33} & t_{34} \\ t_{41} & t_{42} & t_{43} & t_{44} \end{array}\right] \left[\begin{array}{c} \delta_o \\ \theta_o \\ \hline M_o \\ F_o \end{array}\right] = \left[\begin{array}{c} \delta_n \\ \theta_n \\ \hline 0 \\ 0 \end{array}\right]$$

Or, in terms of sub-matrices

$$\begin{bmatrix} \tau_{11} & \tau_{12} \\ \tau_{21} & \tau_{22} \end{bmatrix} \begin{bmatrix} \Delta_o \\ \mathfrak{F}_o \end{bmatrix} = \begin{bmatrix} \Delta_n \\ 0 \end{bmatrix}$$

which give Δ_o and Δ_n in terms of the known $\mathfrak{F}_o$ as follows:

$$\Delta_o = - \tau_{21}^{-1} \tau_{22} \mathfrak{F}_o$$

$$\Delta_n = (- \tau_{11} \tau_{21}^{-1} \tau_{22} + \tau_{12}) \mathfrak{F}_o$$

Hence, B_o and B_n are now known completely and the shear and moment reactions (i.e. discontinuities) at the i^{th} bearing are given by the i^{th} discontinuity vector viz: $K_i \left[T_i \; (I + K_{i-1}) \, T_{i-1} \; (I + K_{i-2}) \; . \; . \; . \; . \; T_1 \right] B_o$

If a complete knowledge of conditions in the interior of the shaft is required, it is necessary to transfer B_o to various locations between the bearings.

The specific way in which the $\mathfrak{T}$ matrix is partitioned will, of course, depend on the actual boundary conditions imposed on the shaft. Also, it is apparent that the $\mathfrak{T}$ matrix is frequency dependent so that the behavior of the beam has to be investigated separately for each frequency.

(2) Transverse vibration coupled in two planes

In general, a ship's propeller shaft will exhibit flexural vibrations in both the vertical and horizontal planes with coupling between the two planes arising at the propeller and at elastic supports. As stated earlier, the distributed coupling due to gyroscopic actions of the shaft itself will not be considered here.

Let $(B_x)_z$ = vector of conditions in the x z plane at the point z

$(B_y)_z$ = vector of conditions in the Y z plane at the point z

A single transfer relation can be written in terms of sub-matrices: -

$$\begin{bmatrix} B_x \\ \hline B_y \end{bmatrix}_z = \begin{bmatrix} T_z & \cdot \\ \hline \cdot & T_z \end{bmatrix} \begin{bmatrix} B_x \\ \hline B_y \end{bmatrix}_o$$

which can be re-ordered into the form

$$\mathbf{B}_z = \begin{bmatrix} \delta_x \\ \theta_x \\ \delta_y \\ \theta_y \\ F_x \\ M_x \\ F_y \\ M_y \end{bmatrix}_z = \mathbf{T}_z \begin{bmatrix} \delta_x \\ \theta_x \\ \delta_y \\ \theta_y \\ F_x \\ M_x \\ F_y \\ M_y \end{bmatrix}_o = \mathbf{T}_z \mathbf{B}_o$$

The arguments advanced previously will still apply and vectors may be transferred to discontinuities, the discontinuities added, and the result transferred to other points.

The major difference arising is in the nature of the matrix which characterizes a discontinuity. This matrix (which will be designated the $\mathbb{K}$ matrix) must include stiffness terms which couple deflections and rotations in one plane with forces and moments in the other plane. In addition, gyroscopic coupling demands the incorporation of matrix elements which couple rotations in one plane with moments in the other.

If the elements of the $\mathbb{B}$ vector are allowed to become complex (to take care of phase differences), then, including the time dependence, the condition vector may be written:

$$\begin{bmatrix} \delta_x \cdot & e^{i\omega t} \\ \theta_x \cdot & e^{i\omega t} \\ \delta_y \cdot & e^{i\omega t} \\ \theta_y \cdot & e^{i\omega t} \\ F_x \cdot & e^{i\omega t} \\ M_x \cdot & e^{i\omega t} \\ F_y \cdot & e^{i\omega t} \\ M_y \cdot & e^{i\omega t} \end{bmatrix}$$

If I_d is the mass moment of inertia of a disc (e.g. propeller) at some location, and the spin velocity of this disc on its axis is Ω_1, then rotational velocities Ω_2 and Ω_3 about axes normal to the spin axis will produce moments $I_d\Omega_1\Omega_2$ and $I_d\Omega_1\Omega_3$ in planes normal to those containing Ω_2, Ω_3. Thus, rotations θ_x and θ_y, with their corresponding rotational velocities $i\omega\theta_x$ and $i\omega\theta_y$ will produce the following moments:

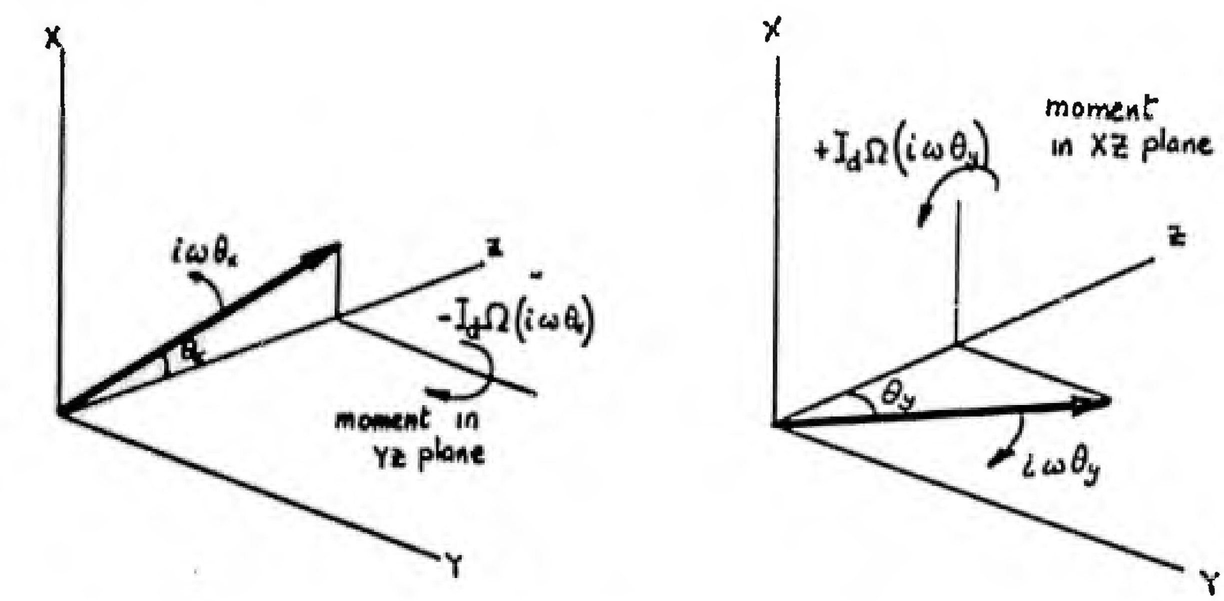

DISC ROTATES CLOCKWISE LOOKING IN Z DIRECTION

The gyroscopic moment in the yz plane can be written as $-ig\theta_x$ and that in the xz plane as $+ig\theta_y$, where g is a coefficient representing the product $(I_d\Omega\omega)$.

If the shaft is supported in a bearing with anisotropic stiffness there will be terms coupling a translation in one plane with a force component in the other, and coupling a rotation in one plane with a moment in the other. At this time it is assumed that there is no coupling between translations and moments, or between rotations and forces, however, such a case can be handled by incorporating appropriate terms in the matrix.

In general then, when both inertial and elastic coupling appear at a discontinuity - e. g. a propeller and bearing close together - the $(\mathbb{I} + \mathbb{K})$ matrix will have the following general appearance:

$$\begin{bmatrix} 1 & 0 & 0 & 0 & 0 & 0 & 0 & 0 \\ 0 & 1 & 0 & 0 & 0 & 0 & 0 & 0 \\ 0 & 0 & 1 & 0 & 0 & 0 & 0 & 0 \\ 0 & 0 & 0 & 1 & 0 & 0 & 0 & 0 \\ k_{51}-m_d\omega^2 & 0 & k_{53} & 0 & 1 & 0 & 0 & 0 \\ 0 & k_{62}-I_d\omega^2 & 0 & k_{64}+ig & 0 & 1 & 0 & 0 \\ k_{71} & 0 & k_{73}-m_d\omega^2 & 0 & 0 & 0 & 1 & 0 \\ 0 & k_{82}-ig & 0 & k_{84}-I_d\omega^2 & 0 & 0 & 0 & 1 \end{bmatrix}$$

The procedure to be followed in building up an overall transfer matrix is the same as before. This now leads to eight simultaneous equations whose solution yields the unknown parts of the boundary conditions. The procedure for finding the bearing reactions is the same as before.

(3) Axial Vibration - coupled extensional/torsional oscillation

Since torsional oscillations of the propeller shaft will result in variations in approach velocity of the propeller, there will be an attendant fluctuation of the axial (thrust) component of blade force. Also, axial movement of the blades will alter the effective angle of incidence and will produce oscillatory components in the blade torque. Both of these mechanisms serve to couple the torsional and extensional modes of vibration of the propeller shaft.

Coupled vibrations of this type can be treated by matrix methods similar in character to those used in the preceding discussions of flexural vibrations.

Thus, the extensional equation $\frac{\partial^2 u}{\partial z^2} = \frac{\rho}{E} \cdot \frac{\partial^2 u}{\partial t^2}$ admits a steady state solution of the form $Ue^{i\omega t}$ where

$$U = C_1 e^{\gamma_1 z} + C_2 e^{\gamma_2 z}$$

and γ_1, γ_2 are roots of the reduced equation corresponding to

$$\frac{d^2U}{dz^2} + \frac{\rho\omega^2}{E} U = 0$$

Hence, axial displacement $= \epsilon = U = \sum_i c_i e^{\gamma_i z} \qquad i = 1,2$

axial force $= \sigma = E a \frac{dU}{dz} = Ea \sum_i \gamma_i c_i e^{\gamma_i z}$

In this, E = Young's modulus

a = area of cross-section of shaft

ρ = density of shaft material

$\omega = 2\pi f$ where f = vibration frequency

$U = \epsilon$ = axial displacement of shaft cross-section

By arguments similar to those used previously, we may write

$$\begin{bmatrix} \varepsilon \\ \sigma \end{bmatrix}_z = \begin{bmatrix} 1 & 1 \\ Ea\gamma_1 & Ea\gamma_2 \end{bmatrix} \begin{bmatrix} e^{\gamma_1 z} & \cdot \\ \cdot & e^{\gamma_2 z} \end{bmatrix} \begin{bmatrix} 1 & 1 \\ Ea\gamma_1 & Ea\gamma_2 \end{bmatrix}^{-1} \begin{bmatrix} \varepsilon \\ \sigma \end{bmatrix}_{z=0}$$

which is again of the form $B_z = T_z \; B_o$

The transfer matrix T_z can be written in the form

$$\begin{bmatrix} \cos\gamma z & \frac{1}{Ea\gamma}\sin\gamma z \\ -Ea\gamma\sin\gamma z & \cos\gamma z \end{bmatrix} \qquad \text{where } \gamma = \sqrt{\frac{\rho\omega^2}{E}}$$

In a similar fashion, the equation governing torsional oscillations

$$\frac{\partial^2 \phi}{\partial z^2} = \frac{\rho}{G} \frac{\partial^2 \phi}{\partial t^2} \qquad G = \text{shear modulus}$$

admits the solution $\Phi \; e^{i\omega t}$ where $\Phi = C_1 e^{\zeta_1 z} + C_2 e^{\zeta_2 z}$

with ζ_1, ζ_2 the roots of the reduced equation corresponding to

$$\frac{d^2 \Phi}{dz^2} + \frac{\rho\omega^2}{G}\Phi = 0$$

Hence, if J_s = polar moment of inertia of shaft cross-section

ϕ = angular displacement

τ = torque

$$\begin{bmatrix} \phi \\ \tau \end{bmatrix}_z = \begin{bmatrix} 1 & 1 \\ J_s G\zeta_1 & J_s G\zeta_2 \end{bmatrix} \begin{bmatrix} e^{\zeta_1 z} & \cdot \\ \cdot & e^{\zeta_2 z} \end{bmatrix} \begin{bmatrix} 1 & 1 \\ J_s G\zeta_1 & J_s G\zeta_2 \end{bmatrix}^{-1} \begin{bmatrix} \phi \\ \tau \end{bmatrix}_{z=0}$$

This is again of the form $B_x = T_x B_o$ where T_x can be written

$$\begin{bmatrix} \cos \zeta x & \dfrac{1}{J_s G \zeta} \sin \zeta x \\ \\ -J_s G \zeta \sin \zeta x & \cos \zeta x \end{bmatrix} \qquad \text{with } \zeta = \sqrt{\frac{\rho \omega^2}{G}}$$

In the transformations shown above, the torsional and extensional modes are, of course, uncoupled. The axial contraction which accompanies torsional deflection (and which would constitute a distributed coupling) has been ignored. However, coupling which arises at discrete points can be taken into account by combining the two transfer relations as was done in the case of coupled flexural vibrations; thus:-

$$\begin{bmatrix} \varepsilon \\ \phi \\ \sigma \\ \tau \end{bmatrix}_x = \begin{bmatrix} \cos \gamma x & 0 & \dfrac{1}{E a \gamma} \sin \gamma x & 0 \\ 0 & \cos \zeta x & 0 & \dfrac{1}{J_s G \zeta} \sin \zeta x \\ -E a \gamma \sin \gamma x & 0 & \cos \gamma x & 0 \\ 0 & -J_s G \zeta \sin \zeta x & 0 & \cos \zeta x \end{bmatrix} \begin{bmatrix} \varepsilon \\ \phi \\ \sigma \\ \tau \end{bmatrix}_{x=0}$$

The $(\mathbb{I} + \mathbb{K})$ matrix which carries the condition vector past a discontinuity involving inertial and elastic effects will be of the following form:

$$\begin{bmatrix} 1 & 0 & 0 & 0 \\ 0 & 1 & 0 & 0 \\ a_{31}+ib_{31} & a_{32}+ib_{32} & 1 & 0 \\ a_{41}+ib_{41} & a_{42}+ib_{42} & 0 & 1 \end{bmatrix}$$

The complex sub-matrix in the lower left hand corner of this will have terms of the following types:

The 3, 1 term represents axial force contributions that are dependent on axial displacements. It will have a real part made up of a stiffness term (e.g. the stiffness of the thrust bearing) and a mass term (e.g. the inertia force of a disc which is proportional to ω^2 times the displacement). An imaginary term will arise when the discontinuity is the propeller. This is due to the fact that a harmonic axial velocity will alter the attack angle of the blades, thereby producing harmonic fluctuations in the thrust and torque. These fluctuations, being velocity dependent, will be in quadrature with the displacement - i.e. the former will contribute an imaginary term in the 3, 1 position, while the latter will contribute an imaginary term in the 4, 1 position. The 4, 1 position represents torque contributions arising from axial displacements and may have a real term corresponding to stiffness coupling between rotation and extension.

The 3, 2 and 4, 2 positions may have real terms arising from stiffness effects but will have imaginary contributions from the propeller action. Thus, torsional oscillations of the shaft result in harmonic variations in the blade approach velocity with attendant oscillations in thrust and torque. The former will produce an imaginary term in the 3, 2 position and the latter an imaginary term in the 4, 2 position. The 4, 2 term will also have a real contribution resulting from angular accelerations produced in the disc.

The theoretical description of thrust and torque oscillations produced by harmonic velocities in the blades is not in a condition to let the results be conveniently incorporated in this work.

Another type of discontinuity of interest in the propulsion train is that which occurs at the reduction gear. If it is assumed that there is no axial sliding between the gears, there will be no discontinuity in the axial displacement ε; however, the other three components of the condition vector will change discontinuously. If the mass and polar inertia of the low speed gear are M_1 and J_1 respectively and those of the high speed pinion are M_2 and J_2, the gear ratio being R, then the vector after the discontinuity is derived from the vector before by multiplication by the following matrix which plays the role of an ($\mathbb{I} + \mathbb{K}$) matrix.

$$\begin{bmatrix} 1 & 0 & 0 & 0 \\ 0 & R & 0 & 0 \\ -\omega^2(M_1+M_2) & 0 & 1 & 0 \\ 0 & -\omega^2\left(\dfrac{J_2R+J_1}{R}\right) & 0 & \dfrac{1}{R} \end{bmatrix}$$

(b) <u>The Calculation of Bearing Reactions</u>

To calculate bearing reactions, the various transfer matrices and discontinuity matrices are formed and the cumulative product described in the preceding paragraphs is obtained. The resulting four equations containing known boundary conditions are solved for the unknown boundary conditions. Starting at one end of the shaft the boundary conditions (now completely known) are transferred up to and beyond each discontinuity. There then results a pair of condition vectors for each discontinuity – one before and one immediately after. The difference in each pair gives the discontinuous change in the elements of the condition vector. In the following paragraphs there is described a simple numerical example.

(c) Illustrative Examples.

For the most part, tne application of these methods to the calculation of bearing reactions in an actual ship presents no great problems. However, there is one major exception. While the various lengths, diameters, etc. necessary to form the transfer matrices can be taken directly from drawings, the information necessary to form the discontinuity matrices is less easily obtained. In particular, the estimation of bearing stiffness is quite difficult. An accurate estimate of bearing stiffness would take account of the contributions from the bearing material (wood, phenolic, rubber, white metal, etc.), the bearing housing, and the struts, pedestal, or other supports which connect the bearing to the floors and plating of the main hull structure. In addition, the main hull structure has some flexibility which contributes to the effective stiffness of the bearing. Jasper [4] and others have devised simple formulas for effective bearing stiffness; however, while these formulas are extremely useful and convenient, there is still no thoroughly satisfactory method of computing stiffness.

The example chosen for calculations in this report is relatively simple and does not demonstrate the full capacity of the program. However, it is useful in that the numerical results can be easily compared with intuitive ideas about shaft behavior. The system considered consisted of a shaft some 117 ft. long with a mass representing a propeller at one end while the other end was free. Two flexible bearings were located 595 in. apart with one of these bearings placed 96 in. from the propeller. The shaft dimensions and bearing flexibilities were based on values chosen by Jasper[4] to represent the shafting of the USS FORRESTAL (CVA 59).

The system response was calculated over the frequency range of 100 to 500 cpm. i. e. slightly more than the speed range. Since it was shown earlier that the forces arising at the propeller are of shaft order (unbalance, etc.) and multiples of blade order, a calculation that includes twice blade order would have to cover frequencies up to 5000 cpm.

Figures 13 and 14 illustrate the response of the system to a unit vertical force at the propeller and it can be seen that the first resonance lies at $\omega = 28$ rad/sec (approx. 270 rpm.). Figure 13 presents the force reaction at each of the two bearings while Figure 14 presents the moment reaction. Table 1 gives the numerical results calculated by the machine for $\omega = 24$ and is given here to illustrate the

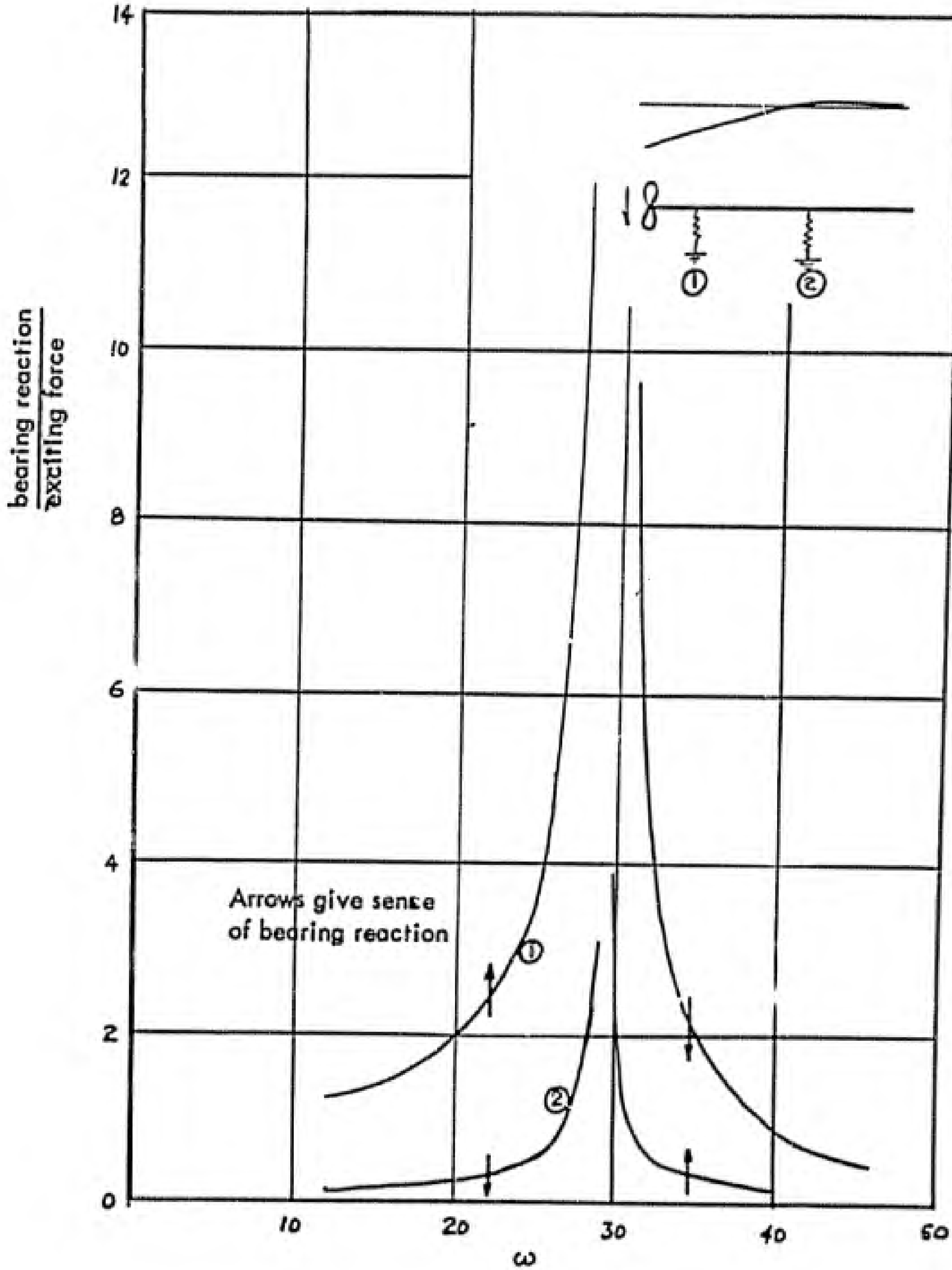

Figure 13 Force reactions at bearings

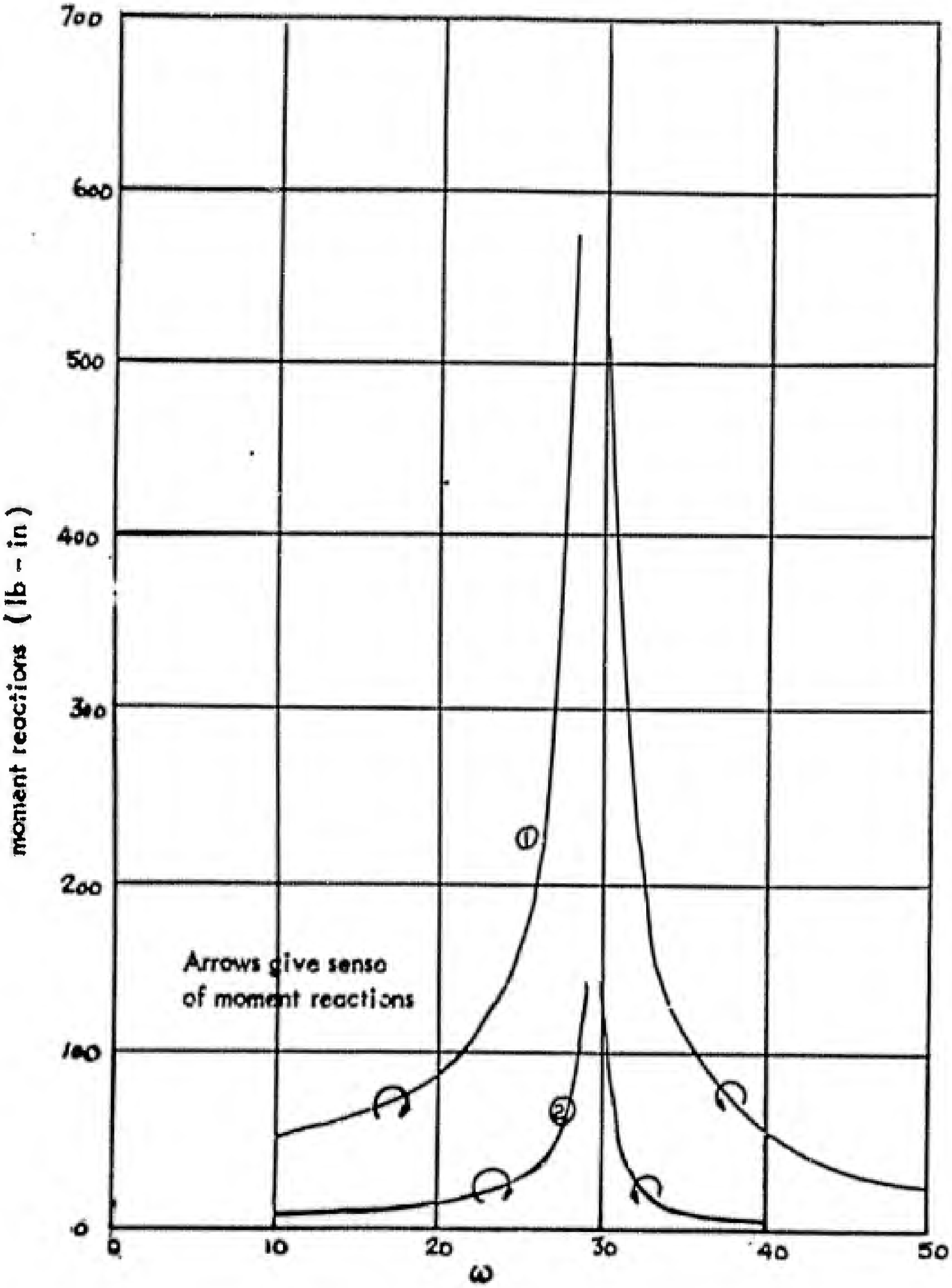

Figure 14 Moment reactions at bearings (unit vertical force at propeller)

TABLE 1

Excerpt from IBM 704 data output for problem illustrated in Fig. 13 Response of shaft at $\omega = 24$.

Location		Displacement (in).	Slope (rads.)	Shear (lb)	Moment (lb-in)
propeller	before	$-..169129 \times 10^{-4}$	$+ .171992 \times 10^{-6}$	$+ .100000 \times 10^{1}$	0
	after	$- .169129 \times 10^{-4}$	$+ .171992 \times 10^{-6}$	$+ .276327 \times 10^{1}$	$- .295221 \times 10^{2}$
1st bearing	before	$- .258962 \times 10^{-5}$	$+ .109302 \times 10^{-6}$	$+ .277215 \times 10^{1}$	$- .295333 \times 10^{3}$
	after	$- .258962 \times 10^{-5}$	$+ .109302 \times 10^{-6}$	$- .322444 \times 10^{0}$	$- .152579 \times 10^{3}$
2nd bearing	before	$+ .330749 \times 10^{-6}$	$- .189256 \times 10^{-7}$	$- .353834 \times 10^{0}$	$+ .492272 \times 10^{2}$
	after	$+ .330749 \times 10^{-6}$	$- .189256 \times 10^{-7}$	$+ .414772 \times 10^{-1}$	$+ .244989 \times 10^{2}$
free end	before	$+ .142399 \times 10^{-5}$	$+ .619548 \times 10^{-8}$	$+ .460968 \times 10^{-1}$	$- .797070 \times 10$
	after	$+ .142399 \times 10^{-5}$	$+ .619548 \times 10^{-8}$	$+ .460968 \times 10^{-1}$	$- .797070 \times 10$

NOTE: The shear and moment at the free end should be zero; as can be seen, there is a residual error. This example was calculated with 'single precision' and the residual errors are substantially reduced when 'double precision' is used.

Translational stiffness of bearing $= .1195 \times 10^{7}$ lb/in

Rotational stiffness of bearing $= .1307 \times 10^{10}$ lb in/rad interpretation of the various signs. It will be recalled that the sign convention adopted was such as to make 'upward' displacements and shear forces positive, and 'anti-clockwise' rotations and moments positive. In Table 1 the deflection at the first bearing is negative (i.e. downward) producing an upward (i.e. positive) force at the bearing yet the calculations show a negative change in shear force. The reason why an upward force produces a negative change in shear force is clear from the following diagram.

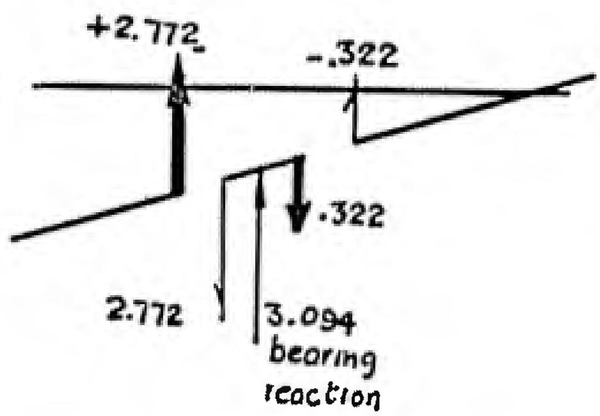

Since the shear forces quoted always refer to the force on the right-hand end of a beam element, the values calculated refer to the heavily outlined arrows on the diagram.

In practice, the sign of the shear change or change in bending moment at a discontinuity can be ignored since the sense of the force or moment will be obvious from the deflection or slope at the point in question.

As would be expected, the reactions are rapidly attenuated as the distance from the bearing to the propeller increases and the main reactions (off-resonance) occur at the first bearing.

NOTE: THE PROGRAM AS WRITTEN USES A DIFFERENT ORDER OF THE ELEMENTS OF THE COLUMN VECTORS TO THAT USED IN THE DERIVATIONS. SHEAR FORCE AND MOMENT ARE INTERCHANGED. THIS STEP WAS TAKEN TO PRODUCE A CONVENIENT SYMMETRY OF THE ELEMENTS OF THE TRANSFER MATRICES.

4. CONCLUDING REMARKS

The object of this study has been to apply the available scientific information in the fields of structural vibration, acoustics and hydrodynamics to the problem of propeller excited hull vibration in ships. In the process of doing this, some advances in applied mechanics have been made. This report presents the following accomplishments of the study:

(a) Methods for computing the dynamic forces and moments that are generated by a propeller working in angularly varying wakes have been developed. These methods include the effects of the fluid inertia upon the amplitude and phase of the generated forces - the "Theodorsen effects". Forms and detailed instructions are given so that the calculations may be carried through with a minimum of effort by design engineers.

(b) A method for computing the free-field pressures generated by a propeller has been developed. This method, since it is based upon the pressures generated by moving forces, does not require corrections for the interactions between sources, and utilizes the actual load distributions on the propeller blades.

(c) Analyses have been made of the effects of pitch and of lift distribution across the blade width upon the free-field pressures generated by a propeller.

(d) A theoretical study of the pressures generated on the surface of a wedge having a small solid angle that is inserted into the pressure field generated by an oscillating dipole is presented. This original work is an important step in evaluating the pressures on the hull - as distinct from the free-field pressures.

(e) Dynamical equations have been developed to determine the reactions in the bearings of the propeller shafting as a consequence of the harmonic forces and moments at the propeller. These equations include the coupling between mutually perpendicular planes of motion that result from gyroscopic action in large masses and from anisotropy in the bearings. The staff of the David Taylor Model Basin have programmed these equations for a digital computer.

(f) Equations have been developed to evaluate the gyroscopic effects of uniform shafting. These equations have been used to show that it is proper to neglect these gyroscopic effects in the calculations of ships' propulsion shafting.

As is usual in a study of this type, there are many facets of the problems that will require further study before the solutions are complete. Among these may be listed the following:

tighten up

(a) A study of the effects of blade width upon the fluctuating forces produced by high frequency stream and gust variations.

(b) The Theodorsen effects that apply to a blade that is moving harmonically in the direction of the stream.

a little

(c) A more complete study should be made of the effects upon the free-field pressures of blade pitch angle and of lift distribution along the blade (also on the face and back of the propeller). Ways of incorporating these effects in a reasonably simple calculation should be included.

(d) The intensification factors for various surfaces should be investigated. These studies should include:

(1) Further studies on the wedge

(2) An infinite circular cylinder (information on this exists but is not in a useable form)

(3) An infinite elliptical cylinder

(4) A cone

(5) A torus or a parabolloid or a hyperbolloid of revolution

(6) An ellipsoid

Each of these studies represents a substantial amount of work.

In addition to these, the theoretical work should be utilized in a procedure by which a designer can determine the intensification factor at a

fit in to 7 ms hold with program (blade shape etc)
blade thickness effects. Applying Breslin's work

[illegible] of shafts

[illegible] mass prop blades

point on a ship's hull.

(e) A study should be made of the effects of structural flexibility at the boundary upon the intensification factors.

(f) Since the stiffness of the bearings has a very important effect upon the accurate calculation of shafting bearing reactions, methods of determining these stiffnesses (both laterally and rotationally in two perpendicular planes) in struts, and stern tubes should be developed. The results should be checked by experiments.

(g) The report contains a procedure for estimating the lowest natural frequency of the propeller blades. This procedure should be compared with experimental determinations. A method of calculating the natural frequency of propeller blades with a higher degree of accuracy should be developed.

(h) It was not possible, within the limitations of this contract, to fully test the computer program for determining bearing reactions. This program should be applied to a system that will utilize its full capabilities. Careful attention should be paid to assuring that the input information completely and accurately represents an actual system and the results compared with experimental data.

The methods developed during this project now make it feasible to study many factors influencing propeller vibration that was not practical to study in the past. Some of these are listed below:

(a). In the experiments on propeller vibration run by Professor Lewis in the past, he has computed the values of the propeller forces generated by irregular wakes and compared them with the forces that he determined experimentally. In general, the amplitudes of these forces agreed reasonably well, but the phases showed poor agreement. It would be desirable to find out whether including the "Theodorsen effects" would give better agreement between the calculated and the experimentally determined forces.

(b) The possibilities of reducing the vibratory forces generated at the propeller by variations in design should be studied. These studies should include:

(1). The effects of skewback and rake.

(2) The possibilities of shaping the hull in such a manner as to change the higher orders of wake variation enough to reduce the propeller forces.

(3) Is it possible to obtain both low vibratory forces and high propulsion efficiency?

(c). The design factors that influence the forces transmitted to the hull by the pressure field surrounding the propeller should be investigated. These studies should include:

(1) The manner in which hull clearance effects the hull forces. At which point on the propeller is hull clearance most important?

(2) What is the influence of the propeller blade shape (rake and skewback) upon the hull pressure forces?

(3) What is the effect of the inclination of the propeller axis to the hull on the forces and moments generated?

(4) Will local hull flexibility in the vicinity of the propellers have an influence upon the vibratory energy transmitted to the hull?

(5) Recognizing that the pressure field from the propeller has a wide variation in phase, is it possible to shape the hull in the vicinity of the propellers in such a way that the hull pressures from the propeller will cancel?

Appendix A

Calculation of Fourier Components of Wake

On the following pages, tables are given for determining the harmonic coefficients for a periodic curve based upon 24 ordinates (15° interval) and 16 ordinates (22 1/2° interval). These tables are based upon the Runge method of harmonic analysis. A discussion of the method and its limitations is given by Manley.[28] Most wake surveys appear to be made in 15° or 22 1/2° intervals. If however, a 20° interval is used, a harmonic analysis form using 18 ordinates that has been developed by the Bureau of Standards[29] may be used, and if a 7 1/2° interval is adopted, a form based upon 48 ordinates is given by Den Hartog.[30]

The use of these tables is self-explanatory and they are applied to a specific example in Appendix I.

SCHEDULE FOR HARMONIC ANALYSIS

24 ORDINATES

y	0 (12)	1 (23)	2 (22)	3 (21)	4 (20)	5 (19)	6 (18)	7 (17)	8 (16)	9 (15)	10 (14)	11 (13)
Sum: c												
Diff: d												

c	0 (6)	1 (11)	2 (10)	3 (9)	4 (8)	5 (7)
Sum: e						
Diff: f						

d	0 (6)	1 (11)	2 (10)	3 (9)	4 (8)	5 (7)
Sum: g						
Diff: h						

e	0 (3)	1 (5)	2 (4)
Sum: k			
Diff: l			

f	0 (3)	1 (5)	2 (4)
Sum: m			
Diff: n			

g	0 (3)	1 (5)	2 (4)
Sum: o			
Diff: p			

h	0 (3)	1 (5)	2 (4)
Sum: q			
Diff: r			

Table A-1(a)

SCHEDULE FOR HARMONIC ANALYSIS
24 ORDINATES

$$y = A_0 + A_1 \cos \theta + A_2 \cos 2\theta + \dots + B_1 \sin \theta + B_2 \sin 2\theta + \dots$$

Sin 15°	f_5	g_1							f_1	g_5			$-f_1$	g_5							$-f_5$	g_1	
Cos 75°																							
0.259																							
Sin 30°	f_4	g_2	l_2	g_1			k_1-k_2		f_4	g_2			f_4	$-g_2$	$-k_1-k_2$				l_2	g_1	f_4	$-g_2$	
Cos 60°																							
0.500																							
Sin 45°	f_3	g_3			h_1-f_3	p_1+g_3			$-f_3$	$-g_3$			f_3	$-g_3$			f_3-h_1	g_3+p_1			$-f_3$	g_3	
Cos 45°																							
0.707																							
Sin 60°	f_2	g_4	l_1	g_2				r_1+r_2	$-f_2$	$-g_4$			$-f_2$	g_4		r_1-r_2			$-l_1$	$-g_2$	f_2	$-g_4$	
Cos 30°																							
0.866																							
Sin 75°	f_1	g_5							f_5	g_1			$-f_5$	g_1							$-f_1$	g_5	
Cos 15°																							
0.966																							
Sin 90°	d_0	d_6	f_0	h_3	d_0-f_4	g_2-d_6	l_0		d_0	d_6	f_0-l_2	g_1-h_3	d_0	$-d_6$	k_0		d_0-f_4	d_6-g_2	f_0	h_3	d_0	$-d_6$	$f_0-k_1+k_2$
Cos 0°																							
Σ																							
	A_1	B_1	A_2	B_2	A_3	B_3	A_4	B_4	A_5	B_5	A_6	B_6	A_7	B_7	A_8	B_8	A_9	B_9	A_{10}	B_{10}	A_{11}	B_{11}	A_{12}
Σ÷12																							

$A_0 = 1/24 \; (k_0 + k_1 + k_2)$

Checks:
$A_1 + A_2 + A_3 + A_4 + A_5 + A_6 + A_7 + A_8 + A_9 + A_{10} + A_{11} + A_{12} = Y_0 - A_0$
$A_1 - A_2 + A_3 - A_4 + A_5 - A_6 + A_7 - A_8 + A_9 - A_{10} + A_{11} - A_{12} = -Y_{12} + A_0$
$2 \sin 60^\circ \, (B_1 + B_2 - B_4 - B_5 + B_7 + B_8 - B_{10} - B_{11}) = d_4$
$2 \, (B_1 - B_3 + B_5 - B_7 + B_9 - B_{11}) = d_6$

Table A-1(b)

SCHEDULE FOR HARMONIC ANALYSIS

16 ORDINATES

y	0 (8)	1 (15)	2 (14)	3 (13)	4 (12)	5 (11)	6 (10)	7 (9)
Sum: c								
Diff: d								

c	0 (4)	1 (7)	2 (6)	3 (5)
Sum: c				
Diff: f				

d	0 (4)	1 (7)	2 (6)	3 (5)
Sum: g				
Diff: h				

e	0 (2)	1 (3)
Sum: k		
Diff: l		

f	0 (2)	1 (3)
Sum: m		
Diff: n		

g	0 (2)	1 (3)
Sum: O		
Diff: p		

h	0 (2)	1 (3)
Sum: q		
Diff: r		

Table A-2(a)

SCHEDULE FOR HARMONIC ANALYSIS

16 ORDINATES

$$y = A_o + A_1 \cos\theta + A_2 \cos 2\theta + \ldots + B_1 \sin\theta + B_2 \sin 2\theta + \ldots$$

Sin 22.5°	f_3	g_1			f_1	$-g_3$			$-f_1$	$-g_3$			$-f_3$	g_1	
Cos 67.5°															
0.3827															
Sin 45°	f_2	g_2	l_1	q_1	$-f_2$	g_2			$-f_2$	$-g_2$	$-l_1$	q_1	f_2	$-g_2$	
Cos 45°															
0.7071															
Sin 67.5°	f_1	g_3			$-f_3$	g_1			f_3	g_1			$-f_1$	g_3	
Cos 22.5°															
0.9239															
Sin 90°	d_o	d_4	f_o	h_2	d_o	$-d_4$	l_o	r_1	d_o	d_4	f_o	$-h_2$	d_o	$-d_4$	$k_o - k_1$
Cos 0°															
Σ															
	A_1	B_1	A_2	B_2	A_3	B_3	A_4	B_4	A_5	B_5	A_6	B_6	A_7	B_7	A_8
1/8 Σ															

$A_o = (k_o + k_1)\ 1/16$

Checks:

$A_1 + A_2 + A_3 + A_4 + A_5 + A_6 + A_7 + A_8 = Y_o - A_o$

$A_1 - A_2 + A_3 - A_4 + A_5 - A_6 + A_7 - A_8 = Y_8 + A_o$

$2\,(B_1 - B_3 + B_5 - B_7) = d_4$

$2\left[(B_2 - B_6) + \sin 45^\circ\,(B_1 + B_3 - B_5 - B_7)\right] = d_2$

Table A-2(b)

Appendix B

Calculation of the Thrust and Tangential Forces Developed by a Radial Blade Element Operating in a Steady Wake

The method of calculating the variable forces and moments developed by a propeller is based upon the determination of the changes in the steady forces acting on radial elements as they are subjected to the varying flow caused by wake fluctuations. The first step is the determination of the steady elemental forces and a method for doing this has been developed by Burrill.[1] Since the method is somewhat difficult to follow without detailed study of the paper, and since the objective of this calculation is different from Burrill's original purpose, a new calculation form was developed. This is presented in Table B-1 and detailed instructions are given for the use of this form. A determiniation of Propeller Section Characteristics is required by this calculation form and Table B-2 is used for this purpose. Table B-3 is a designation sheet used with the instructions. It is necessary to refer to Burrill's paper[1] in using this form.

The application of the calculation forms to a specific example is given in Appendix I. This appendix also includes a check upon the calculation obtained by integrating the elemental forces over the propeller. This calculated result is compared with the propeller characteristics as determined by Model Basin tests.

CALCULATION OF THRUST, TORQUE & EFFICIENCY AT

$x = r/R =$ $\quad$ $J = V/Nd =$

Diam =

Pitch =

V_a (W_l=) =

N =

$\sigma = \frac{B \times C}{2\pi r} =$ ______ =

K_{α_0} = $\quad$ $K_{g\alpha_0}$ =

K_s = $\quad$ K_{gs} =

t =

c =

t/c =

α_0 = $\quad$ =

α_{nt} = $\quad$ =

$\tan\theta = P/2\pi r =$ $\quad$ θ =

$\theta + \alpha_0 + \alpha_{nT}$ =

$-\Delta\alpha_q$ = $\quad$ =

θ_0 =

$\tan\psi = J/\pi x =$ $\quad$ ψ =

$\theta_0 - \psi$ =

α_1			
$\phi = \theta_0 - \alpha_1$ $\beta = \phi - \psi$ $\varepsilon = \phi + \beta$ K_ε $\sin\phi$ $\tan\beta$			
$\alpha_2 = C_2 K_\varepsilon \sin\phi \tan\beta$			
$\tan\phi$ K_ϕ $(1-K_\phi)\frac{\tan\beta}{\tan\phi} \times \alpha_2$			
α_3			

α_1^{*} = $\quad$ =

C_2 = ______ =

$C_{L\,OPT}$ =

C_L =

$C_L - C_{L\,OPT}$ =

$C_{D\,MIN}$ =

=

ΔC_{Dg} = ______ =

C_D =

$\tan\gamma$ =

$(\alpha_3 - \alpha_1)\frac{\beta}{\beta + \alpha_3}$

= ______ =

C_L = ______

$\delta C_L = \frac{1}{2}\times$ =

C_L =

γ =

ϕ =

$\phi + \gamma$ =

$\tan(\phi+\gamma) =$ $\quad$ $\sin(\phi+\gamma) =$ $\quad$ $C_y = \frac{\pi^3 x^3 \sigma}{2 D} =$ $\quad$ $\cos(\gamma) =$

$$a' = \frac{(\tan\phi - \tan\psi)\tan(\phi+\gamma)}{1 + \tan\phi\tan(\phi+\gamma)} = \text{______} =$$

$(1-a')$ =

$K_G' = C_y(1-a')^2(1+\tan^2\phi)C_L\frac{\sin(\phi+\gamma)}{\cos\gamma}$

=

=

$K_Q' = K_G'\,x/2 =$

$K_F' = \frac{K_G'}{\tan(\phi+\gamma)} =$ ______ =

$\eta = \frac{J}{2\pi}\cdot\frac{K_F'}{K_Q'} =$ $\quad$ =

ck. $\eta = \frac{\tan\psi}{\tan(\phi+\gamma)} =$ ______ =

$C_s = \rho n^2 D^3$

=

=

$G = C_s K_G'$

=

$F = C_s K_F'$

=

Table B-1

PROPELLER SECTION CHARACTERISTICS $x = \frac{r}{R} =$

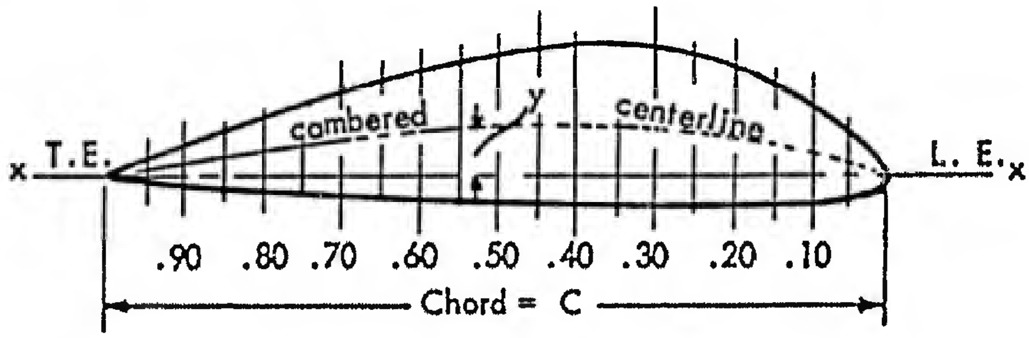

$$\alpha_o^{\bullet}(\text{Theory}) = \frac{1}{C}\,(f_1 y_1 + f_2 y_2 + f_3 y_3 + \ldots f_{19} y_{19})$$

Station	Position from L. E.	Y ins.	Multipliers f_1, f_2 etc.	Functions $(f_1 \times y_1)$etc.
y_1	0.05 C		5.04	
y_2	0.10 C		3.38	
y_3	0.15 C		3.01	
y_4	0.20 C		2.87	
y_5	0.25 C		2.81	
y_6	0.30 C		2.84	
y_7	0.35 C		2.92	
y_8	0.40 C		3.09	
y_9	0.45 C		3.32	
y_{10}	0.50 C		3.64	
y_{11}	0.55 C		4.07	
y_{12}	0.60 C		4.64	
y_{13}	0.65 C		5.44	
y_{14}	0.70 C		6.65	
y_{15}	0.75 C		8.59	
y_{16}	0.80 C		11.40	
y_{17}	0.85 C		17.05	
y_{18}	0.90 C		35.40	
y_{19}	0.95 C		186.20	
			Σ	

Theoretical $\alpha_o^{\bullet} = \dfrac{\Sigma}{\text{Chord}}$

Actual $\alpha_o^{\bullet} = K_{\alpha_o} \times$ Theoretical $\alpha_o^{\bullet}$

Nose - Tail Slope $= \dfrac{\text{Nose rise} - \text{Tail rise}}{\text{Chord}} \times 57.3$

$= \_\_\_\_\_\_\_\_ \times 57.3$

$=$

Table B-2

SPECIFIC INSTRUCTIONS FOR THE USE OF TABLE B-1 ENTITLED "CALCULATION OF THRUST, TORQUE AND EFFICIENCY"

(1) For Designation of Design of Propeller, Speed and Draft.

(2) Location of Section

(3) (7) / (4) x (8)

(4) From Propeller Design.

(5) From Propeller Design at the radius under consideration.

(6) Average longitudinal wake at the radius. From harmonic analysis of the wake survey.

(7) Ship speed x $(1-W_l)$ x 101.33 - in ft/min.

(8) From Propeller Design - in R.P.M.

(9) Maximum thickness of the section.

(10) Length of chord of section.

(11) (9) ÷ (10)

(12) As indicated: B = No. of blades., C = (10), r - radius of action of section in same units of measurement as C.

(13) K_{ao}, A correction to relate the theoretical value of the angle of attack for zero lift in a uniform airfoil of infinite length to that obtained by experiment. Value obtained from Fig. 6 (labelled Fig. 7 in paper). Max. Camber corresponds

1

CALCULATION OF THRUST, TC QUE & EFFICIENCY AT

$x = r/R = $ 2 $\qquad J = V/Nd = $ 3

Diam = 4

Pitch = 5

V_a (w = 6) = 7

N = 8

$\sigma = \frac{B \times C}{2\pi r} = $ ________ = 12

$K_{\alpha_0} = $ 13 $\qquad K_{g\alpha_0} = $ 23

$K_S = $ 14 $\qquad K_{gs} = $ 34

t = 9

c = 10

t/c = 11

$\alpha_0 = $ 15 × 13 = 16

$\alpha_{nt} = $ = 17

$\tan\theta = P/2\pi r = $ 18 $\quad \theta = $ 19

$\theta + \alpha_0 + \alpha_{nT}$ = 20

$-\Delta\alpha_g = -$ 23 × 15 = − 24

θ_0 = 25

$\tan\psi = J/\pi x = $ 21 $\quad \psi = $ 22

$\theta_0 - \psi$ = 26

$\alpha_1^\circ = $ 26 (0.52 − 0.2 2) = 27

$C_2 = \frac{36.48}{(14) \times (12) \times (34)} = $ 35

α_1	27	42	
$\phi = \theta_0 - \alpha_1$	28		
$\beta = \phi - \psi$	29		
$\varepsilon = \phi + \beta$	30		
K_ε	31		
$\sin\phi$	32		
$\tan\beta$	33		
$\alpha_2 = C_2 K_\varepsilon \sin\phi \tan\beta$	36		
$\tan\phi$	37		
$K\phi$	38		
$(1-K\phi)\frac{\tan\beta}{\tan\phi} \times \alpha_2$	39		
α_3	40		

$C_{L\,OPT}$ = 44

C_L = 43

$C_L - C_{L\,OPT}$ = 45

$C_{D\,MIN}$ = 46

= 47

$\Delta C_{Dg} = \frac{(24) \times (43)}{57.3} = $ 48

C_D = 49

$\tan\gamma = \frac{(49)}{(51)} = $ 52

$(\alpha_3 - \alpha_1)\frac{\beta}{\beta + \alpha_3}$

$\frac{(40 - 27)\,29}{29 + 40} = $ 41

$C_L = \frac{(14) \times (42\ \text{final})\ (34)}{9.072}$ 43

$\delta C_L = \frac{1}{2} \times$ 49 (33 fin) 34 = 50

C_L = 51

γ = 53

ϕ = 28f

$\phi + \gamma$ = 54

$\tan(\phi+\gamma) = $ 56 $\qquad \sin(\phi+\gamma) = $ 57 $\qquad C_Y = \frac{\pi^3 x^3 \sigma}{2B} = $ 58 $\qquad \cos(\gamma) = $ 55

$a' = \frac{(\tan\phi - \tan\psi)\tan(\phi+\gamma)}{1 + \tan\phi\tan(\phi+\gamma)} = $ ________ = 59

$(1 - a')$ = 60

$K_G' = C_y (1-a')^2 (1+\tan^2\phi) C_L \frac{\sin(\phi+\gamma)}{\cos\gamma}$

=

= 61

$K_Q' = K_G' \frac{x}{2} = $ 62

$K_F' = \frac{K_G'}{\tan(\phi+\gamma)} = \frac{(61)}{(56)} = $ 63

$\eta = \frac{J}{2\pi} \cdot \frac{K_F'}{K_Q'} = $ = 64

ck. $\eta = \frac{\tan\psi}{\tan(\phi+\gamma)} = $ ________ = 65

$C_g = \rho n^2 D^3$

=

= 66

$G = C_G K_G'$

= 67

$F = C_F K_F'$

= 68

Designation Sheet for Instructions

Table B-3

to maximum y in propeller section characteristics calculation. $t/_c$ corresponds to (11) .

(14) K_s is a correction to the theoretical slope of the lift curve of a uniform airfoil of infinite length to give agreement with experimental results. The value of this is obtained from Figure 7 (mislabelled Fig. 6 in the paper).

(15) A theoretical value of the angle of attack for zero lift is obtained from the Propeller Section Characteristics calculation form, Table B-2, for the section of interest.

(16) (15) corrected by experiment as indicated.

(17) This value is determined at the bottom of the Propeller Section Characteristics Calculation, Table B-2.

(18) As indicated: $\dfrac{(5)}{\pi (4) \times (2)}$

(19) $\tan^{-1} \dfrac{P}{2\pi r}$

(20) sum as indicated.

It is necessary at this point to make a small correction to the no lift angle of attack that is caused by the interference in the circulation around the blades caused by a cascade effect. This correction is obtained from Figure 15. The value of σ is given by (12) . However, the value of ϕ^o is not known and must be estimated. Fortunately, the correction resulting from this cause is small and so an estimated value of ϕ^o may be used. To obtain this, pass down to determining ψ .

(21) (3) /π (2) as indicated.

(22) $\tan^{-1}$ (21) as indicated.

Since $\phi = \theta_o - \alpha_1$, it may be roughly estimated as follows:

α_1 is roughly ((20) - (22)) (0.52 - 0.2x)

ϕ is roughly (20) - α_1

(23) With the value of ϕ as determined by this side calculation enter Figure 15 to find a preliminary value of K_{gao}.

(24) The value of the cascade correction to the zero lift angle now follows as indicated on the form.

(25) This is (20) - (24) as indicated.

(26) This is (25) - (22) as indicated.

(27) An empirical value for the angle of attack from the zero lift value is given by (26) (0.52 - 0.2 (2)) as is indicated on the form.

The value of α_1 is now refined by a trial and error correction procedure as indicated on the left side of the form.

(28) = (25) - (27) as indicated.

(29) = (28) - (22) as indicated.

(30) = (28) + (29) as indicated.

At this point, a factor is introduced to account for the finite length of the propeller blades and the spilling of the circulation over the blade tips. This factor is based upon complicated theoretical calculations which are summed up in Figures 2 and 3.

(31) For the value of ε, (30), and the value of x, (2), enter Figure 3 or Figure 4, depending on the number of blades, to determine the value of K_{ε}, (31).

(32) tan (28)

(33) sin (29)

(34) Since C_2 is required for the next calculation, it is necessary to ascertain its value. To do this, a correction caused by the airfoils being in cascade, and applied to the slope of the infinite airfoil lift curve, must be determined. This is given by Figure 16 as a function of $\phi°$, (28), and σ, (12).

(35) [For Ogival, round-back, Sections see paragraphs at the end of these instructions].

The value of C_2 is:

$$C_2 = \frac{2 \times 57.3}{K_s \times \pi \times \sigma K_{gs}} = \frac{36.48}{(14) \times (12) \times (34)}$$

(36) The value of α_2 as indicated is (35) × (31) × (32) × (33)

(37) = tan (28)

(38) Found by entering Figure 2 or 3 with (28) and (2). It might be well at this point to also check $K_g\, \alpha_0$, (23), in Figure 15 to see whether there has been any significant change in its value.

(39) = (1 - (38)) (33) (36) / (37) as indicated.

(40) $\alpha_3 = \alpha_2$ - (39).

41 Using α_3, it is now possible to find an improved value of α_1, by the procedure outlined. The approximate amount of the change required to improve α_1 is determined by the indicated formula $\delta\ \alpha_1$ = (40 - 27) 29 / (29 + 40).

42 This differential correction to α_1, 41, is added to the previous value, 27, and the whole procedure repeated. Generally, this will give a value of $\alpha_3 = \alpha_1$ but if not, the procedure is repeated again until agreement is reached.

When α_1 is determined, all of the flow angles and corrections are determined. Now the forces corresponding to these flows are computed.

43 [For Ogival, round-back, Sections see paragraphs at the end of these instructions].

$$C_L = \frac{K_s \times 2\pi \times \alpha_1 \times K_{gs}}{57.3} = \frac{⑭ \times \text{final } \alpha_1 \times ㉞}{9.072}$$

This lift coefficient is increased by the cascade effect and the amount of this is related to the drag coefficient of the section as shown by Burrill's paper. The procedure for evaluating the drag coefficient is given on the left side of the form.

44 [For Ogival, round-back, Sections see paragraphs at the end of these instructions]. The optimum lift coefficient, $C_{L\ opt}$, i. e. the lift coefficient at which the drag coefficient is a minimum, is computed by

the use of Figure 9 in which the curves are entered with the $^{t}/_{c}$, (11),
and the location of the maximum camber, i. e. the location of the maximum value of y, as given in the Propeller Section Characteristics Calculation. The value of K_1 taken from these curves is multiplied by $y_{1\,max}/c$ to find $C_{L\,opt}$.

45 /For Ogival, round-back, Sections see paragraphs at the end of these instructions/. The difference between the uncorrected lift coefficient and the optimum lift coefficient is obtained as indicated.

46 /For Ogival, round-back, Sections see paragraphs at the end of these instructions/. Corresponding to C_{Lopt} there is a minimum drag coefficient whose value is:

$$C_{D\,min} = 0.0056 + 0.01\ t/c + 0.10\ \left(\frac{t}{c}\right)^2 + K_2$$

The value of K_2 in this relationship is determined from Figure 10 as determined by the position of the ℄ camber from the leading edge, the amount of center-line camber and the thickness ratio, $\frac{t}{c}$.

47 /For Ogival, round-back, Sections see paragraphs at the end of these instructions/. To this minimum C_D is added an additional quantity that is given by $K_3\ (C_L - C_{L\,opt})^2$, where K_3 is given by Figure 11 or Figure 12.

48 /For Ogival, round-back, Sections see paragraphs at the end of these instructions/. In addition to the above there is an additional drag

resulting from the cascading of the blades. The magnitude of this drag coefficient

$$= \frac{\Delta \alpha g \times C_L}{57.3} \qquad = \frac{(24) \times (43)}{57.3}$$

(49) The total drag coefficient is the sum of the previous values

$$= (46) + (47) + (48)$$

(50) It is now possible to compute the correction to the lift coefficient for for cascade effect. As shown in Appendix III of Bürrill's paper, this is

$\delta C_L = \frac{1}{2} C_D \tan \beta \; K_s$, $\quad \delta C_L = \frac{1}{2}$ (49) $\times$ final value (33) $\times$ (34)

(51) $= C_L + \delta C_L$ as indicated.

(52) The tangent of the drag angle, γ, is defined as $\frac{C_D}{C_L} = \frac{(49)}{(51)}$

(53) Knowing the tangent, (52), γ, may be determined.

(54) The angle of the resultant force on the blades is the sum of $\emptyset + \gamma$ as indicated.

(55) Since the amplitude of the resultant of the lift and drag coefficients is $C_L / \cos \gamma$, $\cos \gamma$ is determined as shown.

(56) For transferring the lift and drag forces into thrust and torque forces the tangent ($\emptyset + \gamma$) is determined as indicated.

(57) Likewise: sin ($\emptyset + \gamma$).

(58) C_4 , a coefficient used in the computation of the force coefficients is determined as indicated $= \frac{\pi^3 \; (2)^3 \; (12)}{2\,B}$

59 The quantity, a', is used to evaluate the stream velocity to the airfoil in terms of the propeller velocities and is computed as shown

$$= \frac{(37f - 21)\ 56}{1 + 37f\ 56}$$

60 $1 - a' = 1 - 59$

61 K_G', the force coefficient for the tangential force, is computed as shown

$$K_G' = \frac{58\ 60^2\ (1 + 37f^2)\ 51\ 57}{55}$$

62 K_Q', the torque coefficient, $= \quad K_Q' \times \frac{x}{2} = 61 \times \frac{2}{2}$

63 $K_F' = \dfrac{K_G'}{\tan(\phi + \gamma)}$

64 Efficiency checks: $\eta = \dfrac{J}{2\pi} \quad \dfrac{K_T'}{K_Q'} = \dfrac{3}{2\pi} \times \dfrac{63}{62}$

65 $\eta = \dfrac{\tan \psi}{\tan(\phi + \gamma)} = \dfrac{22}{56}$

66 To compute the actual force on the blade, a propeller constant $C_5 = \rho n^2 D^3$ is required

For salt water, $\rho = \dfrac{64 \ \#/ft^3}{g} = 1.99$

$n = \dfrac{8}{60}$ in r.p.s.

$D = 4$ in feet.

(67) The tangential force per foot of propeller blade length at the radius being studied = $C_5 \; K_G' =$ (66) (61) .

(68) The thrust force per foot of propeller blade length at the radius being studied = $C_5 \; K_F' =$ (66) (62) .

When working with Ogival sections, the characteristics of the sections are defined more simply than for airfoil sections. Thus it is possible to determine the lift and drag coefficients more directly. The calculation procedure is modified as follows:

(35) $$C_2 = \frac{2 \times 57.3}{K_s \; \pi\sigma + K_{gs} \, (1 - 0.02\alpha)} \doteq \frac{36.48}{(14) \; (12) \; (34) \times (1 - 0.02 \; (15) \;)}$$

(43) $$C_L = \frac{K_s \; K_{gs} \; 2\pi \; \alpha \; (1 - 0.02\alpha)}{57.3} = \frac{(14) \times (34) \times (42f) \; (1 - 0.02 \; (42f) \;)}{9.072}$$

(44) (45) , not applicable.

(46) Determine $\alpha K_{gs} - \alpha_o + \Delta\alpha_g$

$= (42f) \times (34) - (16) + (24)$

With this value, enter Figure 14 at the proper value of t/c, (11) , and ascertain C_{Di}, (46) .

(47) The above drag coefficient is determined with respect to the flat face of the blade. To refer the drag coefficient to the hydrodynamic pitch line

it is necessary to add a correction factor

$$= C_L \, a_o \, (1 - K_{gs}) \times \frac{1}{57.3}$$

$$= 43 \quad 42f \quad (1 - 34) \times \frac{1}{57.3}$$

48 Already included in 46 .

The remainder of the calculation procedure is unchanged.

Appendix C

Calculation of the Vibratory Forces and Moments on a Propeller.

Using harmonic analyses of the longitudinal and tangential wake and the determination of the steady thrust and tangential forces on radial elements of the propeller, a form (Table C-1) is given for the determination of the vibratory forces,and moments on a blade arising from the wake variations. Detailed instructions for the use of this form are included. The determination of the vibratory forces and moments on the whole propeller from these blade values is accomplished in Table C-2.

The application of these forms to a specific problem - the determination of the 4th order forces and moments on a VC2-S-AP3 Propeller - is illustrated in Appendix I.

CALCULATION OF HARMONIC FORCES & MOMENTS

ON ONE BLADE - SHEET 1

________ORDER, n

SHIP SPEED________ PROP. DIA.________ RPM________ Ω________ ω________

	0.30R		0.55R		0.80R		0.90R	
	Ft.		Ft.		Ft.		Ft.	
1. W_{Lo}								
2. $1-W_{Lo}$								
3. $V/\Omega r$								
4. α								
5. φ								
6. $\sin^2\varphi$								
7. $\cos^2\varphi$								
8. $1/\alpha \sin\varphi \cos\varphi$								
9. $U = (1-a')\sqrt{1+\tan^2\varphi}\,\Omega r$								
10. blade chord, c								
11. Freq. parameter $c\,\omega/2U$								
12. W_{Ln}								
13. W_{tn}								
14. $W_{Ln}/(1-W_{Lo})$								
15. $W_{tn}\ V/\Omega r$								
16. $\boxed{14} + \boxed{15}$								
17. $1/\alpha \sin\varphi \cos\varphi\ \boxed{16}$								
18. M+i N (Fig.2)								
19. $\boxed{17} \times \boxed{18}$								
20. $\sin^2\varphi\ W_{Ln}/(1-W_{Lo})$								
21. $\cos^2\varphi\ W_{tn}\ V/\Omega r$								
22. $\boxed{21} - \boxed{20}$								
23. B + i A (Fig.1)								
24. $\boxed{22} \times \boxed{23}$								
25. $\boxed{19} + \boxed{24}$								
26. G_o								
27. F_o								
28. $G_n = \boxed{26} \times \boxed{25}$								
29. $F_n = \boxed{27} \times \boxed{25}$								
30. G_n Resultant + angle								
31. F_n Resultant + angle								

Table C-1 (a)

CALCULATION OF HARMONIC FORCES & MOMENTS

ON ONE BLADE – SHEET 2

________ORDER, n

SHIP SPEED________ PROP. DIA.________ RPM________ Ω________ ω________

	0.30R		0.55R		0.80R		0.90R	
		Ft.		Ft.		Ft.		Ft.
32. Skewback °								
33. Skewback - phase °								
34. G_n-ref. line – R + ∠								
35. F_n-ref. line – R + ∠								
36. G_n-ref. line –Re + Im								
37. F_n-ref. line – Re + Im								
38. Integration Constant								
39. f (G_n)								
40. f (F_n)								
41. f $(r\,G_n)$								
42. f $(r\,F_n)$								
43. f (G_n)								
44. f (F_n)								
45. f $(r\,G_n)$								
46. f $(r\,F_n)$								

Table C- 1(b)

Specific Instructions For the Calculation Of Vibratory Forces And Moments On a Propeller Blade

(CTTE refers to the form entitled "Calculation of Thrust, Torque and Efficiency" - Table B-1 at the radius under consideration)

$\Omega = 2\pi \times \dfrac{\text{Prop. R.P.M.}}{60}$ $\omega = n\Omega$ radius of section, $r, \left(= \dfrac{r}{R} \cdot \dfrac{D}{2}\right)$

1. From harmonic analysis of the wake - also used in CTTE.

2. As indicated.

3. V = (ship speed knots) $(1-W_{Lo})$ (1.689)

4. - angle of attack, α, in radians (42) in CTTE. ÷ 57.3.

5. Final value of (28) in CTTE.

6. Square of final value of (32) in CTTE.

7. 1 - $\boxed{6}$.

8. As indicated.

9. (1-a') is (60) in CTTE, $1 + \tan^2 \phi$ is given in (61) in CTTE, Ω and r from previously listed values.

10. - (10) in CTTE.

11. $\boxed{10}$ × ω (from heading) /2 × $\boxed{9}$ - This is the Theodorsen frequency parameter.

12. From the harmonic analysis of the longitudinal wake at the radius of interest

and for the order being investigated. The real part is the cosine component, the imaginary part, the sine component.

13. From the harmonic analysis of the tangential wake.
14. $\boxed{12} \div \boxed{2}$ as indicated.
15. $\boxed{13} \times \boxed{3}$ as indicated.
16. As indicated.
17. $\boxed{8} \times \boxed{16}$ as indicated, this is $\frac{\alpha_n}{\alpha}$, the ratio of the nth order variation in angle to the steady angle of attack of the section.
18. M and N are taken from Figure 2 at the proper value of the Theodorsen Function, $\boxed{11}$.
19. As indicated, this gives the ratio of the nth order variable lift to the average lift for the variations in angle of attack due to wake.
20. $\boxed{5} \times \boxed{14}$ as indicated.
21. $\boxed{6} \times \boxed{15}$ as indicated.
22. As indicated – this gives the ratio of the nth order variation in stream velocity to the average stream velocity.
23. B and A are taken from Figure 1 at the proper value of the Theodorsen frequency parameter, $\boxed{11}$.
24. As indicated – this gives the ratio of the nth order variable lift to the average lift for the stream variations caused by the variable wake.
25. As indicated – this gives the ratio of the total nth order lift variations to the

average lift for both gust and stream variations.

26. G_o taken from CTTE (67) .

27. F_o taken from CTTE (68) .

28. As indicated - this is the nth order variable tangential force per unit radial distance.

29. As indicated - this is the nth order variable axial force per unit radial distance.

30. The values of thrust and tangential forces are those at the center of the chord of the blade section. When the blade is skewed, this center of the chord falls off of the reference line and the thrust and tangential forces for the section must be corrected for the shift in phase. This is done by changing to amplitude and phase angle adding the corrected phase angle and then returning to real and imaginary components for integration.

Result, $G_n = \sqrt{G\,re_n^2 + G\,Im_n^2}$; $\phi = \tan^{-1} \dfrac{G\,Im_n}{Gre_n}$

31. Result, $F_n = \sqrt{Fre_n^2 + FI\,m_n^2}$; $\phi = \tan^{-1} \dfrac{FIm_n}{Fre_n}$

32. Skewback angle = $\dfrac{\text{distance of center of chord from reference line}}{r} \times 57.3$

(if the offset is in inches, then r should be in inches.

33. This is n times the skewback - n is the order number.

34. and 35. ϕ is decreased by the skewback angle.

36. Gre_n = Result $G_n \cos \phi$ $\qquad$ $G\,Im_n$ = Result $G_n \sin \phi$

37. Fre_n = Result $F_n \cos \phi$ Fim_n = Result $F_n \sin \phi$

38. At 0.30R, the integration factor is D/24.

At 0.55R, the integration factor is D/6.

At 0.80R, the integration factor is 7D/120.

At 0.90R, the integration factor is D/15.

39. and 40. These are $\boxed{36}$ and $\boxed{37}$ each times $\boxed{38}$.

41. and 42. These are $\boxed{39}$ and $\boxed{40}$ each times r.

43.44. and 45. The quantities in the columns are summed giving real and imaginary terms.

Σf (F_n) is the total nth order variable axial force on the blade.

Σf $(r\ G_n)$ is the total nth order variable torque on the blade.

Σf (G_n) and Σf $(r\ F_n)$ are functions used in the determination of the horizontal and vertical forces and moments generated by the blade.

____

ORDER HARMONIC FORCES AND MOMENTS

GENERATED BY PROPELLER WORKING IN THE NON-UNIFORM WAKE

SHIP SPEED ________ RPM ________ DISPLACEMENT ________

PROPELLER DIA. ________ FT. , NUMBER OF BLADES, B ________

WAKE DISTRIBUTION GIVEN BY ____________________

	Real	Imag.	Real	Imag.	Result	Harm. Phase	Prop. Angle
Harmonic Thrust $= \sum_B \sum F_n$							
Harmonic Torque $= \sum_B \sum (r\,G_n)$							
Vertical Harmonic Force $= \sum_B \left[+\frac{1}{2i} \sum (G_{n-1}) \right.$							
$\left. -\frac{1}{2i} \sum (G_{n+1}) \right]$							
Horizontal Harmonic Force $= \sum_B \left[+\frac{1}{2} \sum (G_{n-1}) \right.$							
$\left. +\frac{1}{2} \sum (G_{n+1}) \right]$							
Harmonic Moment About The Horizontal Axis $= \sum_B \left[+\frac{1}{2} \sum (r\,F_{n-1}) \right.$							
$\left. +\frac{1}{2} \sum (r\,F_{n+1}) \right]$							
Harmonic Moment About The Vertical Axis $= \sum_B \left[+\frac{1}{2i} \sum (r\,F_{n-1}) \right.$							
$\left. -\frac{1}{2i} \sum (r\,F_{n+1}) \right]$							

Table C-2

Appendix D

The Effects of Pitch and Chordwise Lift Distribution on the Free-Field Pressures Generated by a Propeller

In the body of the report, the pressure in the free-field resulting from axial and tangential forces concentrated on a line at the center of the propeller blade is developed. This appendix investigates the free-field pressures that a radial element of a blade generates when the pressures are distributed along the chord rather than concentrated at a point. Although in some cases the errors that result from the concentrated load simplification may be large, the more exact treatment is difficult to apply and is not considered to be adviseable until other uncertainties are reduced. To simplify this analysis, it is assumed that the thrust and torque forces at each radial section are uniformly distributed as pressures over the chord.

Because the propeller is rotating about its axis and because of the pitch of the propeller, it is desirable to designate locations on the propeller in cylindrical coordinates. To remove the rotation from the problem, as far as possible, choose a blade reference line (usually the center of the section) and let the angle between this line and the y, vertical, axis be θ. Designate a location on the blade by the radius r and the angle δ measured from this blade reference line. Let the angle of the leading edge of the section be δ_0 and the total subtended angle of the chord, δ_{ch}. Let $\emptyset$ represent the pitch angle of the section. Let the x coordinate of the blade reference line at the radius r be d. These quantities are shown in Figure D-1. The cartesian coordinates of the point on the propeller blade become:

$$x = d + r\delta \tan \emptyset$$

$$y = r \cos (\theta + \delta)$$

$$z = r \sin (\theta + \delta)$$

The pressure at a free-field point, a, b, c, caused by an elemental thrust force $\frac{F\, d\delta}{\delta_{ch}}$ is

$$P_F = \frac{1}{4\pi} \quad \frac{F\,\emptyset\delta}{\delta} \quad \frac{a-x}{S^3}$$

where $S = \sqrt{(a-x)^2 + (b-y)^2 + (c-z)^2}^{\,2}$

The pressure at a, b, c developed by the thrust forces acting over the whole section is:

$$P_F = \frac{F}{4\pi\delta} \int_{\delta_o - \delta}^{\delta_o} \frac{(a-d-r \quad \tan \emptyset)\, d\delta}{\left\{ (a-d-r\delta \tan \emptyset)^2 + \left[b - r\cos(\theta+\delta)\right]^2 + \left[c - r\sin(\theta + \quad)\right]^2 \right\}^{3/2}}$$

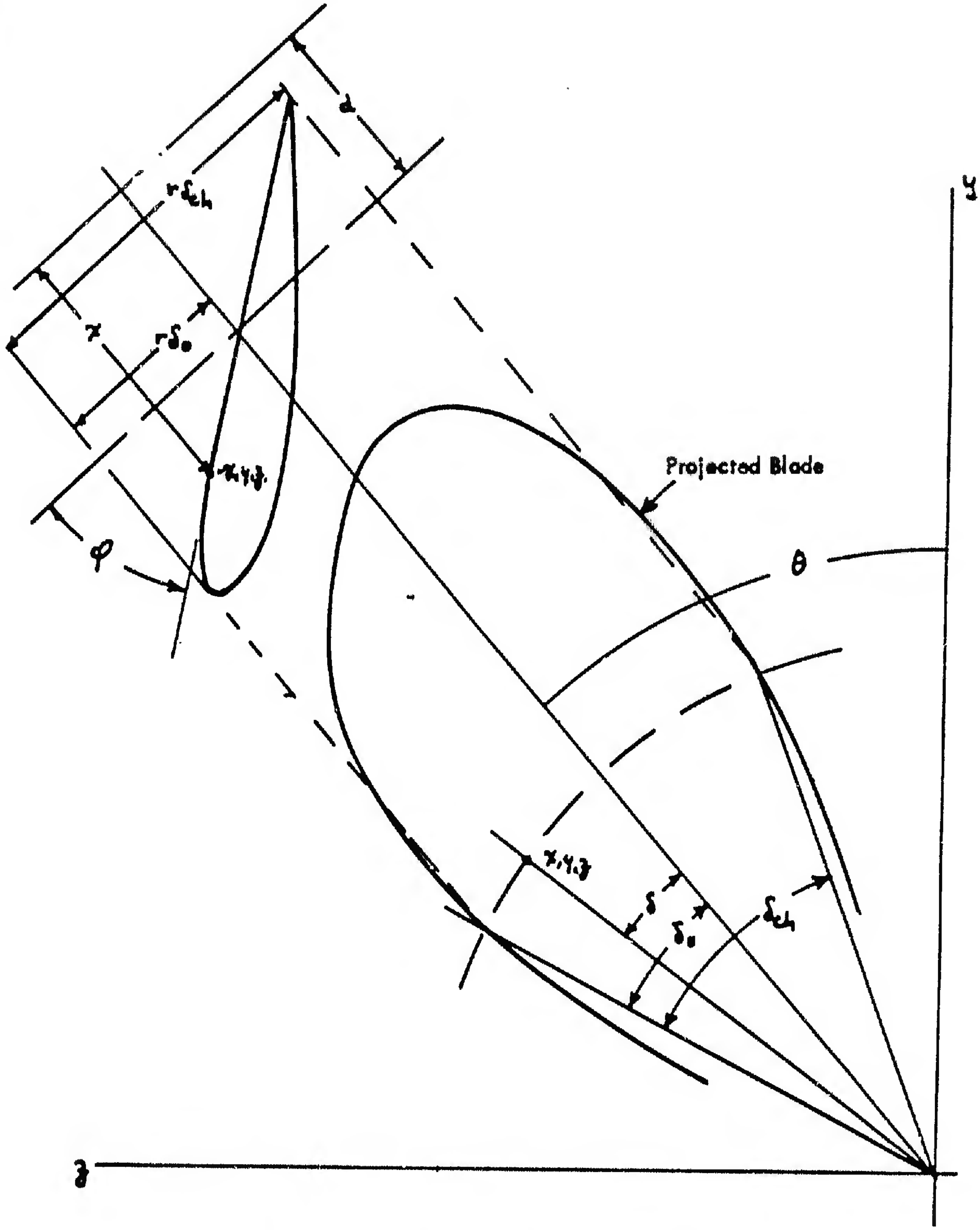

Variables used in Study of Effects of Pitch and
Chordwise Lift Distribution on Free-Field Pressures

Figure D-1

This relationship may be normalized by dividing each distance by R

$$P_F = \frac{F}{4\pi R^2 \delta_{ch}} \int_{\delta_o - \delta_{ch}}^{\delta_o} \frac{\left[\frac{a-d}{R} - \frac{r}{R}\delta \tan \phi\right] d\delta}{\left\{\left[\frac{a-d}{R} - \frac{r\delta}{R}\tan\phi\right]^2 + \left[\frac{b}{R} - \frac{r}{R}\cos(\theta + \delta)\right]^2 + \left[\frac{c}{R} - \frac{r}{R}\sin(\theta + \delta)\right]^2\right\}^{3/2}}$$

To integrate this equation, the sines and cosines of in the denominator are expanded in power series of δ to the second power of δ and then by use of the binomial theorem, the entire denominator is expanded so that it appears in the numerator as a power series of δ .

Thus:

$$\cos(\theta + \delta) = \cos\theta \cos\delta - \sin\theta \sin\delta$$

$$= \left(1 - \frac{\delta^2}{2} \ldots\right)\cos\theta - (\delta + \ldots)\sin\theta$$

$$\sin(\theta + \delta) = \sin\theta\cos\delta + \cos\theta\sin\delta$$

$$= \left(1 - \frac{\delta^2}{2} + \ldots\right)\sin\theta + (\delta + \ldots)\cos\theta$$

and letting $\left(\frac{a-d}{R}\right)^2 + \left(\frac{b}{R}\right)^2 + \left(\frac{c}{R}\right)^2 + \left(\frac{r}{R}\right)^2 = \nu^2$

$$\frac{br}{\nu^2 R^2} = \xi \qquad \frac{cr}{\mu^2 R^2} = \zeta$$

the denominator becomes

$$\Big\{ \nu^2 - 2\xi\nu^2 \cos\theta - 2\zeta\nu^2 \sin\theta + \left[-2\left(\frac{a-d}{R}\right)\left(\frac{r}{R}\right)\tan\phi + 2\nu^2\xi \sin\theta - 2\nu^2\zeta \cos\theta \right]\delta + \left[\left(\frac{r}{R}\right)^2 \tan^2\phi + \nu^2\xi\cos\theta + \nu^2\zeta \sin\theta \right]\delta^2 + \dots \Big\}^{3/2}$$

Expanding the denominator to the minus 3/2 power by the binomial theorem gives the following expression for free-field pressure due to F

$$P_F = \frac{F}{4\pi R^2 \delta_{ch} \nu^3} \frac{1}{(1-2\xi\cos\theta - 2\zeta\sin\theta)^{3/2}} \int_{\delta_o-\delta_{ch}}^{\delta_o} \left[\frac{a-d}{R} + \frac{r}{R}\delta\tan\phi\right]$$

$$\left\{1 - 3A\delta + \left[-\frac{3}{2}B + \frac{15}{2}A^2\right]\delta^2\right\} d\delta$$

where:

$$A = \frac{\frac{1}{\nu^2}\frac{a-d}{R}\frac{r}{R}\tan\phi + \xi\sin\theta - \zeta\cos\theta}{1 - 2\xi\cos\theta - 2\zeta\sin\theta}$$

$$B = \frac{\frac{1}{\nu^2}\left(\frac{r}{R}\right)^2 \tan^2\phi + \xi\cos\theta + \zeta\sin\theta}{1 - 2\xi\cos\theta - 2\zeta\sin\theta}$$

and where $\delta_o = \frac{1}{2}\delta_{ch}$ (the reference line is at the center of the section)

$$P_F = \frac{F\,\frac{a-d}{R}}{4\pi R^2\nu^3\,(1-2\xi\cos\theta - 2\zeta\sin\theta)^{3/2}}$$

$$\left\{1 + \frac{\delta_{ch}^2}{12}\left[-\frac{3}{2}B + \frac{15}{2}A^2 + \frac{3Ar\tan\phi}{a-d}\right] + \dots\right\}$$

Following a similar procedure, it can be shown that the free-field pressure due to the distributed tangential force, G_n is

$$p_G = \frac{G}{4\pi R^2 \nu \left(1 - 2\xi\cos\theta - 2\zeta\sin\theta\right)^{3/2}} \frac{R}{r} \left\{ \left(-\xi\sin\theta + \zeta\cos\theta\right) + \left[\sin\theta\left(\frac{1}{2}\xi + 3\zeta A + \frac{3}{2}\xi B - \frac{15}{2}\zeta A^2\right) + \cos\theta\left(-\frac{1}{2}\zeta + 3\xi A - \frac{3}{2}\zeta B + \frac{15}{2}\zeta A^2\right)\right] \frac{\delta_{ch}^2}{12} \right\}$$

In both cases, the pressure is that due to the concentrated loading plus a correction factor proportional to δ_{ch}^2. It should be recognized that δ_{ch} is not small and that the higher powers of δ_{ch} can only be neglected if their coefficients are small. For propellers whose blades just fail to overlap in the axial projection $\delta_{ch} = 120^\circ = \frac{2}{3}\pi$ for a three bladed and $90^\circ = \pi/2$ for a four bladed propeller.

Checks at critical locations, where the pressure is desired near the propeller and the pitch angle is large, will show that the coefficient of δ^2_{ch} is not always small and negligible. However, it becomes of lesser importance as the distance from the propeller increases and the present state of the art of computing hull forces generated by the propeller does not justify the complications introduced by the more complete treatment.

Appendix E

Diffraction of a Dipole Field by a Wedge

by

Musa Yildiz and

Osman K. Mawardi

1. Introduction

The determination of the diffraction pattern of a wedge in a dipole field is of interest in several situations of practical importance. One such situation, which instigated the work described here, is the study of forced vibrations of the hull of a ship induced by the water-borne pressure fluctuations set up by the propeller. It was shown by Lamb[20] that in the investigation of wave phenomena, a fluctuating force may be represented by an oscillating dipole of the same frequency. Accordingly, a reasonable estimate of the pressure fluctuations on the ship's hull and also in the vicinity of the propeller, can be made by considering the idealized situation of a dipole source close to a rigid wedge of infinite extent.

The general problem of the diffraction of plane sound waves by a wedge has been discussed at great length in the technical literature. The procedure commonly followed in the treatment of these diffraction problems makes use of many valued solutions of the Helmholz wave equation. This fundamental idea originally due to Sommerfeld[31] has turned out to be a very powerful technique for the study of two-dimensional diffraction problems. In the case of three dimensional diffraction problems, however, Sommerfeld's approach is not applicable, and an alternative method of solution for the diffraction field of a wedge had to be explored during the project.

The method that was used was actually developed by Kontorovitch, Lebedev, Titchmarsh, Weyle and others,[32] and makes use of the spectral representation of Green's functions. A common drawback of such spectral representation is that it yields infinite series which are slowly convergent. To remedy this difficulty, a number of artifices, like the saddle point method of integration, are usually introduced to facilitate the calculations. In this report, it has been possible to obviate the above-mentioned difficulty by deriving a closed form for the diffracted field which considerably simplifies the computations.

The present investigation is divided in three parts. In the first part, an expression is obtained for the derivation of the dipole field from a Green's function. The determination of the appropriate Green's function constitutes the bulk of the second part. Finally, in the third part, the pressure distribution on the surface of the wedge is discussed.

2. Statement of problem

The general problem of the diffraction of a dipole field by a rigid wedge can be visualized as a "forced" exterior boundary value problem. This means that the diffraction pattern can be estimated from the solution of the forced scalar wave equation

$$\nabla^2 \Phi + k^2 \Phi = -q(\underline{r}') \qquad (1)$$

In the above equation Φ stands for the velocity potential, and k, the wave number, is the ratio of the radian frequency ω to c, the velocity of sound in open space. The term $q(\underline{r}')$ on the right hand side of (1) is the density distribution function for the dipole sources. The position vector $\underline{r}'$ is reckoned from the edge of the wedge (Fig. 6-1).

The required solution of (1) must be continuous throughout the region exterior to the wedge except over a prescribed region V which coincides with the positions of the dipole sources. The velocity potential must have a vanishing gradient in the direction of the normal to the surface of the rigid wedge. The solution must also satisfy the Sommerfeld's radiation criterion[33]

$$\left(\frac{\partial \Phi}{\partial r} - i k \Phi\right)_{r \to \infty} \sim 0 \qquad (2)$$

in the exterior region as well as on the surface of the wedge.

It is convenient to introduce the Green's function for the exterior region of the wedge. This Green's function $G(\underline{r}, \underline{r}')$ satisfies the inhomogeneous equation.

$$\nabla^2 G(\underline{r}, \underline{r}') + k^2 G(\underline{r}, \underline{r}') = -\delta(\underline{r} - \underline{r}') \qquad (3)$$

where $\underline{r}$ and $\underline{r}'$ are the usual notations for the position vectors of a test point

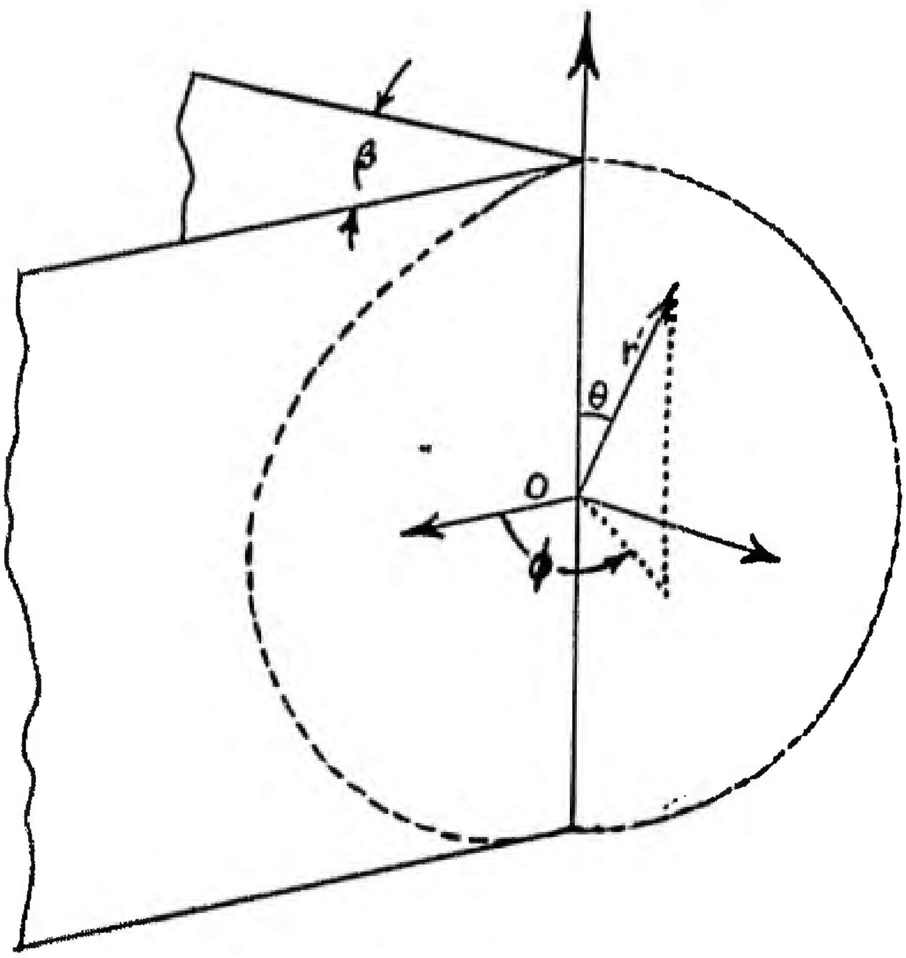

Figure (E-1)

Diagram of coordinate system used.

and source respectively. When the region V over which the sources are distributed reduces to a point, the solution of (1) can be deduced at once from that of (3).

This is shown in the following manner.

The density distribution function $\rho(\underline{r})$ of a point dipole can be written as

$$\rho(\underline{r}') = \lim_{|\Delta \underline{r}'| \to 0} \frac{A(\underline{r}' + \Delta \underline{r}') - A(\underline{r}')}{|\Delta \underline{r}'|}$$

i.e., the resultant of two point sources of equal strength but opposite polarity. In the limit of $|\Delta \underline{r}'|$ tending to zero

$$\rho(\underline{r}') = A\, \partial_{s'} (\delta(\underline{r} - \underline{r}')) \tag{4}$$

where A is the strength of the dipole source and $\partial_{s'}$ is the directional derivative taken along the dipole axis. The differential operator $\partial_{s'}$ affects $\underline{r}'$ only.

From the linearity of the differential equation (3), it follows at once that

$$\Phi(\underline{r}) = A\, \partial_{s'} G(\underline{r}, \underline{r}') \tag{5}$$

The determination of the Green's function consequently completely defines the problem.

3. Green's function for the exterior domain:

The domain exterior to the wedge consists of the region of space inside a sphere of very large radius R, centered at 0 (Fig. E-1) from which the wedge has been subtracted. Because the boundaries of the wedge are easily described by spherical coordinates, these coordinates are introduced as indicated on

Fig. E-1. It is seen that the wedge is defined by the two semi-infinite planes $\phi = 0$ and $\phi = \beta$ whose line of intersection is the polar axis.

The starting point of the argument is an old theorem discussed by Marcuvitz[34] which allows the expression of a Green's function in n dimensions as the integral of the product of n Green's functions in one dimension. The essential points of the proof are reproduced here for convenience.

It is known[35] from the theory of functions that any arbitrary function subject to minor restrictions can be expanded in a series of orthogonal functions which form a complete set. Accordingly, one can express the Green's function $\mathcal{G}(\xi,\eta;\xi',\eta')$ of the wave equation in two dimensions (ξ,η) by means of the series

$$\mathcal{G}(\xi,\eta;\xi',\eta') = \sum_i G_\xi(\xi,\xi',\lambda_i)\,\psi_i(\eta)\,\psi_i(\eta') \tag{6}$$

In the above relation ψ_i is an eigenfunction of the differential equation

$$\mathcal{L}(\psi) = 0 \tag{7}$$

into which the wave equation separates. The relation (6) may be interpreted as an expansion of $\mathcal{G}(\xi,\eta;\xi',\eta')$ in $\psi_i(\eta)$ with coefficients $G_\xi(\xi,\xi';\lambda_i)\,\psi_i(\eta')$. It also turns out that $G_\xi(\xi,\xi';\lambda_i)$ is the Green's function for the "separated" differential equation with separation constant λ_i.

From the theory of spectral representation[36] it can be shown that

$$\sum_i \psi_i(\eta)\psi_i(\eta') = \frac{1}{2\pi i}\oint G_\eta(\eta,\eta';\lambda)\,d\lambda \tag{8}$$

where G_η is the Green's function for Eq. (7) and where the contour integration is taken over the λ - plane. The variable λ stands for the eigenumber of (7). By using Cauchy's theorem, one can write by inspection as a result of (6) and

(8), $$g(\xi,\eta;\xi',\eta') = \frac{1}{2\pi i}\oint G_\xi(\xi,\xi';\lambda)\,G_\eta(\eta,\eta';\lambda)\,d\lambda \qquad (9)$$

The same line of arguments can be extended to three dimensions which proves the original theorem stated above.

Now the three elementary Green's functions which are appropriate to the wedge problem are obtained from

$$\left\{\frac{1}{r^2}\frac{\partial}{\partial r}\left(r^2\frac{\partial}{\partial r}\right)+k^2-\frac{\lambda_1^2}{r^2}\right\}G_r = -\frac{\delta(r-r')}{r^2}\,, \qquad (10)$$

$$\left(\frac{\partial^2}{\partial\phi^2}+\lambda_2^2\right)G_\phi = -\delta(\phi-\phi')\,, \qquad (11)$$

and $$\left\{\frac{1}{\sin\theta}\frac{\partial}{\partial\theta}\sin\theta\frac{\partial}{\partial\theta}-\frac{\lambda_2^2}{\sin^2\theta}+\frac{\lambda_1^2}{\sin\theta}\right\}G_\theta = -\frac{\delta(\theta-\theta')}{\sin\theta'} \qquad (12)$$

In the above equations λ_1, and λ_2 are separation constants. The constant λ_1 is written as $\lambda_1 = n\,(n+1)$. (13)

Since the wedge is rigid, the gradient of all Green's functions in the direction of the normal must vanish. This leads at once to the expansions in orthogonal functions

$$G_\phi = \frac{\cos(\lambda_2 \phi_<)\cos\lambda_2(2\pi-\beta-\phi_>)}{\lambda_2 \sin\lambda_2(2\pi-\beta)} \quad 0<\phi\leqslant 2\pi-\beta \tag{14}$$

$$G_\theta = \frac{\Gamma(\lambda_2+\lambda_1+1)P^{n}_{\lambda_{2+n}}(\cos\theta_<)P^{-n}_{\lambda_{2+n}}\cos\theta_>}{\Gamma(\lambda_2-\lambda_1+1)\sin(\lambda_2-\lambda_1)\pi} \tag{15}$$

$$0\leqslant\theta\leqslant\pi$$

and $$G_r = \frac{i}{K} j_n(Kr_<)h_n^{(1)}(Kr_>), \; 0\leqslant r\leqslant\infty \tag{16}$$

where j_n and $h_n^{(1)}$ stand for the spherical cylindrical functions of order n. The general expression for the Green's function is by analogy to (9):

$$g(r,\phi,\theta;r',\phi',\theta') = \frac{-1}{(2\pi)^2 rr'}\oint d\lambda_1 \oint d\lambda_2\, G_r(\lambda_1)G_\phi(\lambda_2)G_\theta(\lambda_1\lambda_2) \tag{17}$$

The factor rr' appears in the above equation because of the normalization condition[37] for the δ function which requires that

$$r'^2\delta(r-r') = \frac{1}{2\pi i}\oint d\lambda_1\, G_r(\lambda_1) \tag{18}$$

Also the poles of the integrand of (17) occur for

$$\lambda_2 = \frac{m\pi}{(2\pi-\beta)}; \; m = 0, 1, 2, \ldots \tag{19}$$

and for all integral values of n. The estimation of the residues of (17) was made by Marcuvitz[38] for a situation similar to the one considered here. Following a similar technique one finds that the resultant Green's function becomes

$$\mathcal{G}(r,\phi,\theta;r',\phi',\theta')=\frac{1}{(2\pi-\beta)k}\frac{i}{rr'}\sum_m \epsilon_m \cos\frac{m\pi\phi}{2\pi-\beta}\cos\frac{m\pi\phi'}{2\pi-\beta}\sum_{n=m}^{\infty}(2n+1)\frac{\left(n-\frac{m\pi}{2\pi-\beta}\right)!}{\left(n+\frac{m\pi}{2\pi-\beta}\right)!}\times$$

$$\times P_n^{\frac{m\pi}{2\pi-\beta}}(\cos\theta)P_n^{\frac{m\pi}{2\pi-\beta}}(\cos\theta')j_{n+\frac{m\pi}{(2\pi-\beta)}}(kr)h^{(1)}_{n+\frac{m\pi}{(2\pi-\beta)}}(kr') \qquad (20)$$

In the above expression ϵ_m is Neuman's factor which is $\frac{1}{(2-\delta_{om})}$.

The above series can be written in closed form by analogy with a standard expansion[39] for $\frac{e^{ik(\underline{r}-\underline{r}')}}{|\underline{r}-\underline{r}'|}$ which is explicitly

$$\frac{e^{ik|(\underline{r}-\underline{r}')|}}{|\underline{r}-\underline{r}'|}=\frac{1}{2\pi}\frac{\exp ik\left[r^2+r'^2-2rr'(\cos\theta\cos\theta'+\sin\theta\sin\theta'\cos(\phi-\phi')\right]^{\frac{1}{2}}}{\left[r^2+r'^2-2rr'(\cos\theta\cos\theta'+\sin\theta\sin\theta'\cos(\phi-\phi')\right]^{\frac{1}{2}}}$$

$$=\frac{i}{2\pi krr'}\sum_m \epsilon_m \cos m(\phi-\phi')\sum_{n=m}^{\infty}(2n+1)\frac{(n-m)!}{(n+m)!}P_n^m(\cos\theta)\times \qquad (21)$$

$$\times P_n^m(\cos\theta')\times j_{n+m}(kr)h^{(1)}_{n+m}(kr')$$

By inspection, the two series (20) and (21) bear a great deal of similarity to each other and it can be shown that the expression for (20) can be written in closed form as

$$\mathcal{G}(r,\phi,\theta;r',\phi',\theta')=\frac{1}{(2\pi-\beta)}\,\frac{\exp ik\left[r^2+r'^2-2rr'\left(\cos\theta\cos\theta'+\sin\theta\sin\theta'\cos\frac{\pi\phi}{2\pi-\beta}\cos\frac{\pi\phi'}{2\pi-\beta}\right)\right]^{\frac{1}{2}}}{\left[r^2+r'^2-2rr'\left(\cos\theta\cos\theta'+\sin\theta\sin\theta'\cos\frac{\pi\phi}{2\pi-\beta}\cos\frac{\pi\phi'}{2\pi-\beta}\right)\right]^{\frac{1}{2}}} \tag{22}$$

4. <u>Pressure distribution</u>

The distribution of the pressure on the hull can be obtained from Eq. (5). The directional derivative in spherical coordinates is given by the general expression

$$\partial_{s'}=\alpha_1\left(\frac{\partial}{\partial r'}\right)+\alpha_2\left(\frac{1}{r'}\frac{\partial}{\partial\theta'}\right)+\alpha_3\left(\frac{1}{r'\sin\theta'}\frac{\partial}{\partial\phi'}\right) \tag{23}$$

where $\alpha_1, \alpha_2, \alpha_3$ are the direction cosines of the dipole axis referred to a primed frame shown in Fig. E-2 , and the polar axis of which is r'.

From elementary considerations the direction cosines of the primed frame with respect to the unprimed frame is given by the table indicated below.

	x	y	z
$i_{r'}$	$\sin\theta'\cos\phi'$	$\sin\theta'\sin\phi'$	$\cos\theta'$
$i_{\theta'}$	$\cos\theta'\cos\phi'$	$\cos\theta'\sin\phi'$	$-\sin\theta'$
$i_{\phi'}$	$-\sin\phi'$	$\cos\phi'$	0

(24)

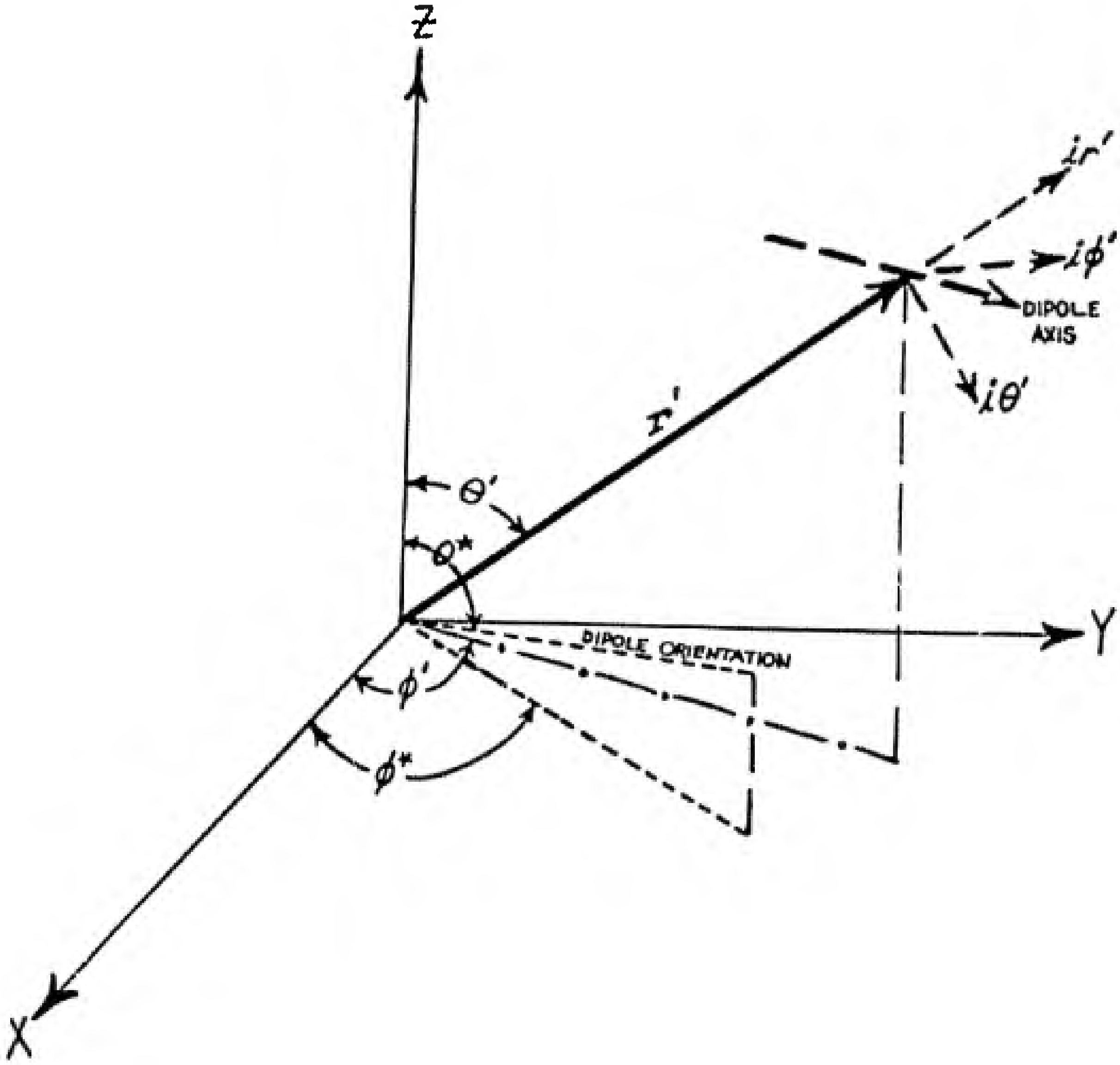

Figure E-2

Frame of reference used in the evaluation of the directional derivative of Eq. (5).

It is easy, but laborious, to derive the coefficients α_1, α_2, α_3 starting from the value of the direction cosines of the dipole axis referred to the unprimed frame. These are found to be

$$\sin\theta^* \cos\phi^* = \sin\theta^* \sin\phi^* : \quad \cos\Theta^* \tag{25}$$

Now the required α's are as shown below

$$\alpha_1 = \cos\theta' \cos\theta^* + \sin\theta' \sin\theta^* \cos(\phi' - \phi^*)$$

$$\alpha_2 = -\cos\theta^* \sin\theta' + \sin\theta^* \cos\theta' \cos(\phi^* - \phi') \tag{26}$$

and $$\alpha_3 = \sin\theta^* \sin(\phi^* - \phi').$$

The general relation for the pressure distribution is then

$$p_w(r,\phi,\theta;r',\phi',\theta') = -\frac{i\omega\rho_0}{(2\pi-\beta)} \frac{(ikR_w - 1)}{R_w^3} \times$$
$$\times e^{ikR_w}\left\{\alpha_1\left[r' - r\left(\cos\theta\cos\theta' + \sin\theta\sin\theta'\cos\frac{\pi\phi}{2\pi-\beta}\cos\frac{\pi\phi'}{2\pi-\beta}\right)\right] - \right.$$
$$-\alpha_2 r\left(\sin\theta\cos\theta'\cos\frac{\pi\phi}{2\pi-\beta}\cos\frac{\pi\phi'}{2\pi-\beta} - \cos\theta\sin\theta'\right) + \tag{27}$$
$$\left. + \alpha_3\frac{\pi r}{2\pi-\beta}\sin\theta\sin\theta'\cos\frac{\pi\phi}{2\pi-\beta}\sin\frac{\pi\phi'}{2\pi-\beta}\right\}$$

when we have written

$$R_w = \left[r^2 + r'^2 - 2rr'\left(\cos\theta\cos\theta' + \sin\theta\sin\theta'\cos\frac{\pi\phi}{2\pi-\beta}\cos\frac{\pi\phi'}{2\pi-\beta}\right)\right]^{\frac{1}{2}} \tag{28}$$

It is convenient to reduce the results to a normalized pressure which gives an indication of the extent of the distortion of the dipole field by the wedge. Accordingly, a diffraction "coefficient" μ is introduced. This coefficient defines the ratio of the pressure on the wedge to the equivalent free-field pressure due to a dipole placed at the same position.

In a similar manner one finds the expression for the free-field of a dipole to be

$$p_f = \frac{-i\omega\rho_o}{2\pi}\,\frac{(ikR_f - 1)}{R_f^3}\,e^{ikR_f}\Big\{\alpha_1\big[r' - r(\cos\theta\cos\theta' + \sin\theta\sin\theta'\cos(\phi-\phi'))\big]$$
$$-\alpha_2 r\big(\sin\theta\cos\theta'\cos(\phi-\phi') - \cos\theta\sin\theta'\big) - \alpha_3 r\sin\theta\sin\theta'\sin(\phi-\phi')\Big\} \tag{29}$$

in which we have set

$$R_f = \left[r^2 + r'^2 - 2rr'(\cos\theta\cos\theta' + \sin\theta\sin\theta'\cos(\phi-\phi'))\right]^{\frac{1}{2}} \tag{30}$$

Upon substitution of the explicit values of the direction cosines from (26), Eqs. (27) and (29) become, after some algebraic manipulations,

$$p_w = \frac{-i\omega\rho_o}{2\pi-\beta}\,\frac{(ikR_w - 1)}{R_w^3}\,e^{ikR_w}\Big\{(r'\cos\theta' - r\cos\theta)\cos\theta^* +$$
$$+\left(r'\sin\theta' - r\sin\theta\,\cos\frac{\pi\phi}{2\pi-\beta}\,\cos\frac{\pi\phi'}{2\pi-\beta}\right)\sin\theta^*\cos(\phi^* - \phi') + \tag{27}$$
$$+\frac{\pi r}{2\pi-\beta}\sin\theta^*\sin(\phi^* - \phi')\sin\theta\sin\theta'\cos\frac{\pi\phi}{2\pi-\beta}\,\sin\frac{\pi\phi'}{2\pi-\beta}\Big\},$$

similarly

$$\mathcal{P}_f = \frac{-i\omega\rho_0}{2\pi}\,\frac{(ik\mathcal{R}_f-1)}{\mathcal{R}_f^{3}}\,e^{ik\mathcal{R}_f}\Big\{\big(r'\cos\Theta' - r\cos\Theta\big)\cos\Theta^{*} +$$

$$+\big(r'\sin\Theta' - r\sin\Theta\cos(\phi-\phi')\big)\sin\Theta^{*}\cos(\phi^{*}-\phi') - \qquad (29)$$

$$-r\sin\Theta^{*}\sin\Theta\,\sin\Theta'\sin(\phi^{*}-\phi')\sin(\phi-\phi')\Big\}.$$

We now consider a number of special cases for which the dipole axis orientation is

i) parallel to the edge of the wedge

ii) parallel to one face of the wedge but perpendicular to the edge

iii) perpendicular to one face of the wedge

For case i) we find that

$\Theta^{*} = 0$; ϕ^{*} is undefined

$\alpha_1 = \cos\Theta'$

$\alpha_2 = -\sin\Theta'$

$\alpha_3 = 0$

the corresponding coefficient is

$$\Big(\qquad \mu = \frac{2\pi}{(2\pi-\beta)}\left(\frac{\mathcal{R}_f}{\mathcal{R}_w}\right)^{3}\frac{(ik\mathcal{R}_w-1)}{(ik\mathcal{R}_f-1)}\,e^{ik(\mathcal{R}_w-\mathcal{R}_f)} \qquad (31)$$

When the dipole is situated on a line perpendicular to the wedge surface (i.e. on the y axis), $\phi' = \Theta' = \frac{\pi}{2}$. Under this assumption, $\mathcal{R}_{f,1}$, $\mathcal{R}_{w,1}$ are the corresponding values of $\mathcal{R}_f, \mathcal{R}_w$ for $\theta' = \frac{\pi}{2}$. More explicitly they are

$$\mathcal{R}_{w,1} = \left[r^2 + r'^2 - 2rr'\sin\theta\cos\left(\frac{\pi\phi}{2\pi-\beta}\right)\cos\left(\frac{\pi^2}{2(2\pi-\beta)}\right)\right]^{\frac{1}{2}} \tag{33}$$

and

$$\mathcal{R}_{f,1} = \left[r^2 + r'^2 - 2rr'\sin\theta\sin\phi\right]^{\frac{1}{2}}. \tag{34}$$

For case (ii) we also find that

$$\theta^* = \frac{\pi}{2}\ ;\ \phi^* = 0$$

$$\alpha_1 = \sin\theta'\cos\phi'$$

$$\alpha_2 = \cos\theta'\cos\phi'$$

$$\alpha_3 = -\sin\phi'$$

The index μ is thus in general for this case:

$$\mu = \frac{2\pi}{2\pi-\beta}\left(\frac{\mathcal{R}_f}{\mathcal{R}_w}\right)^3 \frac{(ik\mathcal{R}_w - 1)}{(ik\mathcal{R}_f - 1)} e^{ik(\mathcal{R}_w - \mathcal{R}_f)} \times f^{(2)}(r, r', \theta, \theta', \phi, \phi') \tag{35}$$

where

$$f^{(2)} = \left\{\cos\phi'\left[r'\sin\theta' - r\sin\theta\cos\frac{\pi\phi}{2\pi-\beta}\cos\frac{\pi\phi'}{2\pi-\beta}\right] - \frac{\pi}{2\pi-\beta}r\sin\phi'\sin\theta\right.$$

$$\left.\sin\theta'\cos\frac{\pi}{2\pi-\beta}\phi\sin\frac{\pi\phi'}{2\pi-\beta}\right\}\left\{\cos\phi'\left[r'\sin\theta'\right.\right.$$

$$\left.\left.-r\sin\theta\cos(\phi-\phi')\right] + r\sin\theta'\sin\phi'\sin\theta\sin(\phi-\phi')\right\}^{-1}$$

Whenever the dipole is placed on the y axis, i. e. $\phi' = \theta' = \frac{\pi}{2}$, μ becomes

$$\mu = \frac{2\pi}{2\pi-\beta}\left(\frac{R_{f,1}}{R_{w,1}}\right)^3\left(\frac{ikR_{w,1}-1}{ikR_{f,1}-1}\right) e^{ik(R_{w,1}-R_{f,1})}\left(\frac{\pi}{2\pi-\beta}\right) \frac{\cos\left(\frac{\pi\phi}{2\pi-\beta}\right)\cos\frac{\pi^2}{2(2\pi-\beta)}}{\cos\phi} \quad (36)$$

Finally, for case (iii), we have

$\theta^* = \frac{\pi}{2}$; $\phi^* = \frac{\pi}{2}$

$\alpha_1 = \sin\theta'\sin\phi'$

$\alpha_2 = \cos\theta'\sin\phi'$

$\alpha_3 = \cos\phi'$

which leads to a corresponding value of the index

$$\mu = \frac{2\pi}{2\pi-\beta}\left(\frac{R_f}{R_w}\right)^3 \frac{(ikR_w-1)}{(ikR_f-1)} e^{ik(R_w-R_f)} \times f^{(3)}(r, r', \theta, \theta', \phi, \phi')$$

$$f^{(3)} = \left\{ \sin\phi' \left[r'\sin\theta' - r\sin\theta\cos\frac{\pi\phi}{2\pi-\beta}\cos\frac{\pi\phi'}{2\pi-\beta}\right] \right. \quad (37)$$

$$\left. + \frac{\pi}{2\pi-\beta}\, r\cos\phi'\sin\theta\sin\theta'\cos\frac{\pi\phi}{2\pi-\beta}\sin\frac{\pi\phi'}{2\pi-\beta} \right\}$$

$$\left\{ \sin\phi'\left[r'\sin\theta' - r\sin\theta\cos(\phi-\phi')\right] - r\cos\phi\sin\theta\sin\theta'\sin(\phi-\phi')\right\}^{-1}$$

Here again when we place the dipole on the y axis, μ reduces to

$$\mu = \frac{2\pi}{2\pi-\beta}\left(\frac{R_{f,1}}{R_{w,1}}\right)^3\left(\frac{ikR_{w,1}-1}{ikR_{f,1}-1}\right)e^{ik(R_{w,1}-R_{f,1})}\;\frac{1-\frac{r}{r'}\sin\theta\cos\frac{\pi\phi}{2\pi-\beta}\cos\frac{\pi^2\phi}{2(2\pi-\beta)}}{1+\frac{r}{r'}\sin\theta\sin\phi} \tag{38}$$

The dependence of μ on some selected values of the dimensionless parameter $\frac{r}{r'}$ is shown in the table below:

Values of μ as a function of $\frac{r}{r'}$ for the values of ϕ and ϕ' indicated and for $\phi^* = 0,\ \theta^* = \frac{\pi}{2},\ \theta' = \theta = \frac{\pi}{2}\quad \beta = 15^\circ$

$\frac{r}{r'}$	$\phi' = \frac{\pi}{2};\ \phi=0$	$\phi' = \frac{\pi}{2};\ \phi=2\pi-\beta$	$\phi' = \frac{2\pi}{3};\ \phi=0$	$\phi' = \frac{2\pi}{3};\ \phi=2\pi-\beta$
0			1.04	1.04
0.1	0.415	0.362	1.193	
0.2	0.425		1.385	0.91
0.3	0.75	0.262		
0.4	0.95			
0.5		0.24	2.015	0.70
0.6	1.427			
0.8	1.781	0.21		
1.0	1.980	.208	2.157	0.424

Table E-1

Appendix F

Programming of Calculation of Dynamic Properties of Propulsion Shafting

For those who are interested in the programming of the calculation of the shaft bearing reactions, the following notes supplied by Dr. Elizabeth Cuthill of the David Taylor Model Basin are given. The engineering analysis from which these notes were developed is in the section of the report on the dynamical properties of the propulsion shafting (pages 60 through 85).

Calculations Performed in GVC I (Preliminary)

A. Option 1. Flexural Vibrations in a Plane

1) Initial Calculations

First the moment of inertia I_s for each section is calculated using

$$(1) \qquad I_s = \frac{\pi}{64}\left(d_o^4 - d_i^4\right)$$

where

d_o is the "outer diameter" of the section,

d_i is the "inner diameter" of the section.

Then the bending rigidity β for each section is also computed using

$$(2) \qquad \beta = EI_s$$

where E is the modulus of elasticity of the section material. Finally, the parameter $\tilde{\alpha}$ is calculated

$$(3) \qquad \tilde{\alpha} = \frac{\alpha^4}{\omega^2} = \frac{\rho\,\pi\,(d_o^2 - d_i^2)}{4\beta}$$

where ρ is the density of the section material, and ω is the excitation frequency.

2) Calculation of the Elements of $(I + K^{(n)})$.

The elements of $I + K^{(n)}$, the discontinuity matrix to be used at the start of section n can be computed directly from the input data and the current value being used for ω , i.e.

$$(4) \quad I + K^{(n)} = \begin{pmatrix} 1 & 0 & 0 & 0 \\ 0 & 1 & 0 & 0 \\ k_{51}^{(n)} - \omega^2 m^{(n)} & k_{52}^{(n)} & 1 & 0 \\ k_{61}^{(n)} & k_{62}^{(n)} - \omega^2 I_d & 0 & 1 \end{pmatrix}$$

for n = 1, 2, 3, ...N + 1.

3) Calculation of the Elements of $\bar{T}^{(n)}$

The elements of $T^{(n)}$ the transfer matrix for section n involve the following combinations of trigonometric and hyperbolic functions:

$$f_1 \ (\alpha , l) = (\sinh \alpha l + \sin \alpha l) \ /2 \alpha$$

$$f_2 \ (\alpha , l) = (\sinh \alpha l - \sin \alpha l) \ /2 \alpha^3$$

$$(5) \qquad f_3 \ (\alpha , l) = (\cosh \alpha l + \cos \alpha l) \ / 2$$

$$f_4 \ (\alpha , l) = (\cosh \alpha l - \cos \alpha l) \ /2 \alpha^2$$

where

l is the section length, and

$$\alpha = \sqrt[4]{\tilde{q} \omega^2}$$

with α given by equation (3). These expressions are approximated as described below. First the maximum value of η is determined so that

$$\frac{\alpha l}{2^{\eta}} < \sqrt{10}$$

(It is assumed that $\eta \leq 5$.) Then the following approximate expressions for the functions f_1, f_2, f_3, f_4 defined by equations (5) are in error by less than 10^{-9}.

(6)

$$f_1\left(\alpha,\frac{\ell}{2^n}\right) \approx \frac{\ell}{2^n}\left[1+\left(\frac{\alpha\ell}{2^n}\right)^4\left[\frac{1}{5!}+\left(\frac{\alpha\ell}{2^n}\right)^4\left[\frac{1}{9!}+\left(\frac{\alpha\ell}{2^n}\right)^4\left[\frac{1}{13!}+\left(\frac{\alpha\ell}{2^n}\right)^4\cdot\frac{1}{17!}\right]\right]\right]\right]$$

$$f_2\left(\alpha,\frac{\ell}{2^n}\right) \approx \left(\frac{\ell}{2^n}\right)^3\left[\frac{1}{3!}+\left(\frac{\alpha\ell}{2^n}\right)^4\left[\frac{1}{7!}+\left(\frac{\alpha\ell}{2^n}\right)^4\left[\frac{1}{11!}+\left(\frac{\alpha\ell}{2^n}\right)^4\left[\frac{1}{15!}+\left(\frac{\alpha\ell}{2^n}\right)^4\cdot\frac{1}{19!}\right]\right]\right]\right]$$

$$f_3\left(\alpha,\frac{\ell}{2^n}\right) \approx 1+\left(\frac{\alpha\ell}{2^n}\right)^4\left[\frac{1}{4!}+\left(\frac{\alpha\ell}{2^n}\right)^4\left[\frac{1}{8!}+\left(\frac{\alpha\ell}{2^n}\right)^4\left[\frac{1}{12!}+\left(\frac{\alpha\ell}{2^n}\right)^4\cdot\frac{1}{16!}\right]\right]\right]\right]$$

$$f_4\left(\alpha,\frac{\ell}{2^n}\right) \approx \left(\frac{\ell}{2^n}\right)^2\left[\frac{1}{2}+\left(\frac{\alpha\ell}{2^n}\right)^4\left[\frac{1}{6!}+\left(\frac{\alpha\ell}{2^n}\right)^4\left[\frac{1}{10!}+\left(\frac{\alpha\ell}{2^n}\right)^4\left[\frac{1}{14!}+\left(\frac{\alpha\ell}{2^n}\right)^4\cdot\frac{1}{18!}\right]\right]\right]\right]$$

Then for $i = 0, 1, 2, \ldots, \eta-1$, let $l_{i+1} = 2l_i$ with $l_o = \frac{\ell}{2^\eta}$. The following recursion relations based on the double angle formulas can now be used to obtain $f_1(a, l)$, $f_2(a, l)$, $f_3(a, l)$, $f_4(a, l)$ where $l = \ell_\eta$:

(7)

$$f_1(a, l_{i+1}) = 2\ f_1(a, l_i)\, f_3(a, l_i) + a\ f_2(a, l_i)\ f_4(a, l_i)$$

$$f_2(a, l_{i+1}) = 2\ f_2(a, l_i)\ f_3(a, l_i) + f_1(a, l_i)\ f_4(a, l_i)$$

$$f_3(a, l_{i+1}) = 1 + 4a\ f_1(a, l_i)\ f_2(a, l_i)$$

$$f_4(a, l_{i+1}) = 4\ f_3(a, l_i)\ f_4(a, l_i)$$

With the availability of approximations to these functions and of values for β and a (labelled β_n and a_n) for section n, the elements of the transfer matrix $T^n_{\underline{z}}$ for section n can now be calculated. In the expression for T_{*}^{n} given below, $f_1^{(n)}$, $f_2^{(n)}$, $f_3^{(n)}$, $f_4^{(n)}$ are used to represent the values of $f_1(\alpha, 1)$, $f_2(\alpha, 1)$, $f_3(\alpha, 1)$, $f_4(\alpha, 1)$ respectively for the n^{th} section.

$$(8)\quad T = \begin{pmatrix} f_3^{(n)} & f_1^{(n)} & -\frac{1}{\beta n} f_2^{(n)} & \frac{1}{\beta n} f_4^{(n)} \\ \alpha_n^4 f_2^{(n)} & f_3^{(n)} & -\frac{1}{\beta n} f_4^{(n)} & \frac{1}{\beta n} f_1^{(n)} \\ -\beta_n \alpha_n^4 f_1^{(n)} & -\beta_n \alpha_n^4 f_4^{(n)} & f_3^{(n)} & -\alpha_n^4 f_2^{(n)} \\ \beta_n \alpha_n^4 f_4^{(n)} & \beta_n \alpha_n^4 f_2^{(n)} & -f_1^{(n)} & f_3^{(n)} \end{pmatrix}$$

4) Calculation of the Cumulative Transfer Matrices $S^{(n)}$ and $T^{(n)}$

Let $S^{(n)} = (A_{ij}^{(n)})$ represent the transfer matrix relating the solution vector following the discontinuity at the start of section n, $n \geq 1$, to the vector representing the initial conditions, and $T^{(n)} = (t_{ij}^{(n)})$ represent the identity matrix for n = 1, and the transfer matrix relating the solution at the end of section n to the vector representing the initial conditions. The elements of the cumulative transfer matrices are computed using the matrix relations:

$$(9)\quad \left.\begin{aligned} S^{(n)} &= (I + K^{(n)})\, T^{(n-1)} \\ T^{(n)} &= T_{*}^{(n)}\, S^{(n)} \end{aligned}\right\} \quad \text{for } n = 1, 2, \ldots, N$$

and finally for the end of the last section:

$$S^{(N+1)} = K^{(N+1)} \quad T^{(N)}$$

These matrix relations are equivalent to the following set of relations:

$$\text{(10)} \quad \left.\begin{aligned} s_{ij}^{(n)} &= \sum_{\nu=1}^{4} (\delta_{i\nu} + K_{i\nu}^{(n)}) t_{\nu j}^{(n-1)} \\ t_{ij}^{(n)} &= \sum_{\nu=1}^{4} t_{z,i\nu}^{(n)} \; s_{\nu j}^{(n)} \end{aligned}\right\} \qquad \begin{aligned} &\text{for } i,j = 1,2,3,4 \\ &n = 1,2,\ldots,N \end{aligned}$$

and

$$s_{ij}^{(N+1)} = \sum_{\nu=1}^{4} (\delta_{i\nu} + K_{i\nu}^{(N+1)}) t_{\nu j}^{(N)} \qquad \text{for } i,j = 1,2,3,4$$

where

$$\delta_{ij} = \begin{cases} 1 \text{ when } i = j \\ 0 \text{ when } i \neq j \end{cases}$$

5) Calculation of the Initial Conditions and Solution Vectors

Let the vector representing the initial conditions be given by

$$\vec{\delta}^{(1)} = \begin{pmatrix} a_1 \\ a_2 \\ a_3 \\ a_4 \end{pmatrix} = \begin{pmatrix} \delta_x^{(1)} \\ \theta_x^{(1)} \\ F_x^{(1)} \\ M_x^{(1)} \end{pmatrix}$$

and the conditions at the end of the last section by:

$$\vec{b}^{\,(N+1)} = \begin{pmatrix} b_1 \\ b_2 \\ b_3 \\ b_4 \end{pmatrix} = \begin{pmatrix} \delta_x^{(N+1)} \\ \theta_x^{(N+1)} \\ F_x^{(N+1)} \\ M_x^{(N+1)} \end{pmatrix}$$

Then suppose that the boundary conditions specified are a_{i_1}, a_{i_2}, b_{e_1}, b_{e_2}, where i_1 and i_2, e_1 and e_2 are each taken from the set of indices 1, 2, 3, 4. Then i_3 and i_4 can be appended to the indices i_1 and i_2 so that i_1, i_2, i_3, i_4 represent a permutation of the indices 1, 2, 3, 4. Let P_i represent the permutation matrix such that

$$P_i \begin{pmatrix} a_1 \\ a_2 \\ a_3 \\ a_4 \end{pmatrix} = \begin{pmatrix} a_{i_1} \\ a_{i_2} \\ a_{i_3} \\ a_{i_4} \end{pmatrix}$$

Similarly, let e_1, e_2, e_3, e_4 also represent a permutation of the indices 1,2,3,4 and let P_e represent the permutation matrix such that

$$P_e \begin{pmatrix} b_1 \\ b_2 \\ b_3 \\ b_4 \end{pmatrix} = \begin{pmatrix} b_{e_1} \\ b_{e_2} \\ b_{e_3} \\ b_{e_4} \end{pmatrix}$$

Now $S^{(N+1)}$ has been so defined that

$$\vec{\delta}^{(N+1)} = S^{(N+1)} \vec{\delta}^{(1)}$$

or equivalently,

$$P_e \vec{\delta}^{(N+1)} = P_e S^{(N+1)} P_i^{-1} P_i \vec{\delta}^{(1)}$$

Thus

$$b_{e_1} = s_{e_1 i_1}^{(N+1)} a_{i_1} + s_{e_1 i_2}^{(N+1)} a_{i_2} + s_{e_1 i_3}^{(N+1)} a_{i_3} + s_{e_1 i_4}^{(N+1)} a_{i_4}$$

(11)

$$b_{e2} = s_{e_2 i_1}^{(N+1)} a_{i_1} + s_{e_2 i_2}^{(N+1)} a_{i_2} + s_{e_1 i_3}^{(N+1)} a_{i_3} + s_{e_1 i_4}^{(N+1)} a_{i_4}$$

giving a system of two linear equation in two unknowns, a_{i_3} and a_{i_4}, the other entries b_{e_1}, b_{e_2}, a_{i_1}, a_{i_2} being the end conditions supplied as input,and the elements $s_{i_j}^{(N+1)}$, $i = e_1, e_2$, $j = 1,2,3,4$ being elements of the transfer matrix $S^{(N+1)}$. Therefore, these equations can be solved for a_{i_3} and a_{i_4} provided matrix of their coefficients is non-singular giving a full set of initial conditions, i.e. all of the elements of the vector $\delta^{(1)}$. Now the set of solution vectors $^{(n)}$ for n = 1, 2, . . . , N+1 can be computing using

$$\vec{\lambda}^{(n)} = S^{(n)} \vec{\delta}^{(1)} \tag{12}$$

In addition, the solution vectors $\delta^{(n1.5)}$ just ahead of the discontinuity at section n for n = 1,2, . . . , N can be calculated using

$$\vec{\delta}^{(n1.5)} = T^{(n)} \vec{\delta}^{(1)} \tag{13}$$

The program is set up so that once the elements of $S^{(n)}$ and $T^{(n)}$ are available, a number of sets of end conditions can be used and the corresponding solution vectors obtained.

B. Option 2. Coupled Flexural Vibrations in Two Planes

1) Initial Calculations

The moment of inertia I_s, the bending rigidity β, and the parameter $\tilde{\alpha}$ are computed for each section using equations (1), (2), and (3), respectively.

2) Calculation of the Elements of $(I + K^{(n)})$.

The elements of $I + K^{(n)}$, the discontinuity matrix to be used at the start of section n can be computed directly from the input data and the current value being used for ω , i.e.

$$
(14) \quad I+K^{(n)} = \begin{pmatrix}
1 & 0 & 0 & 0 & 0 & 0 & 0 & 0 \\
0 & 1 & 0 & 0 & 0 & 0 & 0 & 0 \\
0 & 0 & 1 & 0 & 0 & 0 & 0 & 0 \\
0 & 0 & 0 & 1 & 0 & 0 & 0 & 0 \\
k_{51}^{(n)} - \omega^2 m^{(n)} & k_{52}^{(n)} & k_{53}^{(n)} & k_{54}^{(n)} & 1 & 0 & 0 & 0 \\
k_{61}^{(n)} & k_{62}^{(n)} - \omega^2 I_d^{(n)} & k_{63}^{(n)} & k_{64}^{(n)} + iG^{(n)} & 0 & 1 & 0 & 0 \\
k_{71}^{(n)} & k_{72}^{(n)} & k_{73}^{(n)} - \omega^2 m^{(n)} & k_{74}^{(n)} & 0 & 0 & 1 & 0 \\
k_{81}^{(n)} & k_{82}^{(n)} - i\,G^{(n)} & k_{83}^{(n)} & k_{84}^{(n)} - \omega^2 I_d^{(n)} & 0 & 0 & 0 & 1
\end{pmatrix}
$$

where

$$G^{(n)} = I_d \, \Omega \, \omega$$

3) <u>Calculation of the Elements of $T_{\Xi}^{(n)}$</u>

The elements of $T_{\Xi}^{(n)}$, the transfer matrix for section n, involve the combinations of trigonometric and hyperbolic functions given in equation (5), and they are calculated in the same way as for Option 1. Using the notation of equation (8), the matrix $T_{\text{II}}^{(n)}$ for the current option is given by

$$
(15)\quad T_{\text{II}}^{(n)} = \begin{pmatrix}
f_3^{(n)} & f_1^{(n)} & 0 & 0 & -\frac{1}{\beta_n} f_2^{(n)} & \frac{1}{\beta_n} f_4 & 0 & 0 \\
\alpha_n^4 f_2^{(n)} & f_3^{(n)} & 0 & 0 & -\frac{1}{\beta_n} f_4^{(n)} & \frac{1}{\beta_n} f_1^{(n)} & 0 & 0 \\
0 & 0 & f_3^{(n)} & f_1^{(n)} & 0 & 0 & -\frac{1}{\beta_n} f_2^{(n)} & \frac{1}{\beta_n} f_4^{(n)} \\
0 & 0 & \alpha_n^4 f_2^{(n)} & f_3^{(n)} & 0 & 0 & \frac{1}{\beta_n} f_4^{(n)} & \frac{1}{\beta_n} f_1^{(n)} \\
-\beta_n \alpha_n^4 f_1^{(n)} & -\beta_n \alpha_n^4 f_4^{(n)} & 0 & 0 & f_3^{(n)} & -\alpha^4 f_2^{(n)} & 0 & 0 \\
\beta_n \alpha_n f_4^{(n)} & \beta_n \alpha_n f_2^{(n)} & 0 & 0 & -f_1^{(n)} & f_3^{(n)} & 0 & 0 \\
0 & 0 & -\beta\alpha^4 f_1^{(n)} & -\beta \alpha^4 f_4^{(n)} & 0 & 0 & f_3^{(n)} & -\alpha^4 f_2^{(n)} \\
0 & 0 & \beta\alpha^4 f_4^{(n)} & \beta \alpha^4 f_2^{(n)} & 0 & 0 & -f_1^{(n)} & f_3^{(n)}
\end{pmatrix}
$$

4) Calculation of the Cumulative Transfer Matrices $S^{(n)}$ and $T^{(n)}$

Using the same notation as for Option (1), the elements of the cumulative transfer matrices $S^{(n)}$ and $T^{(n)}$ are calculated using the matrix relations (9). However, in this case K, and therefore S and T may have complex elements, i. e. the elements of these matrices appearing in equations (10), in particular k_{ij} , t_{ij} , and s_{ij} may all be complex numbers in this case. Also, the matrices are of order 8 so that the range of indices i, j is the set of integers from 1 to 8, inclusive.

5) Calculation of the Initial Conditions and Solution Vectors

For this option, the vector representing the initial conditions is given by

$$\vec{\delta}^{(1)} = \begin{pmatrix} a_1 \\ a_2 \\ a_3 \\ a_4 \\ a_5 \\ a_6 \\ a_7 \\ a_8 \end{pmatrix} = \begin{pmatrix} \delta_x^{(1)} \\ \theta_x^{(1)} \\ \delta_y^{(1)} \\ \theta_y^{(1)} \\ F_x^{(1)} \\ M_x^{(1)} \\ F_y^{(1)} \\ M_y^{(1)} \end{pmatrix}$$

and the end conditions be given by

$$\vec{\delta}^{(N+1)} = \begin{pmatrix} b_1 \\ b_2 \\ b_3 \\ b_4 \\ b_5 \\ b_6 \\ b_7 \\ b_8 \end{pmatrix} = \begin{pmatrix} \delta_x^{(N+1)} \\ \theta_x^{(N+1)} \\ \delta_y^{(N+1)} \\ \theta_y^{(N+1)} \\ F_x^{(N+1)} \\ M_x^{(N+1)} \\ F_y^{(N+1)} \\ M_y^{(N+1)} \end{pmatrix}$$

Now, suppose that the boundary conditions specified are a_{i_1}, a_{i_2}, a_{i_3}, a_{i_4} and b_{e_1}, b_{e_2}, b_{e_3}, b_{e_4}, where i_1, i_2, i_3, i_4 is a subset of the integers 1, 2, . . . , 8 and similarly for e_1, e_2, e_3, e_4. Note that the elements of S need not be real. Now in a manner analogous to that used in Option 1, a set of four linear equations in four unknowns can be obtained which has as its solution the remaining initial conditions, a_{i_5}, a_{i_6}, a_{i_7}, a_{i_8} where i_1, i_2, . . . , i_8 represents some permutation of the indices 1, 2, . . . , 8. Once the initial vector $\vec{\delta}^{(1)}$ has been obtained, equations (12) and (13) can be used to calculate the solution vectors for each section.

Preparation of Input for Applied Mathematics Laboratory Problem 199
(Code designation: GVC I)

PRELIMINARY

The input cards required for GVC I are of the following four types:

Title

General data

End values

Section and discontinuity data

A description of the contents of each of these sets of cards is given below. Sample input sheets are attached.

A. Title Card

This card should have a 1 punched in column 1. Columns 2 to 72 are at the disposal of the problem proposer for the identification of his problem. It is recommended that the date be included with this identification.

B. General Data Card

Up to 9 items can be specified on this card. They include:

1) N: the number of sections,

2) M_1: option number indicating type of problem,

3) M_2: option number indicating whether Ω, the speed of shaft rotation, or values of the ratio ω/Ω are given.

4) ω_1 (rad/sec.): The lower limit of the range of excitation frequencies to be used,

5) ω_2 (rad/sec.): The upper limit of the range of excitation frequencies to be used,

6) $\Delta\omega$(rad./sec.): The interval to be used for incrementing the excitation frequency,

7) Ω(rad./sec.): the speed of shaft rotation or up to three values of ω/Ω.

The permitted values of M_1 are 1, 2, 3 and each indicates a type of problem to be solved. The types of problems are given below:

$M_1 = 1$ indicates that flexural vibrations are to be studied in a plane,

$M_1 = 2$ indicates that coupled flexural vibrations in two planes are to be studied,

$M_1 = 3$ indicates that coupled torsional-extensional vibrations are to be studied.

The permitted values of M_2 are 0, 1, 2, 3. These have the following meaning:

$M_2 = 0$ indicates that a value of Ω is given,

$M_2 > 0$ indicates that M_2 values of ω/Ω are given. (Note that $M_2 \leq 3$, so that a maximum of 3 values of the ratio ω/Ω can be specified.)

C. <u>End Value Cards</u>

Up to four end value cards can be included. The first contains information as to which end conditions are given for the left end of the shaft and the real parts of their values. The second contains the imaginary parts for these values. If the imaginary parts are zero, the second card need not be included. The third and fourth cards contain similar information for the right end of the shaft.

The specific conditions are represented by the code numbers given in Table 1.

TABLE 1

Code Number	Quantity
1	δ_x(in): deflection in x-direction
2	θ_x: slope in x-z plane
3	δ_y(in): deflection in y-direction
4	θ_y: slope in y-z plane
5	F_x(ℓb): shear in x-direction
6	M_x(ℓb-in): moment in x-z plane
7	F_y(ℓb): shear in y-direction
8	M_y(ℓb-in): moment in y-z plane

Thus if the left end is a free end, the end conditions are $F_x = M_x = F_y = M_y = 0$, and columns 7 to 10 of the first end value card should read 5678. The real parts of the four left end values would be given as zeros and the second end value card would be omitted since the imaginary parts vanish. Further examples are given in the sample problems.

D. Section and Discontinuity Data Cards

The specific data required for each section depends on the type of problem being solved. The particular type of problem to be done is specified by the value of M_1 on the general data card. The data required for each of the three types of problems permitted is described below.

The data required for each section is given on a set of cards. The number of cards required in each set depends on the type of problem being solved. Each set of cards starts with cards containing the discontinuity data required at the beginning of the section and ends with a card containing the data for the section. Each card contains a card number which includes the following information:

M_1: type of problem

n : section number

C : number of the card in the set of cards for section n.

Data for the last section must be followed by a set of cards on which the indicated section number is the integer following the last section number. A subset of these cards contain the discontinuity data to be used at the end of the last section, and the last card of this set is blank except for the card number. This card is interpreted as a sentinel card indicating the end of the data.

Type 1 Problem (Flexural Vibration in a Plane):

For a problem of type 1, a set of three data cards must be supplied for each section of the shaft, with one additional set of data cards for the end section as already indicated. The first two cards specify the discontinuity data to be used at the beginning of the section; the third card specifies the data required for the section. Each of these cards has an appropriate card number as already discussed. In addition the first card (C=1) of a set contains the following data:

m (ℓb-sec^2/in): the mass of the disc which is attached at the beginning of the section,

I_d(lb-sec^2-in): the diametrical mass moment of inertia of that disc.

The second card (C=2) of a set contains values for the following quantities:

$$\left.\begin{matrix} K_{31} \\ K_{32} \\ K_{41} \\ K_{42} \end{matrix}\right\} \quad \text{These are entries in the K matrix described in Section III.}$$

The third card (C=3) of the set contains the following section data:

ℓ (in): the length of the section,

d_o(in): the outer diameter of the shaft section,

d_i(in): the inner diameter of the shaft section,

$E(\ell b/in^2)$: the elastic modulus of the section material,

$\rho(\ell b\text{-}sec^2/in^4)$: the density of the section material.

Type 2 Problem (Coupled Flexural Vibration in Two Planes)

For a problem of Type 2 a set of six data cards must be specified for each section of the shaft with one additional set of cards for the end section, as already indicated. The first five cards specify the discontinuity data to be used at the beginning of the section; the sixth card specifies the data required for the section. Each of these cards has an appropriate card number as already discussed. In addition, the first card (C=1) of a set is of the same form as for a type 1 problem i. e. it contains values of m and I_d.

The second card (C=2) of a set contains the following entires of the K matrix described in Section III.

$$k_{51}, k_{52}, k_{53}, k_{54},$$

The third card (C=3) contains the following entries of the K matrix:

$$k_{61}, k_{62}, k_{63}, k_{64}.$$

The fourth card (C=4) contains the following K matrix elements:

$$k_{71}, k_{72}, k_{73}, k_{74}.$$

Finally, the fifth card (C=5) contains:

$$k_{81}, k_{82}, k_{83}, k_{84}.$$

The last card (C=6) of a set is of the same form as the last card of a set for a type 1 problem, i.e., it contains values of

$$\ell, d_o, d_i, E, \rho\ .$$

Type 3 Problem (Coupled torsional-extensional vibration)

For a problem of type 3, a set of four data cards must be supplied for each section of the shaft, with one additional set of data cards for the end section as described above. The first three cards specify discontinuity data to be used at the beginning of the section, and the fourth card of a set contains the data required for the section. Each of these cards has an appropriate card number as already discussed. In addition the first card (C = 1) of a set contains

m(ℓb-sec^2/in): the mass of the disc attached to the beginning of the section

J_d(lb-sec^2-in): polar mass moment of inertia

ν, μ for cross coupling between rotational velocities and extensional forces (see definition of K matrix in Section III). The second card (C=2) contains entries for the K matrix:

$k_{31}, k_{32}, k_{41}, k_{42}$

The third card (C=3) contains values of the following quantities when there is a geared discontinuity:

R: ratio of speed of high speed shaft to speed of low speed shaft

m_1: mass of the gear for the high speed shaft

J_1: polar mass moment of inertia of the corresponding gear,

m_2: mass of the gear for the low speed shaft

J_2: polar mass moment of gear for the corresponding gear.

Finally, the last card (C=4) contains in addition to the data required for problems of other types:

$\ell, d_0, d_1, E, \rho,$

the quantity

G(ℓb/in^2) the shear modulus of the section material.

GVC I INPUT DATA SHEET 1.

TITLE CARD

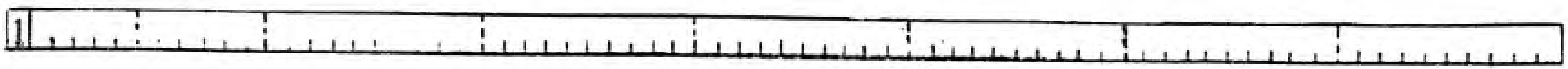

GENERAL DATA CARD

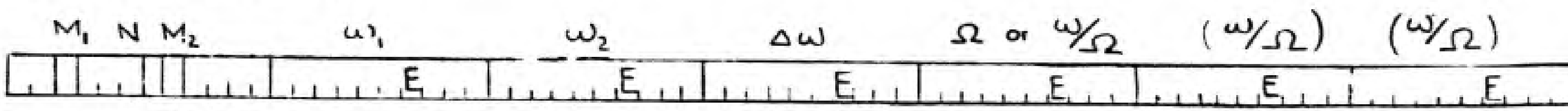

Remarks on data cards:

1) Only columns 1 to 72 are used.

2) Fields in which an E is indicated are 10 column fields to be filled with 'floating point' numbers. For example, -2.54×10^{-6} would be entered as -2.540E-06.

3) Fields which contain zero values need not be filled in

4) If a field has been left blank, the E need not be punched

GVC I INPUT DATA SHEET 2

END VALUES

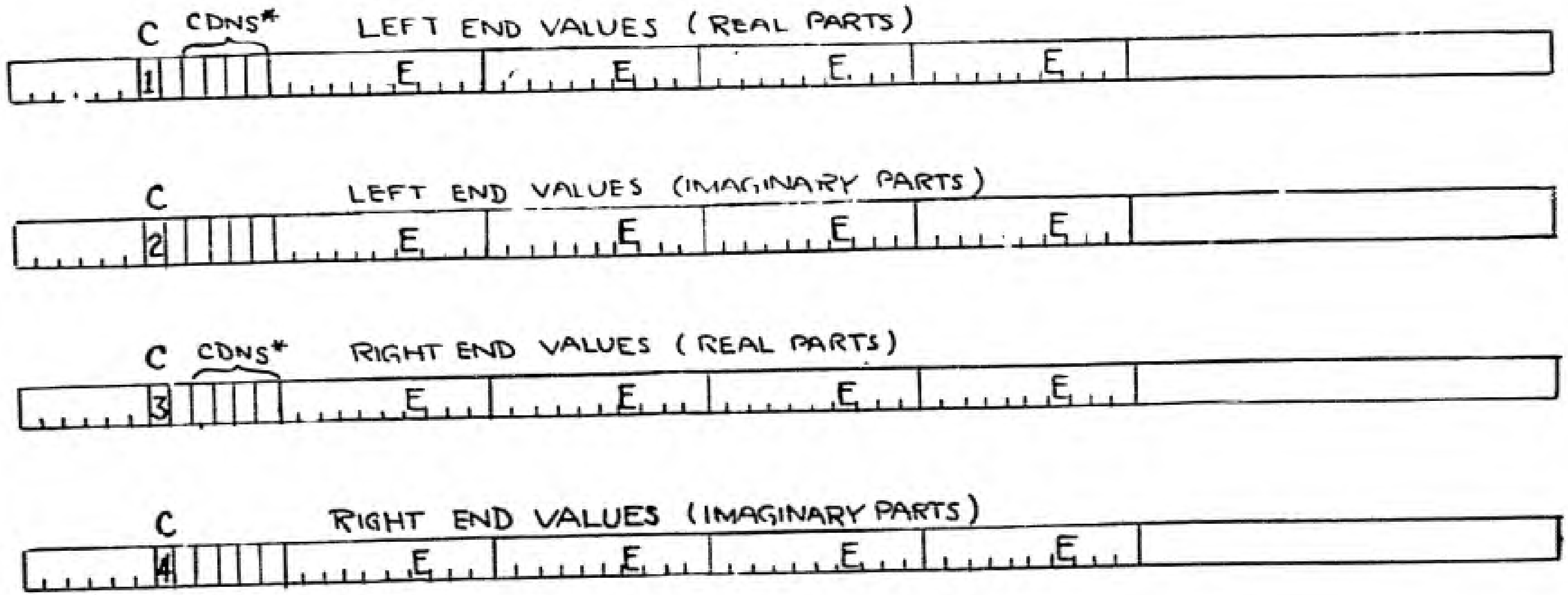

Remark. If all of the end values are real, the above cards with C = 2 and C = 4 can be omitted.

*CNDNS The sequence of end conditions to be used are specified in this four digit field. The numeric correspondance is given by 1, 2, 3, 4, 5, 6, 7, 8 for $\delta_x, \theta_x, \delta_y, \theta_y, F_x, M_x, F_y, M_y$, respectively

GVC I INPUT DATA SHEET

SECTION AND DISCONTINUITY DATA FOR TYPE 1 PROBLEM. FLEXURAL VIBRATION IN A PLANE.

M, n	C	m	I_d				
1	1	E	E				
n		K_{31}	K_{32}	K_{41}	K_{42}		
1	2	E	E	E	E		
n		l	d_o	d_i	E	ρ	
1	3	E	E	E	E	E	
n		m	I_d				
1	1	E	E				
n		K_{31}	K_{32}	K_{41}	K_{42}		
1	2	E	E	E	E		
n		l	d_o	d_i	E	ρ	
1	3	E	E	E	E	E	
n		m	I_d				
1	1	E	E				
n		K_{31}	K_{32}	K_{41}	K_{42}		
1	2	E	E	E	E		
n		l	d_o	d_i	E	ρ	
1	3	E	E	E	E	E	

GVCI INPUT DATA SHEET

SECTION AND DISCONTINUITY DATA FOR TYPE 2 PROBLEM COUPLED FLEXURAL VIBRATION IN TWO PLANES

Card					
M, n, c — 2 1	m	I_d			
n — 2 2	k_{51}	k_{52}	k_{53}	k_{54}	
n — 2 3	k_{61}	k_{62}	k_{63}	k_{64}	
n — 2 4	k_{71}	k_{72}	k_{73}	k_{74}	
n — 2 5	k_{81}	k_{82}	k_{83}	k_{84}	
n — 2 6	l	d_1	d_2	E	ρ

Card					
n — 2 1	m	I_d			
n — 2 2	k_{51}	k_{52}	k_{53}	k_{54}	
n — 2 3	k_{61}	k_{62}	k_{63}	k_{64}	
n — 2 4	k_{71}	k_{72}	k_{73}	k_{74}	
n — 2 5	k_{81}	k_{82}	k_{83}	k_{84}	
n — 2 6	l	d_1	d_2	E	ρ

GVCI INPUT DATA SHEET

SECTION AND DISCONTINUITY DATA FOR TYPE 3 PROBLEM: COUPLED TORSIONAL - EXTENSIONAL VIBRATION

M, n	C	m	J_d	ν	μ		
3	1	E	E	E	E		
n		k_{31}	k_{32}	k_{41}	k_{42}		
3	2	E	E	E	E		
n		m_1	J_1	m_2	J_2	R	
3	3	E	E	E	E	E	
n		ℓ	d_o	d_i	E	ρ	G
3	4	E	E	E	E	E	E

n		m	J_d	ν	μ		
3	1	E	E	E	E		
n		k_{31}	k_{32}	k_{41}	k_{42}		
3	2	E	E	E	E		
n		m_1	J_1	m_2	J_2	R	
3	3	E	E	E	E	E	
n		ℓ	d_o	d_i	E	ρ	G
3	4	E	E	E	E	E	E

Appendix G

The Dynamics of a Rotating Shaft including Gyroscopic Effects.

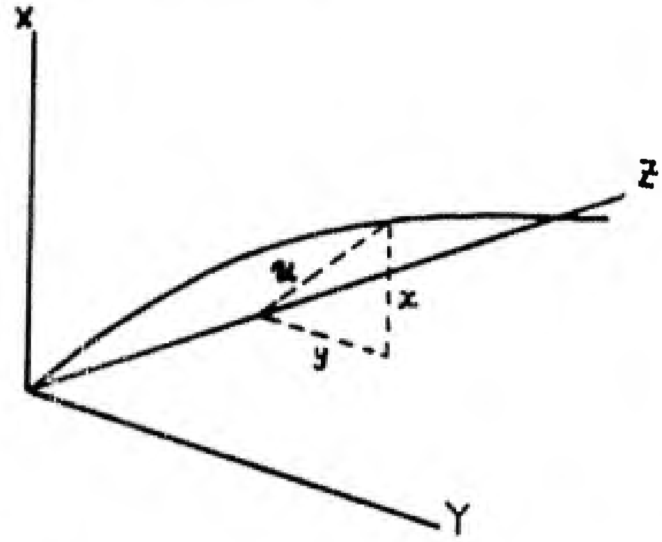

Let M be the moment at some point z in the shaft; M will be the complex quantity $M_y + iM_x$ where M_x and M_y are the moments in the XZ and YZ planes respectively. Let Q be the transverse shear force, i.e. the complex quantity $Q_y + iQ_x$. Let ψ be the inclination of the shaft (to the Z axis) at the point z; this can be written as the complex quantity $\psi_y + i\ \psi_x$ where, for small excursions, ψ_y is the inclination (to the Z axis) of the projection of the shaft in the YZ plane and ψ_x refers to the projection in the XZ plane.

If $u(= y + ix)$ is the displacement of the shaft at a point z and ρ represents the mass density of the material, the first equation of motion is

$$\frac{\partial Q}{\partial z} = \rho a \frac{\partial^2 u}{\partial t^2} \quad \text{where } a = \text{cross-section area}$$

The second equation of motion is

$$\frac{\partial M}{\partial z} + Q \pm i\,(J\rho\Omega)\,\frac{\partial \psi}{\partial t} = \rho\, I\, \frac{\partial^2 \psi}{\partial t^2}$$

where J is the polar moment of inertia of the shaft cross-section and I is the moment of inertia about a diameter - for a circular section $J = 2\,I$. The term on the right is contributed by the rotatory inertia of the section while the imaginary term on the left is the gyroscopic contribution, hence is in quadrature. The sign of the latter term will depend on the sense of rotation of the shaft. Assuming small excursions and ignoring shear deflections we may write the bending relation in the complex form $M = E\,I\,\frac{\partial \psi}{\partial z}$ where $\psi = \frac{\partial u}{\partial z}$

Combining the preceding relations leads to the differential equation

$$EI\,\frac{\partial^4 u}{\partial z^4} + \rho a\,\frac{\partial^2 u}{\partial t^2} + i\,(J\rho\Omega)\,\frac{\partial^3 u}{\partial t\,\partial z^2} - \rho\, I\,\frac{\partial^4 u}{\partial t^2\,\partial z^2} = 0$$

which may be written as:

$$\frac{\partial^4 u}{\partial z^4} + \xi^2\,\frac{\partial^2 u}{\partial t^2} + i\,(2\,\beta^2\Omega)\,\frac{\partial^3 u}{\partial t\,\partial z^2} - \beta^2\,\frac{\partial^4 u}{\partial t^2\,\partial z^2} = 0$$

where $\xi^2 = \frac{\rho a}{EI}$ and $\beta^2 = \frac{\rho}{E}$

In a steady state vibration of the shaft

$$u = r\,e^{i\omega t}$$

Substituting this into the differential equation leads to

$$\frac{d^4 r}{d z^4} + \beta^2 (\omega^2 - 2\omega\Omega) \frac{d^2 r}{d z^2} - \omega^2 \xi^2 r = 0$$

Now r is the complex function of z, $y(z) + i\,x(z)$. If the functions $y(z)$ and $x(z)$ are of different characters, this will imply that the beam will deform into a skewed or twisted curve. However, since all the coefficients in the above equation are real, substituting $y(z) + i\,x(z)$ into the equation and equating real and imaginary parts to zero leads to identical equations for $y(z)$ and $x(z)$, hence if $y(z)$ and $x(z)$ satisfy the same boundary conditions they must then be identical or differ by (at most) a multiplicative constant. Hence, the beam must deform into a plane curve and lie in a plane which rotates about the z axis. It is interesting to note that, in the differential equation for r, the gyroscopic term $2\beta^2\omega\Omega$ appears in combination with the rotatory inertia term $\beta^2\omega^2$ as a coefficient of the second derivative. This means that gyroscopic effects can be included very simply by using a "corrected" moment of inertia of the cross-section!

Consider the whirling of a shaft of length L with simply supported ends. The boundary conditions and the equation are satisfied by the expression

$r = C \sin \frac{\nu \pi z}{L}$ where ν can adopt the values 1,2,3,etc.

Substituting this in the equation leads to

$$\left(\frac{\nu\pi}{L}\right)^4 - \beta^2(\omega^2 - 2\omega\Omega)\left(\frac{\nu\pi}{L}\right)^2 - \omega^2\xi^2 = 0$$

If gyroscopic and rotatory inertia terms are dropped so as to give the simple beam equation, the equivalent frequency equation would be

$$\left(\frac{\nu\pi}{L}\right)^4 - \varpi^2 \xi^2 = 0$$

If the fractional change in critical speed introduced by the inclusion of gyroscopic and rotatory inertia terms is ϵ, i.e. $\omega = \varpi(1+\epsilon)$, then, substituting this expression for ω into the first equation and subtracting the latter gives

$$\epsilon = \frac{\left(\frac{\nu\pi}{L}\beta\right)^2 (2h-1)}{2\left[\left(\frac{\nu\pi\beta}{L}\right)^2 (1-h) + \xi^2\right]}$$

where h is the ratio $\frac{\Omega}{\varpi}$.

For first order whirl, h = 1 and $\epsilon = \frac{1}{2}\left(\frac{\nu\pi}{L}\frac{\beta}{\xi}\right)^2$

Now $\frac{\beta^2}{L^2\xi^2} = \frac{I}{L^2 a} = \left(\frac{\text{radius of gyration}}{\text{length of beam}}\right)^2 = \eta^2$

hence $\epsilon = \frac{1}{2}(\nu\pi\eta)^2$

For a typical example, consider a shaft whose length/diameter ratio is 20, i.e. $\eta = \frac{1}{80}$. The first critical speed ($\nu = 1$) involves an error of $\frac{1}{2}\left(\frac{\pi}{80}\right)^2$ i.e. approx. .08%.

It is of interest to compare the equation of motion derived here (viz.

$$\frac{\partial^4 u}{\partial x^4} + \xi^2 \frac{\partial^2 u}{\partial t^2} + i(2\beta^2\Omega)\frac{\partial^3 u}{\partial t\,\partial x^2} - \beta^2\frac{\partial^4 u}{\partial t^2\,\partial x^2} = 0 \text{)}$$

with those derived by N. H. Jasper (1953), viz.

$$KAG\left[\frac{\partial^2 x}{\partial z^2} - \frac{\partial \psi_x}{\partial z}\right] + P_x - \rho a \ddot{x} = 0$$

$$KAG\left[\frac{\partial x}{\partial z} - \psi_x\right] + N_y + E\,I\frac{\partial^2 \psi_x}{\partial z^2} + \rho J \Omega \dot{\psi}_y - \rho I \ddot{\psi}_x = 0$$

$$KAG\left[\frac{\partial^2 y}{\partial z^2} - \frac{\partial \psi_y}{\partial z}\right] + P_y - \rho a \ddot{y} = 0$$

$$KAG\left[\frac{\partial y}{\partial z} - \psi_y\right] + N_x + EI\frac{\partial^2 \psi_y}{\partial z^2} - \rho J \Omega \dot{\psi}_x - \rho I \ddot{\psi}_y = 0$$

(NOTE: Jasper's notation has been altered to conform with that used here.)

Setting the external loads P_x P_y N_x N_y equal to zero and combining these relations in pairs gives:

$$\rho a \frac{\partial^2 x}{\partial t^2} + EI\frac{\partial^3 \psi_x}{\partial z^3} + \rho J \Omega \frac{\partial^2 \psi_y}{\partial t \partial z} - \rho I \frac{\partial^3 \psi_x}{\partial t^2 \partial z} = 0$$

$$\rho a \frac{\partial^2 y}{\partial t^2} + E\,I\frac{\partial^3 \psi_y}{\partial z^3} - \rho J \Omega \frac{\partial^2 \psi_x}{\partial z \partial t} - \rho I \frac{\partial^3 \psi_y}{\partial t^2 \partial z} = 0$$

Multiplying the first of these by i, adding to the second and replacing y + ix by u and $\psi_y + i\,\psi_x$ by ψ gives

$$E\,I\frac{\partial^3 \psi}{\partial z^3} + \rho a \frac{\partial^2 u}{\partial t^2} + i\,(\rho J \Omega)\frac{\partial^2 \psi}{\partial z \partial t} - \rho I \frac{\partial^3 \psi}{\partial t^2 \partial z} = 0$$

whence, by replacing ψ by $\frac{\partial u}{\partial x}$, we get

$$\frac{\partial^4 u}{\partial x^4} + \xi^2 \frac{\partial^2 u}{\partial t^2} + i\,(2\beta^2 \Omega) \frac{\partial^3 u}{\partial t\,\partial x^2} - \beta^2 \frac{\partial^4 u}{\partial t^2 \partial x^2} = 0$$

Appendix H

An Estimate of the Fundamental Frequency of Propeller Blades in Water when the Hub Is Rigidly Restrained

This section develops an equation for estimating the lowest natural frequency of a ship's propeller blades in water. It is assumed that this frequency is the same as that of a cantilever beam of a uniform cross-section (the same as that of the propeller blade at 0.2R) fixed in a rigid hub at 0.2R and loaded with its weight and its entrained water at 0.7R. The entrained water is taken as that of an elliptical disc having a major diameter equal to the radius of the propeller and a minor diameter equal to the maximum blade width.

An emperical formula for estimating the weight of conventional propeller blades (maximum error in 11 propellers is 1/2%) is:

Weight of blade (beyond 0.2R)

$$= 65 \text{ MWR} \cdot D^2 (\text{BTF} \cdot D + t)$$

where:

D is the propeller diameter, in feet.

MWR is the blade mean width ratio.

BTF is the blade thickness fraction.

t is the tip thickness (extended line of back) in feet

To find the magnitude of the entrained water, use is made of relations developed by Lamb[20] on Page 154.

The kinetic energy of the water surrounding an elliptical disc moving in a direction normal to its surface is:

$$2T = \frac{4/3 \; \pi \; \rho b^2 c^2 \; U^2}{\int_0^{\pi/2} (b^2 \sin^2 \theta + c^2 \cos^2 \theta)^{\frac{1}{2}} \; d\theta}$$

where:

T is the kinetic energy of the fluid.

ρ is the fluid density.

b and c are the semi-axes of the ellipse.

U is the velocity of the ellipse.

Since the kinetic energy of the equivalent mass of water M_{ent} moving with the disc is $1/2 \, M_{ent} U^2$, the value of the entrained mass is:

$$M_{ent} = \frac{4}{3} \pi \rho b^2 c^2 \left[\int_0^{\pi/2} (b^2 \sin^2 \theta + c^2 \cos^2 \theta)^{1/2} \; d\theta \right]^{-1}$$

The integral in the denominator may be expressed in terms of a complete elliptic integral of the second kind (commonly designated as the function E in Tables)

$$\int_0^{\pi/2} (b^2 \sin^2 \theta + c^2 \cos^2 \theta)^{1/2} \, d\theta = c \int_0^{\pi/2} \left[1 - \left(1 - \frac{b^2}{c^2}\right) \sin^2 \theta \right]^{1/2} \, d\theta$$

The values of the semi-axes can be expressed in terms of the diameter and mean width ratio of the propeller.

For elliptical blades, since the maximum blade width is 2b

$$MWR = 0.842 \times 2b/D \quad \text{(Ref. 40 Page 157)}$$

Hence $b = 1.188\ MWR \cdot R$

$$c = 1/2\ R$$

The mass of the entrained water becomes:

$$M_{ent} = 4/3\,\pi\rho\,(1.188\ MWR)^2 \cdot (1/2)^2 R^4 \left(1/2\ R\ E\right)^{-1}$$

$$= \frac{2.952\,\rho\ MWR^2\ R^3}{E}$$

and the total mass of the propeller blade plus entrained salt water becomes:

$$M = 16.2\ MWR\ (BTF + 0.5\frac{t}{R})\ R^3 + 5.88\ (MWR)^2\ R^3/E$$

The next evaluation is for the moment of inertia of the root cross-section.

blade thickness at 0.2R = 0.8 BTF (2R) + 0.2t

$$\text{blade width at } 0.2R = \sqrt{1 - (\frac{0.3}{0.5})^2} \times 2b$$

$$= 0.8 \times 2 \times 1.188\ (MWR)\ R$$

$$= 1.90\ (MWR) R$$

An approximate formula for the moment of inertia, I, of an airfoil section about a longitudinal axis through the center of gravity is:

$$I = 0.046 \text{ width} \times \text{thickness}^3 \quad \text{(Ref. 41 Page 287)}$$

$$= 0.358\ (MWR)\ [BTF + 0.125\ \frac{t}{R}]^3 R^4$$

These values may now be substituted in the relationship for the natural frequency based on the assumptions that are initially stated. Thus,

$$n = \frac{1}{2\pi}\sqrt{\frac{3E'I}{ml^3}}$$

where n is the frequency in cycles per second

E' is the modulus of elasticity of the blade material taken as 16×10^6 #/in² for manganese bronze.

l is the length of the cantilever beam, taken as 0.7R-0.2R = 0.5R

When these values and the mass and moment of inertia are substituted in this relation, and the blade tip thickness is assumed to be 0.01R then the following relationship is obtained:

$$n = \frac{5570}{R}\sqrt{\frac{(BTF + 0.00\,125)^3}{(BTF + 0.005) + \frac{0.364\,MWR}{E}}}$$

A plot of nR for various values of MWR and BTF is given in Figure H-1.

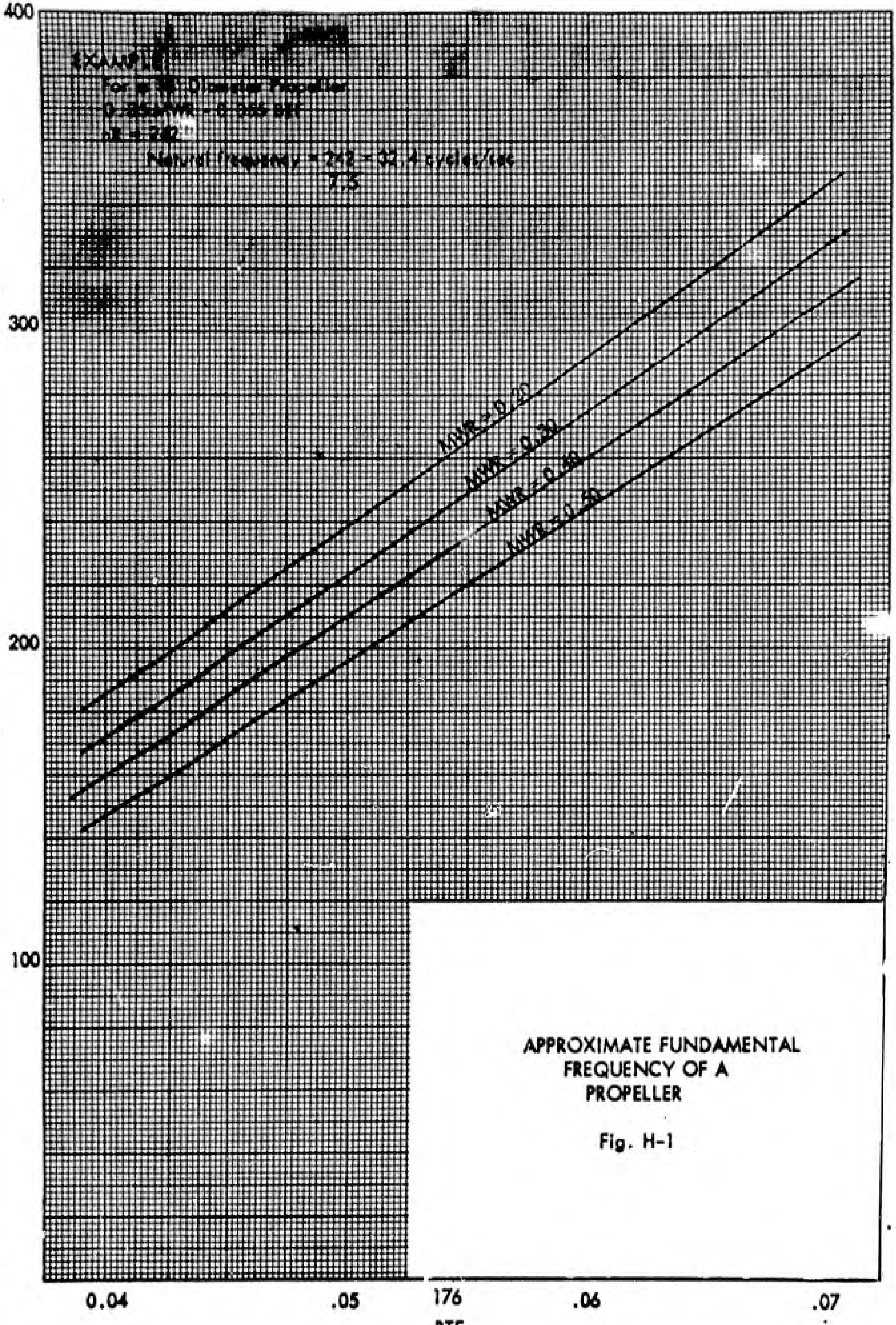

APPROXIMATE FUNDAMENTAL FREQUENCY OF A PROPELLER

Fig. H-1

VC2-S-AP3 - 17.5 KN. - 11,606 Tons

SCHEDULE FOR HARMONIC ANALYSIS

24 ORDINATES

Longitudinal Wake at 0.90R

y	0 (12)	1 (23)	2 (22)	3 (21)	4 (20)	5 (19)	6 (18)	7 (17)	8 (16)	9 (15)	10 (14)	11 (13)
	0.81	0.48	0.35	.27	0.20	.14	0.09	.08	0.07	.07	0.07	0.09
	0.80	0.55	0.36	.25	0.17	.13	0.11	.09	0.08	.08	0.08	0.12
Sum: c	1.61	1.03	0.71	0.52	0.37	0.27	0.20	0.17	0.15	0.15	0.15	0.21
Diff: d	0.01	-.07	-.01	0.02	0.03	0.01	-.02	-.01	-.01	-.01	-.01	-.03

c	0 (6)	1 (11)	2 (10)	3 (9)	4 (8)	5 (7)
	1.61	1.03	0.71	0.52	0.37	0.27
	0.20	0.21	0.15	0.15	0.15	0.17
Sum: e	1.81	1.24	0.86	0.67	0.52	0.44
Diff: f	1.41	0.82	0.56	0.37	0.22	0.10

d	0 (6)	1 (11)	2 (10)	3 (9)	4 (8)	5 (7)
	0.01	-.07	-.01	0.02	0.03	0.01
	-.02	-.03	-.01	-.01	-.01	-.01
Sum: g	-.01	-.10	-.02	0.01	0.02	0
Diff: h	0.03	-.04	0	0.03	0.04	0.02

e	0 (3)	1 (5)	2 (4)
	1.81	1.24	0.86
	0.67	0.44	0.52
Sum: k	2.48	1.68	1.38
Diff: l	1.14	0.80	0.34

f	0 (3)	1 (5)	2 (4)
	1.41	0.82	0.56
	0.37	0.10	0.22
Sum: m	1.78	0.92	0.78
Diff: n	1.04	0.72	0.34

g	0 (3)	1 (5)	2 (4)
	-.01	-.10	-.02
	0.01	0	0.02
Sum: o	0	-.10	0
Diff: p	-.02	-.10	-.04

h	0 (3)	1 (5)	2 (4)
	0.03	-.04	0
	0.03	0.02	0.04
Sum: q	0.06	-.02	0.04
Diff: r	0	-.06	-.04

Table I-1 (a)

Longitudinal Wake at 0.90R

SCHEDULE FOR HARMONIC ANALYSIS
24 ORDINATES

$$y = A_0 + A_1 \cos\theta + A_2 \cos 2\theta + \ldots + B_1 \sin\theta + B_2 \sin 2\theta + \ldots$$

Sin 15°	f_5	g_1							f_1	g_5			$-f_1$	g_5							$-f_5$	g_1	
Cos 75°	0.10	-.10							.82	0			-.82	0							-.10	-.10	
0.259	.026	-.026							.212	0			-.212	0							-.026	-.026	
Sin 30°	f_4	g_2	e_2	g_1			k_1-k_2		f_4	g_2			f_4	$-g_2$	k_1-k_2				e_2	g_1	f_4	$-g_2$	
Cos 60°	.22	-.02	.34	-.02			.30		.22	-.02			.22	.02	-3.06				0.34	-.02	.22	.02	
0.500	.110	-.010	.170	-.010			.150		.110	-.010			.110	.010	-1.530				.170	-.010	.110	.010	
Sin 45°	f_3	g_3			h_1-f_3	p_1+g_3			$-f_3$	$-g_3$			f_3	$-g_3$			f_3-h_1	g_3+p_1			$-f_3$	g_3	
Cos 45°	.37	.01			.35	-.09			-.37	-.01			.37	-.01			-.35	-.09			-.37	.01	
0.707	.262	.007			.247	-.064			-.262	-.007			0.262	-.007			-.247	-.064			-.262	.007	
Sin 60°	f_2	g_4	e_1	g_2				r_1+r_2	$-f_2$	$-g_4$			$-f_2$	g_4		r_1-r_2			$-e_1$	$-g_2$	f_2	$-g_4$	
Cos 30°	.56	-.02	.80	.04				-.10	-.56	-.02			-.56	.02		-.02			-.80	-.04	.56	-.02	
0.866	.485	.017	.693	.035				-.087	-.485	-.017			-.485	.017		-.017			-.693	-.035	.485	-.017	
Sin 75°	f_1	g_5							f_5	g_1			$-f_5$	g_1							$-f_1$	g_5	
Cos 15°	.82	0							.10	-.10			-.10	-.10							-.82	0	
0.966	.792	0							.097	-.097			-.097	-.097							-.792	0	
Sin 90°	d_0	d_6	f_0	h_3	d_0-f_4	g_2-h_1	e_0		d_0	d_6	f_0-e_0	g_1-h_3	d_0	$-d_6$	k_0		d_0-f_4	d_6-g_2	f_0	h_3	d_0	$-d_6$	$e_0-k_1+k_2$
Cos 0°	.01	-.02	1.41	.03	-.21	0	1.14		.01	-.02	1.07	-.05	.01	.02	2.48		-.21	0	1.41	.03	.01	.02	.840
Σ	1.685	-.032	2.273	.055	.037	-.064	1.290	-.087	-.318	-.151	1.07	-.05	-.412	-.057	.950	-.017	-.457	-.064	.887	-.015	-.475	-.006	0.84
	A_1	B_1	A_2	B_2	A_3	B_3	A_4	B_4	A_5	B_5	A_6	B_6	A_7	B_7	A_8	B_8	A_9	B_9	A_{10}	B_{10}	A_{11}	B_{11}	A_{12}
Σ÷12	.140	-.002	.189	.005	.003	-.005	.107	-.007	-.026	-.013	.089	-.004	-.034	-.005	.079	-.001	-.038	-.005	.074	-.001	-.040	.000	.070

$A_0 = 1/24\,(k_0 + k_1 + k_2) = 1/24\,(5.54) = 0.231$, $\quad \frac{1}{12}(k_1 + e_3) = \frac{1}{12}(2.35) = .196$

Checks: $A_1 + A_2 + A_3 + A_4 + A_5 + A_6 + A_7 + A_8 + A_9 + A_{10} + A_{11} + A_{12} = Y_0 - A_0$, $\quad 0.613 + .196 = .809 = .81$

$A_1 - A_2 + A_3 - A_4 + A_5 - A_6 + A_7 - A_8 + A_9 - A_{10} + A_{11} - A_{12} = -Y_{12} + A_0$, $\quad 0.603 + .196 = .799 = .8$

$2 \sin 60° \,(B_1 + B_2 - B_4 - B_5 + B_7 + B_8 - B_{10} - B_{11}) = d_4$, $\quad 2 \times .866(.018) = .031 \approx .03$

$2\,(B_1 - B_3 + B_5 - B_7 + B_9 - B_{11}) = d_6$, $\quad 2(-.010) = -.020 \approx -.02$

Table I-1 (b)

VC2-S-AP3 - 17.55KN - 11,606 Tons

SCHEDULE FOR HARMONIC ANALYSIS

24 ORDINATES

Longitudinal Wake at 0.80R

y	0 (12)	1 (23)	2 (22)	3 (21)	4 (20)	5 (19)	6 (18)	7 (17)	8 (16)	9 (15)	10 (14)	11 (13)
	.77	.48	.36	.27	.19	.15	.10	.08	.07	.07	.08	.11
	.78	.57	.38	.27	.17	.14	.12	.10	.09	.09	.09	.16
Sum: c	1.55	1.05	.74	.54	.36	.29	.22	.18	.16	.16	.17	.27
Diff: d	-.01	-.09	-.02	0	.02	.01	-.02	-.02	-.02	-.02	-.01	-.05

c	0 (6)	1 (11)	2 (10)	3 (9)	4 (8)	5 (7)
	1.55	1.05	.74	.54	.36	.29
	.22	.27	.17	.16	.16	.18
Sum: e	1.77	1.32	.91	.70	.52	.47
Diff: f	1.33	.78	.57	.38	.20	.11

d	0 (6)	1 (11)	2 (10)	3 (9)	4 (8)	5 (7)
	-.01	-.09	-.02	0	.02	.01
	-.02	-.05	-.01	-.02	-.02	-.02
Sum: g	-.03	-.14	-.03	-.02	0	-.01
Diff: h	.01	-.04	-.01	.02	.04	.03

e	0 (3)	1 (5)	2 (4)
	1.77	1.32	.91
	.70	.47	.52
Sum: k	2.47	1.79	1.43
Diff: l	1.07	.85	.39

f	0 (3)	1 (5)	2 (4)
	1.33	.78	.57
	.38	.11	.20
Sum: m	1.71	.89	.77
Diff: n	.95	.67	.37

g	0 (3)	1 (5)	2 (4)
	-.03	-.14	-.03
	-.02	-.01	0
Sum: o	-.05	-.15	-.03
Diff: p	-.01	-.13	-.03

h	0 (3)	1 (5)	2 (4)
	.01	-.04	-.01
	.02	.03	.04
Sum: q	.03	-.01	0.03
Diff: r	-.01	-.07	-.05

Table I-2 (a)

VC2-S-AP3 - 17.55KN. - 11,606 Tons

Longitudinal Wake at 0.80R

SCHEDULE FOR HARMONIC ANALYSIS
24 ORDINATES

$$y = A_o + A_1 \cos\theta + A_2 \cos 2\theta + \ldots + B_1 \sin\theta + B_2 \sin 2\theta + \ldots$$

Sin 15°	f_5	g_1							f_1	g_5			$-f_1$	g_5							$-f_5$	g_1	
Cos 75°	.11	-.14							.78	-.01			-.78	-.01							-.11	-.14	
0.259	.028	-.036							.202	0			-.202	0							-.028	-.036	
Sin 30°	f_4	g_2	l_2	g_1			k_1-k_2		f_4	g_2			f_4	$-g_2$	$-k_1-k_2$				l_2	g_1	f_4	$-g_2$	
Cos 60°	.20	-.03	.39	-.01			.36		.20	-.03			.20	.03	-3.22				.39	-.01	.20	.03	
0.500	.100	-.015	.195	-.005			.180		.100	-.015			.100	.015	-1.61				.195	-.005	.100	.015	
Sin 45°	f_3	g_3			h_1-f_3	p_1+g_3			$-f_3$	$-g_3$			f_3	$-g_3$			f_0-h_1	g_3+p_1			$-f_3$	g_3	
Cos 45°	.38	-.02			.29	-.15			-.38	.02			.38	.02			-.24	-.15			-.38	-.02	
0.707	.269	-.014			.205	-.106			-.269	.014			.269	.014			-.205	-.106			-.269	-.014	
Sin 60°	f_2	g_4	l_1	g_2				h_1+r_2	$-f_2$	$-g_4$			$-f_2$	g_4		h_1-r_2			$-l_1$	$-g_2$	f_2	$-g_4$	
Cos 30°	.57	0	.85	.03				-.12	-.57	0			-.57	0		-.02			-.85	-.03	.57	0	
0.866	.494	0	.736	.026				-.104	-.494	0			-.494	0		-.017			-.736	-.026	.494	0	
Sin 75°	f_1	g_5							f_5	g_1			$-f_5$	g_1							$-f_1$	g_5	
Cos 15°	.78	-.01							.11	-.14			-.11	-.14							-.78	-.01	
0.966	.753	-.097							.106	-.135			-.106	-.135							-.753	-.097	
Sin 90°	d_0	d_6	f_0	h_3	d_0-f_4	g_2-h_3	l_0		d_0	d_6	f_0-l_2	g_1-h_3	d_0	$-d_6$	k_0		d_0-f_4	d_6-g_2	f_0	h_3	d_0	$-d_6$	$f_0-k_1+k_2$
Cos 0°	-.01	-.02	1.33	.02	-.21	-.01	1.07		-.01	-.02	.94	-.03	-.01	.02	2.47		-.21	.01	1.33	.02	-.01	.02	.61
Σ	1.634	-.182	2.261	.041	-.005	-.116	1.25	-.104	-.476	-.156	.94	-.03	-.443	-.086	.860	-.017	-.415	-.096	.789	-.011	-.466	-.112	.61
	A_1	B_1	A_2	B_2	A_3	B_3	A_4	B_4	A_5	B_5	A_6	B_6	A_7	B_7	A_8	B_8	A_9	B_9	A_{10}	B_{10}	A_{11}	B_{11}	A_{12}
Σ÷12	.136	-.015	.188	.003	0	-.010	.104	-.009	-.040	-.013	.078	-.002	-.037	-.007	.072	-.001	-.035	-.008	.066	-.001	-.039	-.009	.051

$A_o = 1/24\ (k_o + k_1 + k_2) = \frac{1}{24}(5.69) = .237,\quad \frac{1}{12}(K_1 + g_3) = \frac{1}{12}(2.49) = .2075$

Checks: $A_1 + A_2 + A_3 + A_4 + A_5 + A_6 + A_7 + A_8 + A_9 + A_{10} + A_{11} + A_{12} = Y_o - A_o,\quad .544 + .208 = .752$

$A_1 - A_2 + A_3 - A_4 + A_5 - A_6 + A_7 - A_8 + A_9 - A_{10} + A_{11} - A_{12} = -Y_{12} + A_o,\quad .574 + .208 = .782$

$2 \sin 60° (B_1 + B_2 - B_4 - B_5 + B_7 + B_8 - B_{10} - B_{11}) = d_4,\quad 2(.866)(.002) = .004$

$2 (B_1 - B_3 + B_5 - B_7 + B_9 - B_{11}) = d_6,\quad 2(-.010) = .02$

Table I-2 (b)

VC2-S-AP3 - 17.55KN.- 11,606 Tons

SCHEDULE FOR HARMONIC ANALYSIS

24 ORDINATES

Longitudinal Wake at 0.55R

y	0 (12)	1 (23)	2 (22)	3 (21)	4 (20)	5 (19)	6 (18)	7 (17)	8 (16)	9 (15)	10 (14)	11 (13)
	.70	.52	.44	.38	.32	.25	.18	.14	.13	.14	.17	.28
	.70	.64	.45	.34	.28	.23	.20	.17	.14	.14	.15	.37
Sum: c	1.40	1.16	0.89	0.72	0.60	.48	.38	.31	.27	.28	.32	.65
Diff: d	0	-.12	-.01	0.04	0.04	0.02	-0.02	-0.03	-0.01	0	.02	-.09

c	0 (6)	1 (11)	2 (10)	3 (9)	4 (8)	5 (7)
	1.40	1.16	0.89	0.72	0.60	0.48
	0.38	0.65	0.32	0.28	0.27	0.31
Sum: e	1.78	1.81	1.21	1.00	0.87	0.79
Diff: f	1.02	0.51	0.57	0.44	0.33	0.17

d	0 (6)	1 (11)	2 (10)	3 (9)	4 (8)	5 (7)
	0	-.12	-.01	0.04	0.04	0.02
	-.02	-.09	.02	0	-.01	-.03
Sum: g	-.02	-.21	0.01	0.04	0.03	-.01
Diff: h	+.02	-.03	-.03	0.04	0.05	0.05

e	0 (3)	1 (5)	2 (4)
	1.78	1.81	1.21
	1.00	0.79	0.87
Sum: k	2.78	2.60	2.08
Diff: l	0.78	1.02	0.34

f	0 (3)	1 (5)	2 (4)
	1.02	0.51	0.57
	0.44	0.17	0.33
Sum: m	1.46	0.68	0.90
Diff: n	.58	0.34	0.24

g	0 (3)	1 (5)	2 (4)
	-.02	-.21	0.01
	0.04	-.01	0.03
Sum: o	0.02	-.22	0.04
Diff: p	-.06	-.20	-.02

h	0 (3)	1 (5)	2 (4)
	0.02	-.03	-.03
	0.04	0.05	0.05
Sum: q	0.06	0.02	0.02
Diff: r	-.02	-.08	-.08

Table I-3 (a)

Longitudinal Wake at 0.55R

SCHEDULE FOR HARMONIC ANALYSIS
24 ORDINATES

$$y = A_o + A_1 \cos\theta + A_2 \cos 2\theta + \ldots + B_1 \sin\theta + B_2 \sin 2\theta + \ldots$$

Sin 15°	f_5	g_1							f_1	g_5			$-f_1$	g_5							$-f_5$	g_1	
Cos 75°	.17	-.21							.51	-.01			-.51	-.01							-.17	-.21	
0.259	.04	-.05							.13	0			-.13	0							-.04	-.05	
Sin 30°	f_4	g_2	ℓ_2	g_1			k_1-k_2		f_4	g_2			f_4	$-g_2$	$-k_1-k_2$				ℓ_2	g_1	f_4	$-g_2$	
Cos 60°	.33	.01	.34	.02			.52		.33	-.01			.33	-.01	-4.68				.34	.02	.33	-.01	
0.500	.16	0	.17	.01			.26		.16	0			.16	0	-2.34				.17	.01	.16	0	
Sin 45°	f_3	g_3			h_1-f_3	g_1+g_3			$-f_3$	$-g_3$			f_3	$-g_3$			f_3-h_1	g_3+g_1			$-f_3$	g_3	
Cos 45°	.44	.04			-.10	-.16			-.44	-.04			.44	-.04			.10	-.16			-.44	.04	
0.707	.31	.03			-.07	-.11			-.31	-.03			.31	-.03			.07	-.11			-.31	.03	
Sin 60°	f_2	g_4	ℓ_1	g_2				h_1+h_3	$-f_2$	$-g_4$			$-f_2$	g_4		h_1-h_3			$-\ell_1$	$-g_2$	f_2	$-g_4$	
Cos 30°	.57	.03	1.02	.02				-.16	-.57	-.03			-.57	.03		0			-1.02	-.02	.57	-.03	
0.866	.49	.03	.88	.02				-.14	-.49	-.03			-.49	.03		0			-.88	-.02	.49	-.03	
Sin 75°	[illegible]	g_5							f_5	g_1			$-f_5$	g_1							$-f_1$	g_5	
Cos 15°	.57	-.01							.17	-.21			-.17	-.21							-.51	-.01	
0.966	.49	-.01							.16	-.20			-.16	-.20							-.49	-.01	
Sin 90°	d_0	d_6	f_0	h_3	d_0-f_4	g_2-d_6	ℓ_0		d_0	d_6	$f_0-\ell_0$	g_1-h_3	d_0	$-d_6$	k_0		d_0-f_4	d_6-g_2	f_0	h_3	d_0	$-d_6$	$k_0-k_1+k_2$
Cos 0°	0	-.02	1.02	.04	-.33	.03	.78		0	-.02	.68	-.02	0	-.02	2.78		-.33	-.03	1.02	.04	0	.02	.26
Σ	1.49	-.02	2.07	.07	-.40	-.08	1.04	-.14	-.35	-.28	.68	-.02	-.31	-.22	.44	0	-.26	-.14	.31	.03	-.19	-.04	.26
	A_1	B_1	A_2	B_2	A_3	B_3	A_4	B_4	A_5	B_5	A_6	B_6	A_7	B_7	A_8	B_8	A_9	B_9	A_{10}	B_{10}	A_{11}	B_{11}	A_{12}
Σ÷12	.124	-.002	.172	.006	-.033	-.007	.087	-.012	-.029	-.023	.057	-.002	-.026	-.018	.037	0	-.022	-.012	.026	.002	-.016	-.003	.022

$A_o = 1/24\ (k_o + k_1 + k_2) = \frac{1}{24}(2.78 + 2.60 + 2.08) = .3108,\ \frac{1}{12}(k_1 + e_3) = \frac{1}{12}(3.60) = 0.300$

Checks: $A_1 + A_2 + A_3 + A_4 + A_5 + A_6 + A_7 + A_8 + A_9 + A_{10} + A_{11} + A_{12} = Y_o - A_o$, $.399 + .300 = 0.70$

$A_1 - A_2 + A_3 - A_4 + A_5 - A_6 + A_7 - A_8 + A_9 - A_{10} + A_{11} - A_{12} = -Y_{12} + A_o$, $0.403 + .300 = 0.70$

$2 \sin 60^o\ (B_1 + B_2 - B_4 - B_5 + B_7 + B_8 - B_{10} - B_{11}) = d_4$, $1.732(.011) = .019 \simeq .04$

$2\ (B_1 - B_3 + B_5 - B_7 + B_9 - B_{11}) = d_6$, $2(-.009) \simeq -.02$

Table I-3 (b)

SCHEDULE FOR HARMONIC ANALYSIS

24 ORDINATES

Longitudinal Wake at 0.3R

	0 (12)	1 (23)	2 (22)	3 (21)	4 (20)	5 (19)	6 (18)	7 (17)	8 (16)	9 (15)	10 (14)	11 (13)
y	0.67	0.61	0.61	0.65	0.69	0.59	0.50	0.50	0.50	0.60	0.95	0.95
	0.65	0.76	0.58	0.61	0.65	0.58	0.50	0.38	0.27	0.35	0.50	0.72
Sum:c	1.32	1.37	1.19	1.26	1.34	1.17	1.00	0.88	0.77	0.95	1.45	1.67
Diff:d	0.02	-0.15	0.03	0.04	0.04	0.01	0	0.12	0.23	0.25	0.45	0.23

	0 (6)	1 (11)	2 (10)	3 (9)	4 (8)	5 (7)
c	1.32	1.37	1.19	1.26	1.34	1.17
	1.00	1.67	1.45	0.95	0.77	0.88
Sum: e	2.32	3.04	2.64	2.21	2.11	2.05
Diff: f	0.32	-.30	-.26	0.31	0.57	0.29

	0 (6)	1 (11)	2 (10)	3 (9)	4 (8)	5 (7)
d	0.02	-0.15	0.03	0.04	0.04	0.01
	0	0.23	0.45	0.25	0.23	0.12
Sum: g	0.02	0.08	0.48	0.29	0.27	0.13
Diff: h	0.02	-.38	-.42	-.21	-.19	-.11

	0 (3)	1 (5)	2 (4)
e	2.32	3.04	2.64
	2.21	2.05	2.11
Sum: k	4.53	5.09	4.75
Diff: l	0.11	0.99	0.53

	0 (3)	1 (5)	2 (4)
f	0.32	-.30	-.26
	0.31	0.29	0.57
Sum: m	0.63	-.01	0.31
Diff: n	0.01	-.59	-.83

	0 (3)	1 (5)	2 (4)
g	0.02	0.08	0.48
	0.29	0.13	0.27
Sum: o	0.31	0.21	0.75
Diff: p	-.27	-.05	0.21

	0 (3)	1 (5)	2 (4)
h	0.02	-.38	-.42
	-.21	-.11	-.19
Sum: q	-.19	-.49	-.61
Diff: r	+.23	-.27	-.23

Table I-4 (a)

VC2-S-AP3 - 17.55KN. - 11,606 Tons

Longitudinal Wake at 0.30R

SCHEDULE FOR HARMONIC ANALYSIS
24 ORDINATES

$$y = A_o + A_1 \cos\theta + A_2 \cos 2\theta + \dots + B_1 \sin\theta + B_2 \sin 2\theta + \dots$$

Sin 15°	f5	g1							f1	g5			-f1	g5							-f5	g1	
Cos 75°	.29	.08							-.30	.13			.30	.13							-.29	.08	
0.259	.07	.02							-.08	.03			.08	.03							-.07	.02	
Sin 30°	f4	g2	e2	g1			k1-k2		f4	g2			f4	-g2	-k1-k2				e2	g1	f4	-g2	
Cos 60°	.57	.48	.53	-.49			.34		0.57	.48			.57	-.48	-.984				.53	-.49	.57	-.48	
0.500	.28	.24	.26	-.24			.17		.28	.24			.28	-.24	-.492				.26	-.24	.28	-.24	
Sin 45°	f3	g3			h1-f3	e1+g3			-f3	-g3			f3	-g3			f3-h1	g3+e1			-f3	g3	
Cos 45°	.31	.29			-.90	.24			-.31	-.29			.31	-.29			.90	.24			-.31	.29	
0.707	.22	.20			-.64	.17			-.22	-.20			.22	-.20			.64	.17			-.22	.20	
Sin 60°	f2	g4	e1	g2				h1+r2	-f2	-g4			-f2	g4		h1-r2			-e1	-g2	f2	-g4	
Cos 30°	-.26	.27	.99	-.61				-.50	.26	-.27			.26	.27		-.04			-.99	.61	-.26	-.27	
0.866	-.23	.23	.86	-.53				-.43	.23	-.23			.23	.23		-.03			-.86	.53	-.23	-.23	
Sin 75°	f1	g5							f5	g1			-f5	g1							-f1	g5	
Cos 15°	-.30	.13							.29	.08			-.29	.08							.30	.13	
0.966	-.29	.13							.28	.08			-.28	.08							.29	.13	
Sin 90°	d0	d6	f0	h3	d0-f4	g2-k2	e0		d0	d6	f0-e2	g1-h3	d0	-d6	k0		d0-f4	d6-g3	f0	h3	d0	-d6	e0-k1+k2
Cos 0°	.02	0	.32	-.21	-.55	.48	.11		.02	0	-.21	.02	.02	0	4.53		-.55	-.48	.32	-.21	.02	0	-.23
Σ	.07	.82	1.44	-.98	-1.19	.65	.27	-.43	.51	-.08	-.21	.02	.55	-.10	-.39	-.03	.09	-.31	-.28	.08	.07	-.12	-.23
	A_1	B_1	A_2	B_2	A_3	B_3	A_4	B_4	A_5	B_5	A_6	B_6	A_7	B_7	A_8	B_8	A_9	B_9	A_{10}	B_{10}	A_{11}	B_{11}	A_{12}
Σ÷12	.006	.068	.120	-.082	-.099	.054	.022	-.036	.042	-.007	-.018	.002	.046	-.008	-.032	-.002	.007	-.026	-.023	.007	.006	-.010	-.019

$A_o = 1/24\ (k_o + k_1 + k_2)$, $\frac{1}{24}(14.37) = 0.599$, $\frac{1}{72}(k_1+e_3) = .608$

Checks: $A_1 + A_2 + A_3 + A_4 + A_5 + A_6 + A_7 + A_8 + A_9 + A_{10} + A_{11} + A_{12} = Y_o - A_o$, $.058 + .608 = 0.666$

$A_1 - A_2 + A_3 - A_4 + A_5 - A_6 + A_7 - A_8 + A_9 - A_{10} + A_{11} - A_{12} = -Y_{12} + A_o$, $.042 + .608 = .650$

$2 \sin 60^\circ\ (B_1 + B_2 - B_4 - B_5 + B_7 + B_8 - B_{10} - B_{11}) = d_4$, $2(.866)(.022) = .038$

$2\ (B_1 - B_3 + B_5 - B_7 + B_9 - B_{11}) = d_6$, $2\,(-.001) = -.002$

Table I-4 (b)

VC2-S-AP3 - 17.55KN - 11,606 Tons

SCHEDULE FOR HARMONIC ANALYSIS

24 ORDINATES

Tangential Wake at 0.9R

y	0 (12)	1 (23)	2 (22)	3 (21)	4 (20)	5 (19)	6 (18)	7 (17)	8 (16)	9 (15)	10 (14)	11 (13)
	1	16	20	20	19	16	11	10	7	5	3	-6
	4	-13	-14	-12	-17	-16	-14	-12	-11	-10	-9	-5
Sum: c	5	3	6	8	2	0	-3	-2	-4	-5	-6	-11
Diff: d	-3	29	34	32	36	32	25	22	18	15	12	-1

c	0 (6)	1 (11)	2 (10)	3 (9)	4 (8)	5 (7)
	5	3	6	8	2	0
	-3	-11	-6	-5	-4	-2
Sum: e	2	-8	0	3	-2	-2
Diff: f	8	14	12	13	6	2

d	0 (6)	1 (11)	2 (10)	3 (9)	4 (8)	5 (7)
	-3	29	34	32	36	32
	25	-1	12	15	18	22
Sum: g	22	28	46	47	54	54
Diff: h	-28	30	22	17	18	10

e	0 (3)	1 (5)	2 (4)
	2	-8	0
	3	-2	-2
Sum: k	5	-10	-2
Diff: l	-1	-6	2

f	0 (3)	1 (5)	2 (4)
	8	14	12
	13	2	6
Sum: m	21	16	18
Diff: n	-5	12	6

g	0 (3)	1 (5)	2 (4)
	22	28	46
	47	54	54
Sum: o	69	82	100
Diff: p	-25	-26	-8

h	0 (3)	1 (5)	2 (4)
	-28	30	22
	17	10	18
Sum: q	-11	40	40
Diff: r	-45	20	4

Table I-5 (a)

Tangential Wake at 0.9R

SCHEDULE FOR HARMONIC ANALYSIS
24 ORDINATES

$y = A_o + A_1 \text{ Cos } \theta + A_2 \text{ Cos } 2\ \theta + \ldots + B_1 \text{ Sin } \theta + B_2 \text{ Sin } 2\ \theta + \ldots$

Sin 15°	f_5	g_1							f_1	g_5			$-f_1$	g_5							$-f_5$	g_1	
Cos 75°	2	28							14	54			-14	54							-2	28	
0.259	0.52	7.25							3.63	13.99			-3.63	13.99							-.52	7.25	
Sin 30°	f_4	g_2	ℓ_2	8_1			k_1-k_2		f_4	g_2			f_4	$-g_2$	$-k_1-k_2$				ℓ_2	8_1	f_4	$-g_2$	
Cos 60°	6	46	2	40			-8		6	46			6	-46	12				2	40	6	-46	
0.500	3	23	1	20			-4		3	23			3	-23	6				1	20	3	-23	
Sin 45°	f_3	g_3			h_1-f_3	p_1+g_3			$-f_3$	$-g_3$			f_3	$-g_3$			f_3-h_1	g_3+p_1			$-f_3$	g_3	
Cos 45°	13	47			-1	21			-13	-47			13	-47			1	21			-13	47	
0.707	9.19	33.23			-.71	14.85			-9.19	-33.23			9.19	-33.23			0.71	14.85			-9.19	33.23	
Sin 60°	f_2	g_4	ℓ_1	8_2				r_1+r_2	$-f_2$	$-g_4$			$-f_2$	g_4		r_1-r_2			$-\ell_1$	-8_2	f_2	$-g_4$	
Cos 30°	12	54	-6	40				24	-12	-54			-12	54		16			6	-40	12	-54	
0.866	10.39	46.76	-5.20	34.64				20.78	-10.39	-46.76			-10.39	46.76		13.86			5.20	-34.64	10.39	-46.76	
Sin 75°	f_1	g_5							f_5	g_1			$-f_5$	g_1							$-f_1$	g_5	
Cos 15°	14	54							2	28			-2	28							-14	54	
0.966	13.52	52.16							1.93	27.05			-1.93	27.05							-13.52	52.16	
Sin 90°	d_0	d_6	f_0	h_3	d_0-f_4	g_3-d_6	ℓ_0		d_0	d_6	$f_0-\ell_2$	g_1-h_3	d_0	$-d_6$	k_0		d_0-f_4	d_6-g_3	f_0	h_3	d_0	$-d_6$	$\ell_0-k_1+k_2$
Cos 0°	-3	25	8	17	-9	21	-1		-3	25	6	23	-3	-25	5		-9	-21	8	17	-3	-25	7
Σ	33.62	187.40	3.80	71.64	-9.71	35.85	-5	20.78	-14.02	9.05	6	23	-6.76	6.57	11	13.86	-8.29	-6.15	14.20	2.36	-12.84	-2.12	7
	A_1	B_1	A_2	B_2	A_3	B_3	A_4	B_4	A_5	B_5	A_6	B_6	A_7	B_7	A_8	B_8	A_9	B_9	A_{10}	B_{10}	A_{11}	B_{11}	A_{12}
Σ÷12	2.802	15.617	0.317	5.970	-.809	2.987	-.417	1.732	-1.168	.754	0.500	1.917	-.563	.547	.917	1.155	-.691	-.512	1.183	.197	-1.070	-.177	.583

$A_o = 1/24\ (k_o + k_1 + k_2) = \frac{1}{24}(-7) = -0.292$ $\quad A_o' = \frac{1}{2}(k_1 + e_5) = \frac{1}{12}(-7) = -0.583$

Checks: $A_1 + A_2 + A_3 + A_4 + A_5 + A_6 + A_7 + A_8 + A_9 + A_{10} + A_{11} + A_{12} = Y_o - A_o,\ 1.584 - 0.583 = 1$

$A_1 - A_2 + A_3 - A_4 + A_5 - A_6 + A_7 - A_8 + A_9 - A_{10} + A_{11} - A_{12} = -Y_{12} + A_o,\ 4.582 - 0.583 = 4$

$2 \text{ Sin } 60^\circ\ (B_1 + B_2 - B_4 - B_5 + B_7 + B_8 - B_{10} - B_{11}) = d_4,\ 1.732(20.783) = 35.996 \approx 36$

$2\ (B_1 - B_3 + B_5 - B_7 + B_9 - B_{11}) = d_6,\ 2(12.502) = 25.004 \approx 25$

Table I-5 (b)

SCHEDULE FOR HARMONIC ANALYSIS

24 ORDINATES

Tangential Wake at 0.8R

y	0 (12)	1 (23)	2 (22)	3 (21)	4 (20)	5 (19)	6 (18)	7 (17)	8 (16)	9 (15)	10 (14)	11 (13)
	1	15	20	21	20	17	13	10	7	4	2	-7
	4	-11	-13	-16	-17	-16	-15	-14	-12	-11	-9	-3
Sum: c	5	4	7	5	3	1	-2	-4	-5	-7	-7	-10
Diff: d	-3	26	33	37	37	33	28	24	19	15	11	-4

c	0 (6)	1 (11)	2 (10)	3 (9)	4 (8)	5 (7)
	5	4	7	5	3	1
	-2	-10	-7	-7	-5	-4
Sum: e	3	-6	0	-2	-2	-3
Diff: f	7	14	14	12	8	5

d	0 (6)	1 (11)	2 (10)	3 (9)	4 (8)	5 (7)
	-3	26	33	37	37	33
	28	-4	11	15	19	24
Sum: g	25	22	44	52	56	57
Diff: h	-31	30	22	22	18	9

e	0 (3)	1 (5)	2 (4)
	3	-6	0
	-2	-3	-2
Sum: k	1	-9	-2
Diff: l	5	-3	2

f	0 (3)	1 (5)	2 (4)
	7	14	14
	12	5	8
Sum: m	19	19	22
Diff: n	-5	9	6

g	0 (3)	1 (5)	2 (4)
	25	22	44
	52	57	56
Sum: o	77	79	100
Diff: p	-27	-35	-12

h	0 (3)	1 (5)	2 (4)
	-31	30	22
	22	9	18
Sum: q	-9	39	40
Diff: r	-53	21	4

Table I-6 (a)

VC2-S-AP3 - 17.55 K N. - 11,606 Tons

Tangential Wake at 0.8R

SCHEDULE FOR HARMONIC ANALYSIS
24 ORDINATES

$$y = A_0 + A_1 \cos\theta + A_2 \cos 2\theta + \ldots + B_1 \sin\theta + B_2 \sin 2\theta + \ldots$$

Sin 15°	f_5	g_1							f_1	g_5			$-f_1$	g_5							$-f_5$	g_1	
Cos 75°	5	22							14	57			-14	57							-5	22	
0.259	1.30	5.70							3.63	14.76			-3.63	14.76							-1.30	5.70	
Sin 30°	f_4	g_2	e_2	g_1			k_1-k_2		f_4	g_2			f_4	$-g_2$	$-k_1-k_2$				e_2	g_1	f_4	$-g_2$	
Cos 60°	8	44	2	39			-7		8	44			8	-44	11				2	39	8	-44	
0.500	4.00	22.00	1.00	19.50			3.50		4.00	22.00			4.00	-22.00	5.50				1	19.50	4	-22.00	
Sin 45°	f_3	g_3			h_1-f_3	p_1+g_3			$-f_3$	$-g_3$			f_3	$-g_3$			f_3-h_1	g_3+p_1			$-f_3$	g_3	
Cos 45°	12	52			-3	17			-12	-52			12	-52			3	17			-12	52	
0.707	8.48	36.76			-2.12	12.02			-8.48	-36.76			8.48	-36.76			2.12	12.02			-8.48	36.76	
Sin 60°	f_2	g_4	e_1	g_2				h_1+h_2	$-f_2$	$-g_4$			$-f_2$	g_4		h_1-h_2			$-e_1$	$-g_2$	f_2	$-g_4$	
Cos 30°	14	56	-3	40				25	-14	-56			-14	56		17			3	-40	14	-56	
0.866	12.12	48.50	-2.60	34.64				21.65	-12.12	-48.50			-12.12	48.50		14.72			2.60	-34.64	12.12	-48.50	
Sin 75°	f_1	g_5							f_5	g_1			$-f_5$	g_1							$-f_1$	g_5	
Cos 15°	14	57							5	22			-5	22							-14	57	
0.966	13.52	55.06							4.83	21.25			-4.83	21.25							-13.52	55.06	
Sin 90°	d_0	d_6	f_0	h_3	d_0-f_0	g_2-k_2	e_0		d_0	d_6	f_0-e_0	g_1-h_3	d_0	$-d_6$	k_0		d_0-f_0	d_6-g_2	f_0	h_3	d_0	$-d_6$	$e_0-k_1+k_2$
Cos 0°	-3	28	7	22	-11	16	5		-3	28	5	17	-3	-28	1		-11	-16	7	22	-3	-28	12
Σ	36.42	76.02	5.40	76.14	-13.12	28.02	1.50	21.65	-11.14	0.75	5	17	-11.10	-2.25	6.50	14.72	-8.88	-3.98	10.60	6.86	-10.18	-0.98	12
	A_1	B_1	A_2	B_2	A_3	B_3	A_4	B_4	A_5	B_5	A_6	B_6	A_7	B_7	A_8	B_8	A_9	B_9	A_{10}	B_{10}	A_{11}	B_{11}	A_{12}
Σ÷12	3.035	6.335	.450	6.345	-1.093	2.335	.125	1.804	-.928	.062	.417	1.417	-.925	-.187	.542	1.227	-.740	-.332	.883	.572	-.848	-.082	1.000

$A_0 = 1/24\ (k_0 + k_1 + k_2) = \frac{1}{24}(-10) = -0.417, \quad A_0' = \frac{1}{2}(k_1 + e_3) = -.917$

Checks: $A_1 + A_2 + A_3 + A_4 + A_5 + A_6 + A_7 + A_8 + A_9 + A_{10} + A_{11} + A_{12} = Y_0 - A_0,\ 1.917 - .917 \simeq 1$ ✓

$A_1 - A_2 + A_3 - A_4 + A_5 - A_6 + A_7 - A_8 + A_9 - A_{10} + A_{11} - A_{12} = -Y_{12} + A_0,\ 4.917 - .917 \simeq 4$ ✓

$2 \sin 60^\circ\ (B_1 + B_2 - B_4 - B_5 + B_7 + B_8 - B_{10} - B_{11}) = d_4,\ 1.732\ (21.359) = 36.985 \approx 37$ ✓

$2\ (B_1 - B_3 + B_5 - B_7 + B_9 - B_{11}) = d_6,\ 2(13.999) = 27.998 \simeq 28$ ✓

Table I-6 (b)

VC2-S-AP3 - 17.55KN.- 11,606 Tons

SCHEDULE FOR HARMONIC ANALYSIS

24 ORDINATES

Tangential Wake at 0.55R

y	0 (12)	1 (23)	2 (22)	3 (21)	4 (20)	5 (19)	6 (18)	7 (17)	8 (16)	9 (15)	10 (14)	11 (13)
	2	7	13	15	15	14	13	10	6	2	-2	-7
	6	-6	-8	-12	-15	-15	-14	-13	-11	-9	-6	+4
Sum: c	8	1	5	3	0	-1	-1	-3	-5	-7	-8	-3
Diff: d	-4	13	21	27	30	29	27	23	17	11	4	-11

c	0 (6)	1 (11)	2 (10)	3 (9)	4 (8)	5 (7)
	8	1	5	3	0	-1
	-1	-3	-8	-7	-5	-3
Sum: e	7	-2	-3	-4	-5	-4
Diff: f	9	4	13	10	5	2

d	0 (6)	1 (11)	2 (10)	3 (9)	4 (8)	5 (7)
	-4	13	21	27	30	29
	27	-11	4	11	17	23
Sum: g	23	2	25	38	47	52
Diff: h	-31	24	17	16	13	6

e	0 (3)	1 (5)	2 (4)
	7	-2	-3
	-4	-4	-5
Sum: k	3	-6	-8
Diff: l	11	2	2

f	0 (3)	1 (5)	2 (4)
	9	4	13
	10	2	5
Sum: m	19	6	18
Diff: n	-1	2	8

g	0 (3)	1 (5)	2 (4)
	23	2	25
	38	52	47
Sum: o	61	54	72
Diff: p	-15	-50	-22

h	0 (3)	1 (5)	2 (4)
	-31	24	17
	16	6	13
Sum: q	-15	30	30
Diff: r	-47	18	4

Table I-7 (a)

VC2-S-AP3 - 17.55KN. - 11,606 Tons

Tangential Wake at 0.55R

SCHEDULE FOR HARMONIC ANALYSIS
24 ORDINATES

$$y = A_o + A_1 \cos\ \theta + A_2 \cos 2\ \theta + \ldots + B_1 \sin\ \theta + B_2 \sin\ 2\ \theta + \ldots$$

Sin 15°	f_5	g_1							f_1	g_5			$-f_1$	g_5							$-f_5$	g_1	
Cos 75°	2	2							4	52			-4	52							-2	2	
0.259	0.52	0.52							1.04	13.47			-1.04	13.47							-.52	.52	
Sin 30°	f_4	g_2	ℓ_2	g_1			k_1-k_2		f_4	g_2			f_4	$-g_2$	[illegible]				ℓ_2	g_1	f_4	$-g_2$	
Cos 60°	5	25	2	30			2		5	25			5	-25	14				2	30	5	-25	
0.500	2.50	12.50	1.00	15.00			1.00		2.50	12.50			2.50	-12.50	7.00				1.00	15.00	2.50	-12.50	
Sin 45°	f_3	g_3			h_1-f_3	p_1+g_3			$-f_3$	$-g_3$			f_3	$-g_3$			f_3-h_1	g_3+p_1			$-f_3$	g_3	
Cos 45°	10	38			-8	-12			-10	-38			10	-38			8	-12			-10	38	
0.707	7.07	26.87			-5.66	-8.48			-7.07	-26.87			7.07	-26.87			5.66	-8.48			-7.07	26.87	
Sin 60°	f_2	g_4	ℓ_1	g_2				h_1+h_2	$-f_2$	$-g_4$			$-f_2$	g_4		h_1-h_2			$-\ell_1$	$-g_2$	f_2	$-g_4$	
Cos 30°	13	47	2	30				22	-13	-47			-13	47		14			-2	-30	13	-47	
0.866	11.26	40.70	1.73	25.98				19.05	-11.26	-40.70			-11.26	40.70		12.12			-1.73	-25.98	11.26	-40.70	
Sin 75°	f_1	g_5							f_5	g_1			$-f_5$	g_1							$-f_1$	g_5	
Cos 15°	4	52							2	2			-2	2							-4	52	
0.966	3.86	50.23							1.93	1.93			-1.93	1.93							-3.86	50.23	
Sin 90°	d_0	d_6	f_0	h_3	d_0-f_4	g_2-d_6	ℓ_0		d_0	d_6	$f_0-\ell_2$	g_1-h_3	d_0	$-d_6$	k_0		d_0-f_4	d_6-g_2	f_0	h_3	d_0	$-d_6$	$\ell_0-k_1+k_2$
Cos 0°	-4	27	9	16	-9	-2	11		-4	27	7	14	-4	-27	3		-9	2	9	16	-4	-27	9
Σ	21.21	157.82	11.73	58.98	-14.66	-10.48	12.00	19.05	-16.86	12.67	7	14	-8.66	-10.27	10.00	12.12	-3.34	-6.48	8.27	[illegible]	-1.69	-2.58	9
	A_1	B_1	A_2	B_2	A_3	B_3	A_4	B_4	A_5	B_5	A_6	B_6	A_7	B_7	A_8	B_8	A_9	B_9	A_{10}	B_{10}	A_{11}	B_{11}	A_{12}
Σ÷12	1.767	13.152	0.977	4.748	-1.222	-.873	1.000	1.587	-1.405	1.056	.583	1.167	-.722	-.856	.833	1.010	-.278	-.540	.689	.418	-.141	-.215	.750

$A_o = 1/24\ (k_o + k_1 + k_2) = \frac{1}{24}(-11) = 0.458$, $\frac{1}{2}(k_1 + e_5) = \frac{1}{2}(-10) = -0.8333$

Checks: $A_1 + A_2 + A_3 + A_4 + A_5 + A_6 + A_7 + A_8 + A_9 + A_{10} + A_{11} + A_{12} = Y_o - A_o$, $2.831 - 0.833 \approx 2$

$A_1 - A_2 + A_3 - A_4 + A_5 - A_6 + A_7 - A_8 + A_9 - A_{10} + A_{11} - A_{12} = -Y_{12} + A_o$, $6.833 - 0.833 \approx 6.00$

$2 \sin 60° (B_1 + B_2 - B_4 - B_5 + B_7 + B_8 - B_{10} - B_{11}) = d_4$, $2(0.866)(17.320) = 29.998 \approx 30$

$2(B_1 - B_3 + B_5 - B_7 + B_9 - B_{11}) = d_6$, $2(13.50) = 27 \approx 27$

Table 1-7 (b)

VC2-S-AP3 - 17.55KN. - 11,606 Tons

SCHEDULE FOR HARMONIC ANALYSIS

24 ORDINATES

Tangential Wake at 0.3R

y	0 (12)	1 (23)	2 (22)	3 (21)	4 (20)	5 (19)	6 (18)	7 (17)	8 (16)	9 (15)	10 (14)	11 (13)
	9	-10	-7	-3	+1	7	+11	7	+1	-6	-11	-4
	+8	+4	0	1	0	-8	-10	-9	-7	0	+10	+21
Sum: c	17	-6	-7	-2	1	-1	1	-2	-6	-6	-1	17
Diff: d	1	-14	-7	-4	1	15	21	16	8	-6	-21	-25

c	0 (6)	1 (11)	2 (10)	3 (9)	4 (8)	5 (7)
	17	-6	-7	-2	1	-1
	1	17	-1	-6	-6	-2
Sum: e	18	11	-8	-8	-5	-3
Diff: f	16	-23	-6	+4	+7	+1

d	0 (6)	1 (11)	2 (10)	3 (9)	4 (8)	5 (7)
	1	-14	-7	-4	1	15
	21	-25	-21	-6	8	16
Sum: g	22	-39	-28	-10	9	31
Diff: h	-20	+11	+14	+2	-7	-1

e	0 (3)	1 (5)	2 (4)
	18	11	-8
	-8	-3	-5
Sum: k	10	8	-13
Diff: l	26	14	-3

f	0 (3)	1 (5)	2 (4)
	16	-23	-6
	4	+1	+7
Sum: m	20	-22	+1
Diff: n	12	-24	-13

g	0 (3)	1 (5)	2 (4)
	22	-39	-28
	-10	31	9
Sum: o	12	-8	-19
Diff: p	32	-70	-37

h	0 (3)	1 (5)	2 (4)
	-20	+11	+14
	+4	-1	-7
Sum: q	-16	+10	+7
Diff: r	-24	+12	+21

Table I-8 (a)

Tangential Wake at 0.3R

SCHEDULE FOR HARMONIC ANALYSIS
24 ORDINATES

$$y = A_o + A_1 \cos\theta + A_2 \cos 2\theta + \dots + B_1 \sin\theta + B_2 \sin 2\theta + \dots$$

Sin 15°	f_5	g_1							f_1	g_5			$-f_1$	g_5							$-f_5$	g_1	
Cos 75°	1	-39							-23	31			23	31							-1	-39	
0.259	0.26	-10.10							-5.96	8.03			5.96	8.03							-.26	-10.10	
Sin 30°	f_4	g_2	l_2	g_1			k_1-k_2		f_4	g_2			f_4	$-g_2$	$-k_1-k_2$				l_2	g_1	f_4	$-g_2$	
Cos 60°	7	-28	-3	10			21		7	-28			7	28	5				-3	10	7	28	
0.500	3.50	-14.00	-1.50	5.00			10.50		3.50	-14.00			3.50	14.00	2.50				-1.50	5.00	3.50	14.00	
Sin 45°	f_3	g_3			h_1-f_3	p_1+g_3			$-f_3$	$-g_3$			f_3	$-g_3$			f_3-h_1	g_3+p_1			$-f_3$	g_3	
Cos 45°	4	-10			-28	-80			-4	10			4	10			28	-80			-4	-10	
0.707	2.83	-7.07			-19.80	-56.56			-2.83	7.07			2.83	7.07			19.80	-56.56			-2.83	-7.07	
Sin 60°	f_2	g_4	l_1	g_2				n_1+n_2	$-f_2$	$-g_4$			$-f_2$	g_4		n_1-n_2			$-l_1$	$-g_2$	f_2	$-g_4$	
Cos 30°	-6	9	14	7				33	6	-9			6	9		-9			-14	-7	-6	-9	
0.866	-5.20	7.79	12.12	6.06				28.58	5.20	-7.79			5.20	7.79		-7.79			-12.12	6.06	-5.20	-7.79	
Sin 75°	f_1	g_5							f_5	g_1			$-f_5$	g_1							$-f_1$	g_5	
Cos 15°	-23	31							1	-39			-1	-39							23	31	
0.966	-22.22	29.95							0.97	37.67			-.97	-37.67							22.22	29.95	
Sin 90°	d_0	d_6	f_0	h_3	d_0-f_4	g_2-d_6	l_0		d_0	d_6	f_0-l_2	g_1-h_3	d_0	$-d_6$	k_0		d_0-f_4	d_6-g_2	f_0	h_3	d_0	$-d_6$	$l_2-k_1+k_2$
Cos 0°	1	21	16	2	-6	-49	26		1	21	19	8	1	-21	10		-6	49	16	2	1	-21	5
Σ	-19.83	22.57	26.62	13.06	-2.58	-105.56	36.50	28.58	1.88	-23.36	19	8	17.52	-21.78	12.50	-7.79	13.80	-7.56	2.		13	-2.01	5
	A_1	B_1	A_2	B_2	A_3	B_3	A_4	B_4	A_5	B_5	A_6	B_6	A_7	B_7	A_8	B_8	A_9	B_9	A_{10}	B_{10}	A_{11}	B_{11}	A_{12}
Σ÷12	-1.652	1.297	2.218	1.088	-.215	-8.797	3.042	2.382	.157	-1.947	1.583	.667	1.460	-1.815	1.042	-.649	1.150	-.630	.198	.078	1.536	-.167	.417

$A_o = 1/24\ (k_o + k_1 + k_2)$ $\frac{1}{24} \times 5 = 0.208$, $\frac{1}{2}(k_1 + e_3) = \frac{1}{2} \times 0 = 0$

Checks: $A_1 + A_2 + A_3 + A_4 + A_5 + A_6 + A_7 + A_8 + A_9 + A_{10} + A_{11} + A_{12} = Y_o - A_o$, $9.000 + 0 \approx 9$

$A_1 - A_2 + A_3 - A_4 + A_5 - A_6 + A_7 - A_8 + A_9 - A_{10} + A_{11} - A_{12} = -Y_{12} + A_o$, $7.999 + 0 \approx 8$

$2 \sin 60° (B_1 + B_2 - B_4 - B_5 + B_7 + B_8 - B_{10} - B_{11}) = d_4$, $2 \times 0.866 (0.575) = 0.996 \approx 1$

$2 (B_1 - B_3 + B_5 - B_7 + B_9 - B_{11}) = d_6$, $2(10.499) = 20.998 \approx 21$

Table 1-8 (b)

VC2-S-AP3 Victory Ship

PROPELLER SECTION CHARACTERISTICS $x = \frac{r}{R} = 0.70$

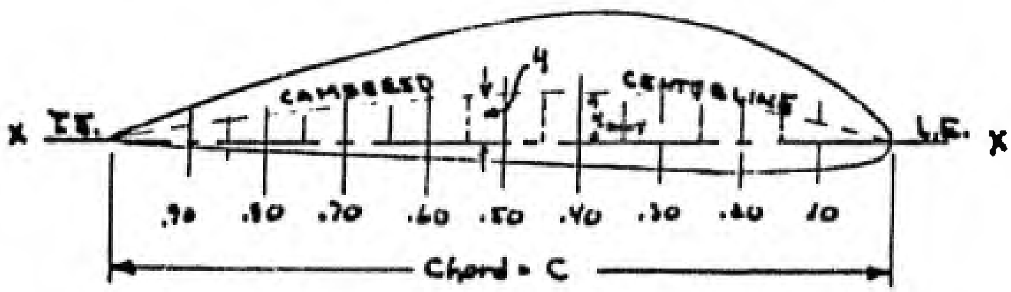

$$\alpha_0^\circ(\text{Theory}) = \frac{1}{C}\left(f_1y_1 + f_2y_2 + f_3y_3 + \cdots f_{19}y_{19}\right)$$

STATION	POSITION FROM LEADING EDGE	y INS.	MULTIPLIERS f_1 f_2 etc.	FUNCTIONS $(f_1 \times y_1)$ etc.
y_1	0.05C	.323	5.04	
y_2	0.10C	.507	3.38	
y_3	0.15C	.635	3.01	
y_4	0.20C	.73	2.87	
y_5	0.25C	.785	2.81	
y_6	0.30C	.84	2.84	
y_7	0.35C	.855	2.92	
y_8	0.40C	.87	3.07	
y_9	0.45C	.866	3.32	
y_{10}	0.50C	.863	3.64	
y_{11}	0.55C	.836	4.07	
y_{12}	0.60C	.809	4.69	
y_{13}	0.65C	.760	5.44	
y_{14}	0.70C	0.710	6.65	
y_{15}	0.75C	0.636	8.59	
y_{16}	0.80C	0.562	11.40	
y_{17}	0.85C	0.455	17.05	
y_{18}	0.90C	0.348	35.40	
y_{19}	0.95C	0.207	186.20	
				109.64

Theoretical $\alpha_0^\circ = \frac{\Sigma}{\text{Chord}} = \frac{109.64}{48.45} = 2.26^\circ$

Actual $\alpha_0^\circ = K\alpha_0 \times \text{Theoretical } \alpha_0^\circ$

Nose-Tail Slope $= \frac{\text{Nose rise} - \text{Tail rise}}{\text{Chord}} \times 57.3$

$= \frac{0.065}{48.45} \times 57.3 =$

$= 0.07^\circ$ $\qquad$ 2.33°

PROPELLER SECTION CHARACTERISTICS $x = \frac{r}{R} = 0.8$

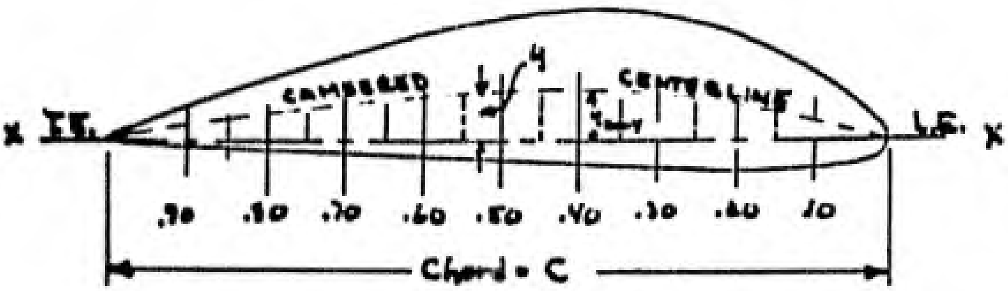

$$\alpha_0^\circ(\text{Theory}) = \frac{1}{c}\left(f_1 y_1 + f_2 y_2 + f_3 y_3 + \cdots \cdots f_{19} y_{19}\right)$$

STATION	POSITION FROM LEADING EDGE	y INS.	MULTIPLIERS $f_1 f_2$ etc.	FUNCTIONS $(f_1 \cdot y_1)$ etc.
y_1	0.05C	0.46	5.04	
y_2	0.10C	0.89	3.38	
y_3	0.15C	1.00	3.01	
y_4	0.20C	[illegible]	2.87	
y_5	0.25C	1.24	2.81	
y_6	0.30C	1.32	2.84	
y_7	0.35C	1.34	2.92	
y_8	0.40C	1.37	3.09	
y_9	0.45C	1.35	3.32	
y_{10}	0.50C	1.34	3.64	
y_{11}	0.55C	1.27	4.07	
y_{12}	0.60C	1.21	4.64	
y_{13}	0.65C	1.12	5.44	
y_{14}	0.70C	1.03	6.65	
y_{15}	0.75C	.90	8.59	
y_{16}	0.80C	0.78	11.40	
y_{17}	0.85C	0.61	17.05	
y_{18}	0.90C	0.452	35.40	
y_{19}	0.95C	0.248	186.20	
				149.332

$$\text{Theoretical } \alpha_0^\circ = \frac{\Sigma}{\text{Chord}} = \frac{149.332}{62.0} = 2.41^\circ$$

$$\text{Actual } \alpha_0^\circ = K\alpha_0 \times \text{Theoretical } \alpha_0^\circ$$

$$\text{Nose-Tail Slope} = \frac{\text{Nose rise} - \text{Tail rise}}{\text{Chord}} \times 57.3$$

$$= \frac{0.13}{62.0} \times 57.3$$

$$= 0.12^\circ$$

2.53°

Table 1-10

VC2-S-AP3 Victory Ship

PROPELLER SECTION CHARACTERISTICS $x = \frac{r}{R} = 0.55R$

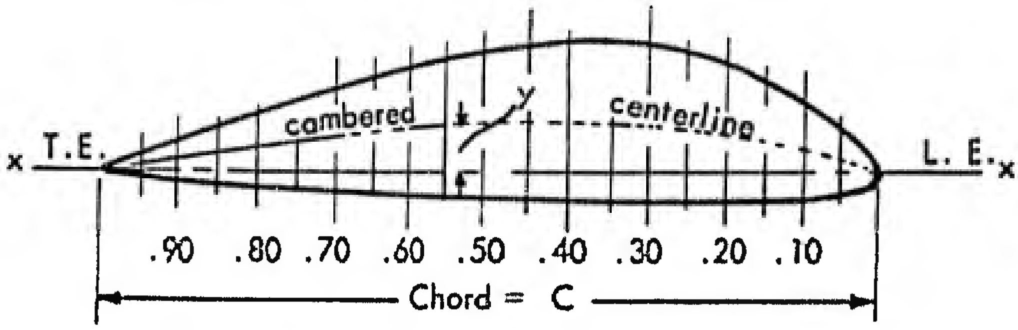

$$\dot{\alpha}_o\text{(Theory)} = \frac{1}{C}\left(f_1 y_1 + f_2 y_2 + f_3 y_3 + \ldots f_{19} y_{19}\right)$$

Station	Position from L. E.	Y ins.	Multipliers f_1, f_2 etc.	Functions $(f_1 \times y_1)$ etc.
y_1	0.05 C	0.83	5.04	
y_2	0.10 C	1.46	3.38	
y_3	0.15 C	1.88	3.01	
y_4	0.20 C	2.12	2.87	
y_5	0.25 C	2.23	2.81	
y_6	0.30 C	2.33	2.84	
y_7	0.35 C	2.35	2.92	
y_8	0.40 C	2.36	3.09	
y_9	0.45 C	2.27	3.32	
y_{10}	0.50 C	2.21	3.64	
y_{11}	0.55 C	2.08	4.07	
y_{12}	0.60 C	1.95	4.64	
y_{13}	0.65 C	1.78	5.44	
y_{14}	0.70 C	1.60	6.65	
y_{15}	0.75 C	1.38	8.59	
y_{16}	0.80 C	1.15	11.40	
y_{17}	0.85 C	0.90	17.05	
y_{18}	0.90 C	0.64	35.40	
y_{19}	0.95 C	0.33	186.20	
			Σ	225.79

$$\text{Theoretical } \dot{\alpha}_o = \frac{\Sigma}{\text{Chord}} = \frac{225.79}{68.15} = 3.31^\circ$$

$$\text{Actual } \dot{\alpha}_o = K_{\alpha_o} \times \text{Theoretical } \dot{\alpha}_o$$

$$\underline{\text{Nose - Tail Slope}} = \frac{\text{Nose rise - Tail rise}}{\text{Chord}} \times 57.3$$

$$= \frac{0.64}{68.15} \times 57.3$$

$$= 0.538 \qquad \Sigma = 3.85^\circ$$

Table 1-11

VC2-S-AP3 - Victory Ship

PROPELLER SECTION CHARACTERISTICS $x = \frac{r}{R} = 0.30$

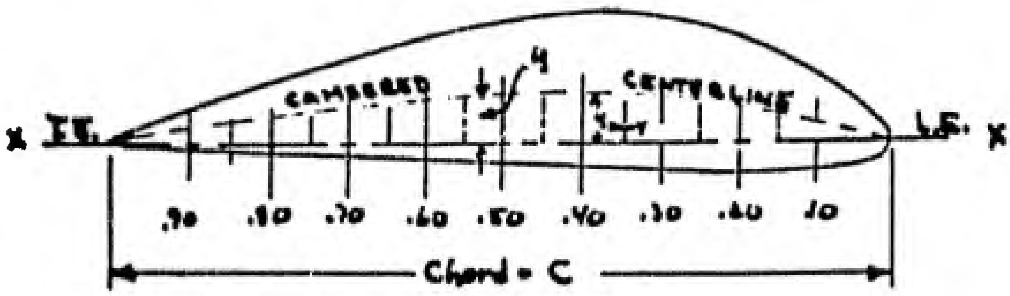

$\alpha_0^\circ(\text{Theory}) = \frac{1}{C}\left(f_1 y_1 + f_2 y_2 + f_3 y_3 + \cdots f_{19} y_{19}\right)$

Station	Position From Leading Edge	y ins.	Multipliers f_1 f_2 etc.	Functions $(f_1 \times y_1)$ etc.
y_1	0.05C	0.756	5.04	
y_2	0.10C	1.362	3.38	
y_3	0.15C	1.631	3.01	
y_4	0.20C	2.079	2.87	
y_5	0.25C	2.192	2.81	
y_6	0.30C	2.306	2.84	
y_7	0.35C	2.270	2.92	
y_8	0.40C	2.233	3.09	
y_9	0.45C	2.131	3.32	
y_{10}	0.50C	2.030	3.64	
y_{11}	0.55C	1.861	4.07	
y_{12}	0.60C	1.672	4.69	
y_{13}	0.65C	1.473	5.44	
y_{14}	0.70C	1.254	6.65	
y_{15}	0.75C	0.995	8.59	
y_{16}	0.80C	0.736	11.40	
y_{17}	0.85C	0.462	17.05	
y_{18}	0.90C	0.188	35.40	
y_{19}	0.95C	0.079	186.20	
				137.95

Theoretical $\alpha_0^\circ = \frac{\Sigma}{\text{Chord}} = \frac{137.95}{54.94} = 2.511^\circ$

Actual $\alpha_0^\circ = K\alpha_0 \times$ Theoretical α_0°

Nose-Tail Slope $= \frac{\text{Nose rise} - \text{Tail rise}}{\text{Chord}} \times 57.3$

$= \frac{2.26 - 0.84}{54.94} \times 57.3 =$

$= 1.48^\circ$

$\Sigma = 3.99^\circ$

Table I-12

VC2-S-AP3   17.55 Kn   11,606T

CALCULATION OF THRUST, TORQUE & EFFICIENCY AT

$x = r/R = 0.90$ $J = V/nd = 0.8555$

Diam = 20.5'
Pitch = 22.90'
V_a [w_L = .231] = 1368
N = 78   n = 1.3

$\sigma = \frac{B \times C}{2\pi r} = \frac{4 \times 48.45}{12\pi \times 20.5 \times 0.9} = 0.2786$

$K_{\alpha_0} = 0.905$ $K_{g\alpha_0} = 0.01$

$K_S = 0.950$ $K_{gs} = 0.961$

t = 1.82	t/c = 0.0376
c = 48.45	

$\alpha_0 = 2.26 \times .905$ =	2.05
α_{nt} =	.07
$\tan\theta = P/2\pi r = .3951$ θ =	21.56
$\theta + \alpha_0 + \alpha_{nT}$ =	23.68
$-\Delta\alpha_g = 2.26 \times 0.01$ =	− .02
θ_0 =	23.66
$\tan\psi = J/\pi x = .3026$ ψ =	16.84
$\theta_0 - \psi$ =	6.82

$\alpha_1^\circ = 6.82(0.52-0.18) = 2.32$

$C_2 = \frac{36.48}{.950 \times .2786 \times .961} = 143.4$

α_1	2.32	2.07
$\phi = \theta_0 - \alpha_1$	21.34	21.59
$\beta = \phi - \psi$	4.50	4.75
$\varepsilon = \phi + \beta$	25.84	26.34
K_ε	.522	.518
$\sin\phi$	.3638	.3679
$\tan\beta$	.0787	.0831
$\alpha_2 = C_2 K_\varepsilon \sin\phi \tan\beta$	2.143	2.271
$\tan\phi$	.3906	.3957
K_ϕ	.583	.580
$(1-K_\phi)\frac{\tan\beta}{\tan\phi} \times \alpha_2$	.180	.200
α_3	1.963	2.071

$C_{L\,opt}$ =	—
C_L =	.2083
$C_L - C_{L\,opt}$ =	—

$C_{D\,min}$ =	.0069
=	—
$\Delta C_{Dg} = \frac{0.02 \times .208}{57.3}$ =	.0002
C_D =	.0071

$(\alpha_3 - \alpha_1)\frac{\beta}{\beta + \alpha_3} = \frac{-.357 \times 4.50}{6.463} = -.250$

$C_L = \frac{2.07 \times .950 \times .961}{9.072}$	.2083
$\delta C_L = \frac{1}{2} \times .0071 \times .0831 \times .961 =$	.0003
C_L =	.2086

$\tan\gamma = .0340$

γ =	1.95°
ϕ =	21.59°
$\phi + \gamma$ =	23.54°

$\tan(\phi+\gamma) = .4356$ $\sin(\phi+\gamma) = .3993$ $C_y = \frac{\pi^2 x^2 \sigma}{2 B} = .7872$ $\cos(\gamma) = .9994$

$a' = \frac{(\tan\phi - \tan\psi)\tan(\phi+\gamma)}{1 + \tan\phi \tan(\phi+\gamma)} = \frac{.0931 \times .4356}{1 + .3957 \times .4356} = .0346$

$(1-a') = .9654$

$K_Q' = C_y (1-a')^2 (1+\tan^2\phi) C_L \frac{\sin(\phi+\gamma)}{\cos\gamma}$
$= .7872\,(.9654)^2 (1.1566)(.2086)\frac{(.3993)}{.9994}$
$= 0.07072$

$K_Q' = K_Q' \frac{x}{2} = .03182$

$K_F' = \frac{K_Q'}{\tan(\phi+\gamma)} = \frac{0.07072}{.4356} = 0.1624$

$\eta = \frac{J}{2\pi} \cdot \frac{K_F'}{K_Q'} = \frac{.8555 \times .1624}{2\pi \times .03182} = .695$

ck. $\eta = \frac{\tan\psi}{\tan(\phi+\gamma)} = \frac{.3026}{.4356} = .695$

$C_S = \rho n^2 D^3$
$= 1.99\,(1.3)^2 \times (20.5)^3$
$= 28,858$

$G = C_S K_Q'$
$= 2,041$

$F = C_S K_F'$
$= 4,687$

Table I-13

VC2-S-AP3   17.55 Kn.   11,606T

CALCULATION OF THRUST, TORQUE & EFFICIENCY AT

$x = r/R = 0.80$ $J = V/nd = 0.8487$

Diam = 20.5'
Pitch = 22.70'
V_a [w_t=.237] = 1357
N = 78   n = 1.3

$\sigma = \frac{Z \times C}{2\pi r} = \frac{4 \times 62}{12\pi \times 20.5 \times .8} = 0.4011$

$K_{\alpha_0} = 0.920$ $K_{g\alpha_0} = 0.041$

$K_s = 0.950$ $K_{gs} = 0.867$

t = 2.90
c = 62.0
t/c = 0.0469

$\alpha_0 = 2.41° \times 0.920 =$	2.22
$\alpha_{nt} =$	0.12
$\tan\theta = P/2\pi r = .4445$ $\theta =$	23.76
$\theta + \alpha_0 + \alpha_{nT} =$	36.30
$-\Delta\alpha_g = 0.041 \times 2.41 =$	-.10
$\theta_0 =$	26.20
$\tan\psi = J/\pi x = .3377$ $\psi =$	18.66
$\theta_0 - \psi =$	7.54

$\alpha_1° = 7.54\,(0.52 - 0.16) = 2.72$

$C_2 = \frac{36.48}{.4011 \times .867 \times .950} = 110.42$

α_1	2.72	2.55
$\phi = \theta_0 - \alpha_1$	23.48	23.65
$\beta = \phi - \psi$	4.82	4.99
$\varepsilon = \phi + \beta$	28.30	28.64
K_ε	.695	.692
$\sin\phi$	.3984	.4012
$\tan\beta$	.0843	.0873
$\alpha_2 = C_2 K_\varepsilon \sin\phi \tan\beta$	2.577	2.676
$\tan\phi$	.4344	.4379
K_ϕ	.764	.761
$(1-K_\phi)\frac{\tan\beta}{\tan\phi} \times \alpha_2$	.118	.127
α_3	2.459	2.549

$C_{L\,opt}$	$11.2 \times \frac{1.372}{62.0} =$	.248
C_L	$=$	.2315
$C_L - C_{L\,opt}$	$=$	-.0165

$C_{D\,min} =$	.0068
$=$	—
$\Delta C_{Dg} = \frac{.10 \times .2315}{57.3} =$	.0004
$C_D =$	.0072

$\tan\gamma = .0311$

$(\alpha_3 - \alpha_1)\frac{\beta}{\beta + \alpha_3} = \frac{-.261 \times 4.87}{7.219} = -.173$

$C_L = \frac{2.55 \times .950 \times .867}{9.072}$	.2315
$\delta C_L = \frac{1}{2} \times .0072 \times .0873 \times SCF$	.0003
$C_L =$	.2318

$\gamma =$	1.78°
$\phi =$	23.65°
$\phi + \gamma =$	25.43°

$\tan(\phi+\gamma) = .4753$ $\sin(\phi+\gamma) = .4292$ $C_y = \frac{\pi^3 x^3 \sigma}{2B} = .7959$ $\cos(\gamma) = .9995$

$a' = \frac{(\tan\phi - \tan\psi)\tan(\phi+\gamma)}{1 + \tan\phi \tan(\phi+\gamma)} = \frac{.1002 \times .4753}{1 + .4379 \times .4753} = 0.0394$

$(1 - a') = 0.9606$

$K_G' = C_y (1-a')^2 (1+\tan^2\phi) C_L \frac{\sin(\phi+\gamma)}{\cos\gamma}$
$= .7959\,(.9606)^2 (1.1917)(.2318)(.4292)\frac{1}{.9995}$
$= 0.08714$

$K_Q' = K_G' \frac{x}{2} = 0.03485$

$K_T' = \frac{K_G'}{\tan(\phi+\gamma)} = \frac{0.08714}{.4753} = 0.1833$

$\eta = \frac{J}{2\pi} \cdot \frac{K_T'}{K_Q'} = \frac{.8487 \times .1833}{2\pi \times .03485} = 0.710$

ck. $\eta = \frac{\tan\psi}{\tan(\phi+\gamma)} = \frac{.3377}{.4753} = 0.710$

$C_S = \rho n^2 D^3$
$=$
$= 28,858$

$G = C_S K_G'$
$= 2,515$

$F = C_S K_T'$
$= 5,290$

Table I-14

VC2-S-AP3 - 17.55KN. - 11,606T.

CALCULATION OF THRUST, TORQUE & EFFICIENCY AT

$x = r/R = 0.55$ $J = V/nd = 0.7661$

Diam	=	20.5
Pitch	=	22.86
V_a [w_L = .211]	=	1225
N	= 78	n = 1.3

$\sigma = \frac{B \times C}{2\pi r} = \frac{4 \times 68.15}{\pi \times 20.5 \times .55 \times 12} = 0.6413$

$K_{\alpha_0} = 0.920$ $K_{g\alpha_0} = 0.148$

$K_s = 0.946$ $K_{gs} = 0.742$

$t = 5.56$, $c = 68.15$, $t/c = 0.0816$

$\alpha_0 = 3.31 \times 0.920$ =	3.04
α_{nt} =	.54
$\tan\theta = P/2\pi r = .6454$ θ =	32.84
$\theta + \alpha_0 + \alpha_{nT}$ =	36.42
$-\Delta\alpha_g = 0.148 \times 3.31$ =	-.49
θ_0 =	35.93
$\tan\psi = J/\pi x = .4434$ ψ =	23.91
$\theta_0 - \psi$ =	12.02

$\alpha_1^\circ = 12.02(.52 - .11) = 4.94^\circ$

$C_2 = \frac{36.48}{0.946 \times .6413 \times .742} = 80.80$

α_1	4.94	4.72	
$\phi = \theta_0 - \alpha_1$	30.99	31.21	
$\beta = \phi - \psi$	7.08	7.30	
$\varepsilon = \phi + \beta$	38.07	38.51	
K_ε	.897	.894	
$\sin\phi$	.5148	.5181	
$\tan\beta$	.1242	.1281	
$\alpha_2 = C_2 K_\varepsilon \sin\phi \tan\beta$	4.634	4.794	
$\tan\phi$	.6005	.6058	
K_ϕ	.937	.937	
$(1-K_\phi)\frac{\tan\beta}{\tan\phi} \times \alpha_2$	0.060	.064	
α_3	4.574	4.730	

$C_{L\,opt}$ $9.4 \times \frac{2.36}{68.15}$ =	.325
C_L =	.3652
$C_L - C_{L\,opt}$ =	.040

$C_{D\,min}$ =	.0155
=	—
$\Delta C_{Dg} = \frac{0.49 \times 0.365}{57.3}$ =	.0031
C_D =	.0186

$\tan\gamma = .0508$

$(\alpha_3 - \alpha_1)\frac{\beta}{\beta + \alpha_3} = \frac{-.366 \times 7.08}{11.67} = -.222$

$C_L = \frac{0.946 \times 4.72 \times .742}{9.072}$	0.3652
$\delta C_L = \frac{1}{2} \times .0186 \times .1281 \times .742$	.0009
C_L =	0.3661

$\gamma = 2.91^\circ$, $\phi = 31.21$, $\phi + \gamma = 34.12^\circ$

$\tan(\phi+\gamma) = 0.6776$ $\sin(\phi+\gamma) = 0.5609$ $C_y = \frac{\pi^3 x^3 \sigma}{2B} = 0.4135$ $\cos(\gamma) = .9987$

$a' = \frac{(\tan\phi - \tan\psi)\tan(\phi+\gamma)}{1 + \tan\phi \tan(\phi+\gamma)} = \frac{.1624 \times .6776}{1 + .6058 \times .6776} = .0780$

$(1 - a') = 0.9220$

$K_Q' = C_y(1-a')^2(1+\tan^2\phi)C_L \frac{\sin(\phi+\gamma)}{\cos\gamma}$

$= .4135(.9220)^2(1.3670)(.3661)\frac{.5609}{.9987}$

$= 0.0988$

$K_Q' = K_Q' \frac{x}{2} = 0.02717$

$K_F' = \frac{K_Q'}{\tan(\phi+\gamma)} = \frac{0.0988}{0.6776} = 0.1458$

$\eta = \frac{J}{2\pi} \cdot \frac{K_F'}{K_Q'} = \frac{.7661}{2\pi} \times \frac{.1458}{.02717} = 0.654$

ck. $\eta = \frac{\tan\psi}{\tan(\phi+\gamma)} = \frac{.4434}{.6776} = 0.654$

$C_s = \rho n^2 D^3$

=

= 28,858

$G = C_s K_G'$

= 2,851

$F = C_s K_F'$

= 4207

Table I-15

VC2 - S - AP3 - 17.55KN - 11.60FT.

CALCULATION OF THRUST, TORQUE & EFFICIENCY AT

$x = r/R = 0.30$ $J = V/nd = 0.450$

Diam = 20.5

Pitch = 20.31

$V_a[(1-w_x)=0.44] = 713$

N = 78 n = 1.3

$\sigma = \frac{BxC}{2\pi r} = \frac{4 \times 54.94}{2\pi \times .15 \times 20.5 \times 12} = 0.948$

$K_{\alpha_0} = 0.925$ $K_{g\alpha_0} = 0.275$

$K_s = 0.912$ $K_{gs} = 0.63$

t = 8.28

c = 54.94

t/c = 0.151

$\alpha_0 = 2.511° \times 0.925 =$	2.32°
$\alpha_{nt} =$	1.48°
$\tan\theta = P/2\pi r = 1.051$ $\theta =$	46.43°
$\theta + \alpha_0 + \alpha_{nT} =$	50.23°
$-\Delta\alpha_g = 2.511 \times 0.275 =$	−.69°
$\theta_0 =$	49.54°
$\tan\psi = J/\pi x = 0.4775$ $\psi =$	25.52°
$\theta_0 - \psi =$	24.02°

$\alpha_1° = 24.02(0.52 - 0.06) = 11.04°$

$C_2 = \frac{36.48}{.912 \times .948 \times .63} = 66.98$

α_1	11.04°	10.32	10.45
$\phi = \theta_0 - \alpha_1$	38.50	39.22	39.07
$\beta = \phi - \psi$	12.98	13.70	13.57
$\varepsilon = \phi + \beta$	51.48	52.92	52.64
K_ε	1.022	1.035	1.031
$\sin\phi$	0.6225	.6323	.6305
$\tan\beta$	0.2306	.2438	.2414
$\alpha_2 = C_2 K_\varepsilon \sin\phi \tan\beta$	9.826	10.687	10.511
$\tan\phi$	0.7954	.8161	.8124
K_ϕ	0.983	.983	.983
$(1-K_\phi)\frac{\tan\beta}{\tan\phi} \times \alpha_2$	0.048	.054	.053
α_3	9.778	10.633	10.458

$C_{L\,opt}$ 4.8 $\frac{2.30}{54.94}$ =	0.2012
C_L =	0.6618
$C_L - C_{L\,opt}$ =	0.4606

$C_{D\,min}$ =	.0109
=	.0015
$\Delta C_{Dg} = \frac{0.69° \times 0.662}{57.3} =$	.0080
C_D =	0.0204

$\tan\gamma = 0.0308$

$(\alpha_3 - \alpha_1)\frac{\beta}{\beta + \alpha_3} = \frac{-1.26 \times 12.98}{22.76} = -0.719$

$C_L = \frac{0.912 \times 10.45 \times 0.63}{9.072}$	0.6618
$\delta C_L = \frac{1}{2} \times .0204 \times .2414 \times .63 =$	.0016
C_L =	0.6634

γ =	1.768°
ϕ =	39.07°
$\phi + \gamma$ =	40.86°

$\tan(\phi+\gamma) = 0.8650$ $\sin(\phi+\gamma) = 0.6542$ $C_y = \frac{\pi^2 x^3 \sigma}{2B} = 0.09939$ $\cos(\gamma) = .9995$

$a' = \frac{(\tan\phi - \tan\psi)\tan(\phi+\gamma)}{1 + \tan\phi \tan(\phi+\gamma)} = \frac{.3349 \times .8650}{1 + .8124 \times .8650} = 0.1701$

$(1-a') = 0.8299$

$K_Q' = C_y(1-a')^2(1+\tan^2\phi)C_L \frac{\sin(\phi+\gamma)}{\cos\gamma}$

$= 0.09939 \times (.8299)^2 (1.6600)(.6634) \frac{0.6542}{0.9995}$

$= 0.04934$

$K_Q' = K_Q' \frac{x}{2} = 0.0074$

$K_T' = \frac{K_Q'}{\tan(\phi+\gamma)} = \frac{0.04934}{0.8650} = 0.05704$

$\eta = \frac{J}{2\pi} \cdot \frac{K_T'}{K_Q'} = \frac{0.450 \times 0.05704}{6.283 \times .0074} = 0.552$

ck. $\eta = \frac{\tan\psi}{\tan(\phi+\gamma)} = \frac{0.4775}{0.8650} = 0.5520$

$C_s = \rho n^2 D^3$

$= 1.99(1.3)^2(20.5)^3$

$= 28,858$

$G = C_s K_Q'$

$= 1,424$

$F = C_s K_T'$

$= 1,646$

Table I-16

Total Steady Thrust and Torque of the Propeller

Radius	F	Integr. Const.	f(F)	G	rG	f(r.G)
0.3R	1,646	1.7083	2,812	1,424	4,379	7,481
0.55R	4,207	3.4167	14,374	2,851	16,065	54,889
0.8R	5,290	1.1958	6,326	2,515	20,623	24,661
0.9R	4,687	1.3667	6,406	2,041	18,818	25,719
			29,918			112,750

Total force on 4 blades = 119,672 pounds.

Total Torque on 4 blades = 451,000 pound feet.

The model basin test gave a thrust of 121,000 pounds and a torque of 455,000 pound feet.[24] (page 12)

The slight increase may result from the thrust and torque of the sections adjacent to the hub.

Table I-17

CALCULATION OF HARMONIC FORCES & MOMENTS

ON ONE BLADE - SHEET 1

Third ORDER, n

SHIP SPEED 17.55 Kn. PROP. DIA. 20.5' RPM 78 Ω 8.168 ω 24.50

	0.30R		0.55R		0.80R		0.90R	
	3.075 Ft.		5.6375 Ft.		8.20 Ft.		9.225 Ft.	
1. W_{Lo}	0.599		0.311		0.237		0.231	
2. $1-W_{Lo}$	0.401		0.689		0.763		0.769	
3. V/Ω_r	0.4732		0.4425		0.3377		0.3025	
4. α	0.1824		0.08.4		0.0445		0.0362	
5. φ	39.09°		31.21°		23.65°		21.59°	
6. $Sin^2 \varphi$	0.3975		0.2684		0.1610		0.1354	
7. $Cos^2 \varphi$	0.6025		0.7316		0.8390		0.8646	
8. $1/\alpha \ Sin \varphi \ cos \varphi$	2.683		5.378		8.258		9.450	
9. $U = (1-a')\sqrt{1+Tan^2\varphi} \ \Omega r$	26.856		49.643		70.232		78.227	
10. blade chord, c	4.578'		5.679'		5.167'		4.038'	
11. Freq. parameter $c \ \omega/2U$	2.088		1.401		0.9011		0.832	
12. W_{Ln}	-.099	.054j	-.033	-.007j	0	-.010j	.003	-.005j
13. W_{tn}	-.022	-.088j	-.012	-.009j	-.011	.023j	-.008	.030j
14. $W_{Ln}/(1-W_{Lo})$	-.246	.135j	-.048	-.010j	0	-.013j	.004	-.007j
15. $W_{tn} \ V/\Omega r$	-.046	-.186j	-.027	-.020j	-.033	.068j	-.026	.099j
16. $\boxed{14} + \boxed{15}$	-.292	-.051j	-.075	-.030j	-.033	.055j	-.022	.092j
17. $1/\alpha \ Sin \varphi \ cos \varphi \ \boxed{16}$	-.783	-.137j	-.403	-.161j	-.273	.454j	-.208	.867j
18. M+i N (Fig. 2)	.058	.271j	.232	.218j	.373	.100j	.473	0
19. $\boxed{17} \times \boxed{18}$	-.008	-.220j	-.058	-.125j	-.147	.142j	-.098	.411j
20. $Sin^2 \varphi \ W_{Ln}/(1-W_{Lo})$	-.098	.054j	-.013	-.003j	0	-.002j	.001	-.001j
21. $cos^2 \varphi \ W_{tn} \ V/\Omega r$	-.028	-.112j	-.020	-.015j	-.028	.057j	-.022	.086j
22. $\boxed{21} - \boxed{20}$	.070	-.166j	-.007	-.012j	-.028	.059j	-.023	.087j
23. B + i A (Fig. 1)	1.518	.980j	1.523	.618j	1.541	.350j	1.666	.103j
24. $\boxed{22} \times \boxed{23}$	.269	-.183j	-.003	-.023j	-.064	.081j	-.047	-.142j
25. $\boxed{19} + \boxed{24}$	.261	.037j	-.061	-.148j	-.211	.223j	-.145	.269j
26. G_o	1,424		2,851		2,515		2,041	
27. F_o	1,646		4,207		5,290		4,687	
28. $G_n = \boxed{26} \times \boxed{25}$	369	53j	-174	-422j	-531	561j	-296	549j
29. $F_n = \boxed{27} \times \boxed{25}$	430	61j	-257	-623j	-1,116	1180j	-680	1261j
30. G_n Resultant + angle					772	133.33°	624	118.34°
31. F_n Resultant + angle					1624	133.33°	1433	118.34°

Table I-18(a)

CALCULATION OF HARMONIC FORCES & MOMENTS

ON ONE BLADE - SHEET 2

Third ORDER, n

SHIP SPEED 17.55Kn PROP. DIA. 20.5' RPM 78 Ω 8.168 ω 24.50

	0.30R		0.55R		0.80R		0.90R	
	3.075 Ft.		5.6375 Ft.		8.20 Ft.		9.225 Ft.	
32. Skewback °					2.22°		4.18°	
33. Skewback - phase °					6.66°		12.54°	
34. G_n-ref. line - R + ∠					772	126.67°	624	105.80°
35. F_n-ref. line - R + ∠					1624	126.67°	1433	105.80°
36. G_n-ref. line -Re + Im	369	53j	-174	-422j	-461	619j	-170	600j
37. F_n-ref. line - Re + Im	430	61j	-257	-623j	-970	1302j	-390	1379j
38. Integration Constant	0.8541		3.4167		1.1958		1.3667	
39. $f\,(G_n)$	315	45j	-595	1442j	-551	740j	-232	820j
40. $f\,(F_n)$	367	52j	-878	2129j	-1160	1557j	-533	1885j
41. $f\,(r\,G_n)$	969	137j	-3351	8128j	-4518	6068j	-2143	7565j
42. $f\,(r\,F_n)$	1129	160j	-4950	12,[illegible]0j	-9511	12,767j	-4917	17,386j
43. $f\,(G_n)$	-1063	3047j						
44. $f\,(F_n)$	-2204	5623j						
45. $f\,(r\,G_n)$	-9043	21,900j						
46. $f\,(r\,F_n)$	-18,249	42,313j						

Table I-18(b)

CALCULATION OF HARMONIC FORCES & MOMENTS

ON ONE BLADE - SHEET 1

Fourth ORDER, n

SHIP SPEED 17.55 Kn. PROP. DIA. 20.5' RPM 78 Ω 8.168 ω 32.67

	0.30R		0.55R		0.80R		0.90R	
	3.075 Ft.		5.6375 Ft.		8.20 Ft.		9.225 Ft.	
1. W_{Lo}								
2. $1-W_{Lo}$								
3. $V/\Omega r$								
4. α			See					
5. φ			Third order					
6. $\sin^2 \varphi$			Calculations					
7. $\cos^2 \varphi$								
8. $1/\alpha \sin\varphi \cos\varphi$								
9. $U = (1-a')\sqrt{1+\tan^2\varphi}\,\Omega r$								
10. blade chord, c								
11. Freq. parameter $c\,\omega/2U$	2.784		1.868		1.202		0.843	
12. W_{Ln}	.022	-.036j	0.87	-.012j	.104	-.009j	.107	-.007j
13. W_{tn}	.030	.024j	.010	.016j	.001	.018j	-.004	.017j
14. $W_{Ln}/(1-W_{Lo})$	.055	-.090j	.127	-.017j	.136	-.012j	.139	-.009j
15. $W_{tn}\ V/\Omega r$	.063	.051j	.023	.036j	.003	.053j	-.013	.056j
16. $\boxed{14} + \boxed{15}$	.118	.039j	.150	.019j	.139	.041j	.126	.047j
17. $1/\alpha \sin\varphi \cos\varphi\ \boxed{16}$	.317	.105j	.807	.102j	1.148	.339j	1.191	.444j
18. M+i N (Fig.2)	-.103	.210j	.111	.271j	.292	.177j	.378	.083j
19. $\boxed{17} \times \boxed{18}$	-.054	.056j	.062	.230j	.275	.302j	.437	.276j
20. $\sin^2\varphi\ W_{Ln}/(1-W_{Lo})$	.022	.036j	.034	-.005j	.022	-.002j	.019	-.001j
21. $\cos^2\varphi\ W_{tn}\ V/\Omega r$	.038	.031j	.017	.026j	.003	.044j	-.011	.048j
22. $\boxed{21} - \boxed{20}$	.016	-.005j	-.017	.031j	-.019	.046j	-.030	.049j
23. B + i A (Fig.1)	1.503	1.347j	1.520	.854j	1.530	.513j	1.544	0.313j
24. $\boxed{22} \times \boxed{23}$	.031	.014j	-.052	.033j	-.053	.061j	-.062	.066j
25. $\boxed{19} + \boxed{24}$	-.023	.070j	.010	.263j	.222	.363j	.375	.342j
26. G_o	1,424		2,851		2,515		2,041	
27. F_o	1,646		4,207		5,290		4,687	
28. $G_n = \boxed{26} \times \boxed{25}$	-33	100j	29	750j	558	913j	765	698j
29. $F_n = \boxed{27} \times \boxed{25}$	-38	115j	42	1106j	1174	1920j	1758	1603j
30. G_n Resultant + angle					1070	58.56°	1036	42.55°
31. F_n Resultant + angle					2250	58.65°	2379	42.55°

Table I-19(a)

CALCULATION OF HARMONIC FORCES & MOMENTS

ON ONE BLADE - SHEET 2

Fourth ORDER, n

SHIP SPEED 17.55Kn. PROP. DIA. 20.5' RPM 78 Ω 8.168 ω 32.67

	0.30R		0.55R		0.80R		0.90R	
	3.075 Ft.		5.6375 Ft.		8.20 Ft.		9.225 Ft.	
32. Skewback °					2.22°		4.18°	
33. Skewback - phase °					8.88°		16.72°	
34. $G_{n\text{-ref. line}}$ - R + ∠					1070	49.68°	1036	25.83°
35. $F_{n\text{-ref. line}}$ - R + ∠					2250	49.68°	2379	25.83°
36. $G_{n\text{-ref. line}}$ -Re + Im	-33	100j	29	750j	692	816j	933	451j
37. $F_{n\text{-ref. line}}$ - Re+ Im	-38	115j	42	1106j	1456	1715j	2141	1036j
38. Integration Constant	0.8541		3.4167		1.1958		1.3667	
39. f (G_n)	-28	85j	99	256j	827	976j	1275	616j
40. f (F_n)	-32	78j	144	3779j	1741	2051j	2926	1416j
41. f $(r\,G_n)$	-87	263j	559	1444j	6785	8001j	11,763	5,686j
42. f $(r\,F_n)$	-100	302j	809	21,303j	14,277	16,816j	26,993	13,062j
43. f (G_n)	2173	1399j						
44. f (F_n)	4779	7344j						
45. f $(r\,G_n)$	19620	13,394j						
46. f $(r\,F_n)$	41,979	57,483j						

Table I-19(b)

CALCULATION OF HARMONIC FORCES & MOMENTS

ON ONE BLADE - SHEET 1

Fifth ORDER, n

SHIP SPEED 17.55k. PROP. DIA. 20.5' RPM 78 Ω 8.168 ω 40.84

	0.30R		0.55R		0.80R		0.90R	
	3.075 Ft.		5.6375		8.20 Ft.		9.225 Ft.	
1. W_{Lo}								
2. $1-W_{Lo}$								
3. $V/\Omega r$								
4. α								
5. φ			See Third Order Calculations					
6. $\sin^2\varphi$								
7. $\cos^2\varphi$								
8. $1/\alpha \sin\varphi \cos\varphi$								
9. $U=(1-a')\sqrt{1+\tan^2\varphi}\,\Omega r$								
10. blade chord, c.								
11. Freq. parameter $c\,\omega/2U$	3.481		2.336		1.502		1.054	
12. W_{Ln}	.042	-.007j	-.029	-.023j	-.040	-.013j	-.026	-.018j
13. W_{tn}	.002	-.019j	-.014	-.011j	-.009	.001j	-.012	.008j
14. $W_{Ln}/(1-W_{Lo})$	.105	-.017j	-.042	-.033j	-.052	-.017j	-.034	-.017j
15. $W_{tn}\ V/\Omega r$	.004	.040j	-.032	-.025j	-.027	.003j	-.040	.026j
16. $\boxed{14} + \boxed{15}$	.109	-.057j	-.074	-.058j	-.079	-.014j	-.074	.009j
17. $1/\alpha \sin\varphi \cos\varphi\ \boxed{16}$	.292	-.153j	-.378	-.312j	-.652	-.116j	-.679	.085j
18. M+i N (Fig. 2)	-.196	.086j	-.002	.261j	.210	.232j	.331	.142j
19. $\boxed{17} \times \boxed{18}$	-.044	.055j	.082	-.103j	-.110	-.176j	-.243	-.071j
20. $\sin^2\varphi\ W_{Ln}/(1-W_{Lo})$	.042	-.007j	-.011	-.009j	-.008	-.003j	-.005	-.002j
21. $\cos^2\varphi\ W_{tn}\ V/\Omega r$	.002	-.024j	-.023	-.018j	-.023	.003j	-.036	.022j
22. $\boxed{21} - \boxed{20}$	-.040	-.017j	-.012	-.009j	-.015	.006j	-.031	.024j
23. B + i A (Fig. 1)	1.500	1.705j	1.576	1.108j	1.520	0.670j	1.538	.427j
24. $\boxed{22} \times \boxed{23}$	-.031	-.074j	-.008	-.023j	-.027	-.001j	-.058	.024j
25. $\boxed{19} + \boxed{24}$	-.075	-.037j	.074	-.130j	-.137	-.177j	-.301	-.047j
26. G_o	1,424		2,851		2,515		2,041	
27. F_o	1,646		4,207		5,290		4,687	
28. $G_n = \boxed{26} \times \boxed{25}$	-107	-56j	211	-371j	-345	-445j	-614	-96j
29. $F_n = \boxed{27} \times \boxed{25}$	-123	-64j	311	-547j	-725	-936j	-1411	-220j
30. G_n Resultant + angle					563	232.21°	621	188.86°
31. F_n Resultant + angle					1128	232.21°	1428	188.86°

Table I-20(a)

CALCULATION OF HARMONIC FORCES & MOMENTS

ON ONE BLADE - SHEET 2

Fifth ORDER, n

SHIP SPEED 17.55 Kn. PROP. DIA. 20.5' RPM 78 Ω 8.168 ω 40.84

	0.30R		0.55R		0.80R		0.90R	
	3.075 Ft.		5.6375 Ft.		8.20 Ft.		9.225 Ft.	
32. Skewback °					2.22°		4.18°	
33. Skewback - phase °					11.10°		20.90°	
34. G_n-ref. line - R + ∠	--				563	221.11°	621	167.96°
35. F_n-ref. line - R + ∠					1128	221.11°	1428	167.96°
36. G_n-ref. line -Re + Im	-107	-56j	211	-371j	-424	-370j	-607	129j
37. F_n-ref. line - Re + Im	-123	-64j	311	-547j	-850	-742j	-1397	278j
38. Integration Constant	0.8541		3.4167		1.1958		1.3667	
39. $f\,(G_n)$	-91	-48j	721	-1268j	-507	-442j	-830	176j
40. $f\,(F_n)$	-105	-55j	1063	-1869j	-1016	-887j	-1907	407j
41. $f\,(r\,G_n)$	-281	-147j	4064	-7146j	-4157	-3628j	-7653	1626j
42. $f\,(r\,F_n)$	-323	-168j	5990	-10,5[illegible]j	-8335	-7276j	-17,613	3757j
43. $f\,(G_n)$	-707	-1582j						
44. $f\,(F_n)$	-1967	-2404j						
45. $f\,(r\,G_n)$	-8027	-9295j						
46. $f\,(r\,F_n)$	-20,281	-14,223j						

Table I-20(b)

VC 2 - S - AP3

Fourth ORDER HARMONIC FORCES AND MOMENTS

GENERATED BY PROPELLER WORKING IN THE NON-UNIFORM WAKE

SHIP SPEED 17.5 Kn. RPM 78 DISPLACEMENT 11,606 Tons.

PROPELLER DIA. 20.5 FT. , NUMBER OF BLADES, B 4

WAKE DISTRIBUTION GIVEN BY DTMB Tests of 20 May 1955

	Real	Imag.	Real	Imag.	Result	Harm. Phase	Prop. Angle
Harmonic Thrust = $\sum_B \sum F_n$			19,116	29,376	35,048	56.75°	14.49°
Harmonic Torque = $\sum_B \sum (r\, G_n)$			76,080	53,576	93,051	35.16°	8.79°
Vertical Harmonic Force = $\sum_B \left[+ \frac{1}{2i} \sum (G_{n-1}) \right.$	1524	632j	1315	179j	1,327	7.75°	1.94°
$\left. - \frac{1}{2i} \sum (G_{n+1}) \right]$	791	-353j					
Horizontal Harmonic Force = $\sum_B \left[+ \frac{1}{2} \sum (G_{n-1}) \right.$	-532	1524j	-885	733j	1,149	140.36°	35.09°
$\left. + \frac{1}{2} \sum (G_{n+1}) \right]$	-353	-791j					
Harmonic Moment About = $\sum_B \left[+ \frac{1}{2} \sum (r\, F_{n-1}) \right.$	-9,124	21,156j	-19,264	14,044j	23,840	143.91°	35.98°
The Horizontal Axis $\left. + \frac{1}{2} \sum (r\, F_{n+1}) \right]$	-10,140	-7,112j					
Harmonic Moment About = $\sum_B \left[+ \frac{1}{2i} \sum (r\, F_{n-1}) \right.$	21,156	9,124j	28,268	-1,016j	28,286	357.94°	89.48°
The Vertical Axis $\left. - \frac{1}{2i} \sum (r\, F_{n+1}) \right]$	7,112	-10,140j					

Table I-21

REFERENCES:

1. Burrill, L. C.
Calculation of Marine Propeller Characteristics
N. E. Cst. Instn. Engrs. Shipb. Trans. V. 60 (1943-1944)

2. Ritger, Paul D. and Breslin, John P.
A Theory for the Quasi-Steady and Unsteady Thrust and Torque of a Propeller in a Ship Wake
Experimental Towing Tank, Stevens Inst. of Tech. Rep. 686 (Mar. 1958)

3. Jasper, Norman H.
A Theoretical Approach to the Problem of Critical Whirling Speeds of Shaft-Disk Systems
David W. Taylor Mod. Basin Rep. 827 (Dec. 1954)

4. Jasper, Norman H.
A Design Approach to the Problem of Critical Whirling Speeds of Shaft-Disk Systems
David W. Taylor Mod. Basin Rep. 890 (Dec. 1954)

5. Lewis, Frank M.
Propeller Vibration
SNAME V. 43 (1935)

6. Lewis, Frank M.
Propeller Vibration
SNAME V. 44 (1936)

7. Lewis, Frank M. and Tachmindji, A. J.
Propeller Forces Exciting Hull Vibration
SNAME V. 62 (1954)

8. Tachmindji, A. J. and Dickerson, M. C.
Measurement of Oscillating Pressures in the Vicinity of Propellers
David W. Taylor Mod. Basin Rep. 1130 (Apr. 1957)

9. Breslin, J. P.
The Unsteady Pressure Field near a Ship Propeller and the Vibratory Forces Produced on an adjacent Structure
Experimental Towing Tank, Stevens Inst. of Tech. Rep. 609 (June 1950)

10. Breslin, J. P..
The Pressure Field near a Ship Propeller
J. Ship Res. V. 1 No. 4 (Mar. 1958) pp. 57-67

11. Breslin, J. P.
A New Interpretation of the Free-Space Pressure Field near a Ship Propeller
Experimental Towing Tank, Stevens Inst. of Tech. Rep. 687 (Feb. 1958)

12. Breslin, J. P.
A Theory for the Vibratory Effects produced by a Propeller on a Large Plate
Experimental Towing Tank, Stevens Inst. of Tech. Rep. 689 (Feb. 1958)
J. Ship Res. V. 3 No. 3 (Dec. 1959) pp. 1-10

13. Gutin, L.
Über das Schallfeld einer Ratierenden Luftschraube
Phys. Zeitschrift der Sowjetunion Band 9 Heft 1 (1936)
NACA NM 1195 (1948)

14. Hubbard, Harvey H. and Regier, Arthur A.
Free Space Oscillating Pressures Near the Tips of Rotating Propellers
NACA Rep. 996 (1950) (Supersedes NACA TN 1870)

15. Garrick, I. E., and Watkins, Charles E.
A Theoretical Study of the Effect of Forward Speed on the Free-Space Sound-Pressure Field around Propellers
NACA Rep. 1198 (1954) (Supersedes NACA TN 3018)

16. Watkins, Charles E., and Durling, Barbara J.
A Method for Calculation of Free-Space Sound Pressures near a Propeller in Flight including Considerations of the Chordwise Blade Loading
NACA TN 3809 (1956)

17. Isaacs, Rufus
Airfoil Theory for Flows of Variable Velocity
J. Aero. Sci. V. 12 No. 1 (Jan 1945)

18. Greenberg, J. Mayo
Airfoil in Sinusoidal Motion in a Pulsating Stream
NACA TN 1326 (June 1947)

19. Bisplinghoff, R. L., Ashley, H. and Halfman, R. L.
Aeroelasticity
Addison-Wesley Publishing Co. Inc. Reading, Mass. (1955)

20. Lamb, Sir Horace
Hydrodynamics
6th Ed. (1945) Dover Publications, New York

21. Von Karman, T. and Burgers, J. M.
General Aerodynamic Theory of Perfect Fluids. Division E, V. II of "Aerodynamic Theory" (Editor: W. F. Durand)
Durand Reprinting Committee, Pasadena, Cal. (1943)

22. Theodorsen, T.
General Theory of Aerodynamics
Instability and the Mechanism of Flutter
NACA Rep. 496 (1935)

23. Scanlan, R. H. and Rosenbaum, R.
Introduction to the Study of Aircraft Vibration and Flutter
The MacMillan Co. N. Y. (1951)

24. Noonan, Knopfle and Feldman, Silver Spring, Md.
Propeller Shaft Bending Stresses on the USNS LT. JAMES E. ROBINSON
For SNAME (Sept. 1955)

25. Prandtl, L. and Tietjens, O. G.
Fundamentals of Hydro-Aeromechanics
McGraw-Hill Book Co. Inc., New York, (1934)

26. Prandtl, L. and Tietgens, O. G.
Applied Hydro-Aeromechanics
McGraw-Hill Book Co., Inc. New York, (1934)

27. Hubbard, Harvey H. and Regier, Arthur A.
Free-Space Oscillating Pressures near the Tips of Rotating Propellers
NACA Rep. 996 (1950)

28. Manley, R. G.
Waveform Analysis
John Wiley and Sons, Inc., New York, (1946)

29. Bulletin of the Bureau of Standards
V. 9 p. 646

30. Den Hartog, J. P.
Mechanical Vibrations, Second Edition, (1940)
McGraw-Hill Book Company, Inc., New York

31. See for instance, Baker, B. B. and Copson, E. T.
The Mathematical Theory of Huygen's Principle"
Clarendon Press, Oxford, (1939) p. 124 ff., wherein
Sommerfeld's theory is discussed in detail

32. Felsen, L. B.
Trans. I. R. E. (Apr. 1959) pp. 168-180 gives a survey of some of
the underlying concepts

33. Sommerfeld, A.
Jahresber. Deutschen Math
Vereinigung V. 21 (1912) p. 312

34. Marcuvitz, N.
Symposium on Electromagnetic Theory
Acad. Press, New York (1951) p. 263 ff.

35. Morse, P. M. and Feshbach, H.
Methods of Theoretical Physics V. 1 p. 828 ff.
McGraw Hill Book Co., New York (1953)

36. Titchmarsh, E. C.
Eigenfunction Expansions
Clarendon Press, Oxford (1946) p. 19 ff.

37. Lebedev, N. N.
Dokl. Acad. Nauk. USSR V. 58 (1947) p. 1007

38. Ref. 34. p. 297

39. Morse, P. M. and Feshbach, H.
Methods of Theoretical Physics V. 2 p. 1466
McGraw Hill Book Co., New York (1953)

40. Rossell, H. E. and Chapman, L. B., Editors
Principles of Naval Architecture, V. 2
Soc. Nav. Arch. Mar. Engrs., New York (1939)

41. Seward, H. L., Editor
Marine Engineering, V. 1.
Soc. Nav. Arch. Mar. Engrs., New York (1942)

CONESCO, Arlington, Massachusetts. Report No. F-101-2. SHIP HULL VIBRATIONS - 2. THE DISTRIBUTION OF EXCITING FORCES GENERATED BY PROPELLERS, by F. E. Reed and R. T. Bradshaw. June 1960. xiii, 214 p. graphs, tables, refs. (Index No. NS712-100 S-1 T-2, Contract NObs 77150) UNCLASSIFIED

A study of the forces acting on a hull as a consequence of propeller action. Develops calculation forms for computing the dynamic forces and moments generated by a propeller operating in a variable wake. Describes a program for computing the shaft bearing reactions resulting from these propeller forces. Presents a method of computing hull pressure forces resulting from the propeller pressure field.

The various procedures are illustrated by numerical examples.

1. Propellers (marine) - performance
2. Ship hulls - propeller pressure field
3. Propeller shafts - vibration

I. F. E. Reed
II. R. T. Bradshaw

CONESCO, Arlington, Massachusetts. Report No. F-101-2. SHIP HULL VIBRATIONS - 2. THE DISTRIBUTION OF EXCITING FORCES GENERATED BY PROPELLERS, by F. E. Reed and R. T. Bradshaw. June 1960. xiii, 214 p. graphs, tables, refs. (Index No. NS712-100 S-1 T-2, Contract NObs 77150) UNCLASSIFIED

A study of the forces acting on a hull as a consequence of propeller action. Develops calculation forms for computing the dynamic forces and moments generated by a propeller operating in a variable wake. Describes a program for computing the shaft bearing reactions resulting from these propeller forces. Presents a method of computing hull pressure forces resulting from the propeller pressure field.

The various procedures are illustrated by numerical examples.

1. Propellers (marine) - performance
2. Ship hulls - propeller pressure field
3. Propeller shafts - vibration

I. F. E. Reed
II. R. T. Bradshaw

CONESCO, Arlington, Massachusetts. Report No. F-101-2. SHIP HULL VIBRATIONS - 2. THE DISTRIBUTION OF EXCITING FORCES GENERATED BY PROPELLERS, by F. E. Reed and R. T. Bradshaw. June 1960. xiii, 214 p. graphs, tables, refs. (Index No. NS712-100 S-1 T-2, Contract NObs 77150) UNCLASSIFIED

A study of the forces acting on a hull as a consequence of propeller action. Develops calculation forms for computing the dynamic forces and moments generated by a propeller operating in a variable wake. Describes a program for computing the shaft bearing reactions resulting from these propeller forces. Presents a method of computing hull pressure forces resulting from the propeller pressure field.

The various procedures are illustrated by numerical examples.

1. Propellers (marine) - performance
2. Ship hulls - propeller pressure field
3. Propeller shafts - vibration

I. F. E. Reed
II. R. T. Bradshaw

CONESCO, Arlington, Massachusetts. Report No. F-101-2. SHIP HULL VIBRATIONS - 2. THE DISTRIBUTION OF EXCITING FORCES GENERATED BY PROPELLERS, by F. E. Reed and R. T. Bradshaw. June 1960. xiii, 214 p. graphs, tables, refs. (Index No. NS712-100 S-1 T-2, Contract NObs 77150) UNCLASSIFIED

A study of the forces acting on a hull as a consequence of propeller action. Develops calculation forms for computing the dynamic forces and moments generated by a propeller operating in a variable wake. Describes a program for computing the shaft bearing reactions resulting from these propeller forces. Presents a method of computing hull pressure forces resulting from the propeller pressure field.

The various procedures are illustrated by numerical examples.

1. Propellers (marine) - performance
2. Ship hulls - propeller pressure field
3. Propeller shafts - vibration

I. F. E. Reed
II. R. T. Bradshaw

CONESCO, Arlington, Massachusetts. Report No. F-101-2.
SHIP HULL VIBRATIONS - 2. THE DISTRIBUTION OF EXCITING FORCES GENERATED BY PROPELLERS, by F. E. Reed and R. T. Brodshaw. June 1960. xiii, 214 p. graphs, tables, refs. (Index No. NS712-100 S. T. 2, Contract NObs 77150)
UNCLASSIFIED

A study of the forces acting on a hull as a consequence of propeller action. Develops calculation forms for computing the dynamic forces and moments generated by a propeller operating in a variable wake. Describes a program for computing the shaft bearing reactions resulting from these propeller forces. Presents a method of computing hull pressure forces resulting from the propeller pressure field.
The various procedures are illustrated by numerical examples.

1. Propellers (marine) - performance
2. Ship hulls - propeller pressure field
3. Propeller shafts - vibration

I. F. E. Reed
II. R. T. Brodshaw

CONESCO, Arlington, Massachusetts. Report No. 101-2.
SHIP HULL VIBRATIONS - 2. THE DISTRIBUTION OF EXCITING FORCES GENERATED BY PROPELLERS, by F. E. Reed and R. T. Brodshaw. June 1960. xiii, 214 p. graphs, tables, refs. (Index No. NS712-100 S. T. 2, Contract NObs 77150)
UNCLASSIFIED

A study of the forces acting on a hull as a consequence of propeller action. Develops calculation forms for computing the dynamic forces and moments generated by a propeller operating in a variable wake. Describes a program for computing the shaft bearing reactions resulting from these propeller forces. Presents a method of computing hull pressure forces resulting from the propeller pressure field.
The various procedures are illustrated by numerical examples.

1. Propellers (marine) - performance
2. Ship hulls - propeller pressure field
3. Propeller shafts - vibration

I. F. E. Reed
II. R. T. Brodshaw

CONESCO, Arlington, Massachusetts. Report No. F-101-2.
SHIP HULL VIBRATIONS - 2. THE DISTRIBUTION OF EXCITING FORCES GENERATED BY PROPELLERS, by F. E. Reed and R. T. Brodshaw. June 1960. xiii, 214 p. graphs, tables, refs. (Index No. NS712-100 S. T. 2; Contract NObs 77150)
UNCLASSIFIED

A study of the forces acting on a hull as a consequence of propeller action. Develops calculation forms for computing the dynamic forces and moments generated by a propeller operating in a variable wake. Describes a program for computing the shaft bearing reactions resulting from these propeller forces. Presents a method of computing hull pressure forces resulting from the propeller pressure field.
The various procedures are illustrated by numerical examples.

1. Propellers (marine) performance
2. Ship hulls - propeller pressure field
3. Propeller shafts - vibration

I. F. E. Reed
II. R. T. Brodshaw

CONESCO, Arlington, Massachusetts. Report No. F-101-2.
SHIP HULL VIBRATIONS - 2. THE DISTRIBUTION OF EXCITING FORCES GENERATED BY PROPELLERS, by F. E. Reed and R. T. Brodshaw. June 1960. xiii, 214 p. graphs, tables, refs. (Index No. NS712-100 S. T. 2; Contract NObs 77150)
UNCLASSIFIED

A study of the forces acting on a hull as a consequence of propeller action. Develops calculation forms for computing the dynamic forces and moments generated by a propeller operating in a variable wake. Describes a program for computing the shaft bearing reactions resulting from these propeller forces. Presents a method of computing hull pressure forces resulting from the propeller pressure field.
The various procedures are illustrated by numerical examples.

1. Propellers (marine)-performance
2. Ship hulls - propeller pressure field
3. Propeller shafts - vibration

I. F. E. Reed
II. R. T. Brodshaw

BLANK PAGE